Cape Peninsula University of Technology

PICO-SCALE WIND TURBINE SYSTEM FOR SUSTAINABLE ELECTRICITY PROVISION IN OFF-GRID RURAL REGIONS

by

JOHN BUSAYO TEMILOLA

Thesis submitted in fulfillment of the requirements for the degree

Master of Engineering: Mechanical Engineering

in the Faculty of Engineering & the Built Environment

at the Cape Peninsula University of Technology

Supervisor: Dr. Olukayode Lawrence Ayodele
Co-supervisor: Prof. Tiyamike Nyozani Ngonda

Bellville
August 2025

DECLARATION

I, **John Busayo Temilola**, affirm that the content of this thesis is the result of my independent work and has not been previously submitted or published for the award of any academic degree. All external sources of literature, data, or contributions referenced in this thesis have been properly credited and are fully listed in the references section.

	August 2025
Signed	**Date**

ABSTRACT

This research investigates the practical feasibility of deploying pico-scale vertical-axis wind turbines (VAWTs), specifically of the Darrieus configuration, as decentralized power generation solutions for remote rural communities without access to grid electricity. The overarching goal is to provide sustainable, low-cost electrical energy for essential end-uses such as mobile phone charging, small communication devices, and LED lighting. The Darrieus VAWT topology was selected for its compact footprint, omnidirectional wind capture capability, and relatively favorable aerodynamic performance in low to moderate wind speed regimes.

A transient Computational Fluid Dynamics (CFD) model of a pico-scale Darrieus VAWT was developed in ANSYS Fluent. The simulation employed a Six Degrees of Freedom (6DOF) dynamic mesh solver, enabling free rotation of the rotor driven solely by aerodynamic forces, thereby capturing realistic self-starting and operational behavior. The analysis covered wind speeds ranging from 2 m/s to 10 m/s and angles of attack (AoA) between 0° and 25°. Aerodynamic performance metrics—such as torque, lift force, and power coefficient (Cp)were evaluated using the Realizable k-ε model turbulence model to accurately resolve boundary layer separation, dynamic stall, and wake vortex structures. A mesh sensitivity study was conducted to ensure grid convergence and numerical stability.

Simulation results revealed that the turbine achieved peak performance at an electrical output of 38.29 W, corresponding to wind speeds of 6–8 m/s and AoA values of 5°–10°. Below 4 m/s, torque generation was insufficient to overcome bearing and aerodynamic losses due to inadequate lift production. Conversely, AoA values exceeding 15° induced pronounced dynamic stalls, characterized by flow separation, elevated pressure drag, and reduced Cp. These findings indicate that the design is best suited to steady, moderate-wind environments and is less effective under persistently low or highly turbulent wind conditions.

The study concludes that pico-scale Darrieus VAWTs offer viable potential for small-scale rural electrification but are most effective when integrated into hybrid renewable energy systems. Coupling the turbine with photovoltaic modules and battery storage would mitigate the intermittency of wind resources, enhance supply reliability and support broader rural electrification initiatives aligned with the United Nations' Sustainable Development Goals (SDGs). Real-world prototyping and experimental validation are

recommended to refine aerodynamic predictions and confirm long-term performance under field conditions.

Keywords: Pico-scale wind turbine, small wind energy systems, Off-grid electrification, Rural energy access, Sustainable energy, Vertical-axis wind turbine (VAWT)

ACKNOWLEDGEMENTS

All glory belongs to God without which this output would not have been possible. My sincere appreciation goes to all the members of my family for their unflinching support in all ramifications.

TABLE OF CONTENTS

LIST OF FIGURES

LIST OF TABLES

GLOSSARYS

AFPM – Axial Flux Permanent Magnet: A type of generator in which the magnetic flux travels along the axis of rotation.

AoA – Angle of Attack: Describes the angle formed between a turbine blade's chord line and the direction of oncoming wind, which directly affects how much lift or drag is generated during operation.

BEMT – Blade Element Momentum Theory: A method used to model turbine performance by combining blade element theory with momentum conservation.

BLF – Bloemfontein: Geographic shorthand used for wind resource data referencing this location.

BLWT2 – Boundary Layer Wind Tunnel 2: A specific wind tunnel facility used for experimental aerodynamic studies.

CFD – Computational Fluid Dynamics: A digital simulation technique used to study how air moves around turbine components, helping predict aerodynamic behavior and performance without physical testing.

COE – Cost of Energy: A financial metric indicating the unit cost of generated electricity over a system's lifetime.

Cp – Power Coefficient: A dimensionless measure of a wind turbine's efficiency in capturing wind energy.

CPT – Cape Town: Abbreviation for the city used in regional wind analysis.

DPSM – Dynamic Positioning System Mechanism: A mechanism or control system used for real-time orientation adjustments.

DRB – Durban: Regional abbreviation used in site-specific evaluations.

ELD – East London: Another South African region abbreviation referenced for wind data.

ESS – Energy Storage Systems: Technologies used to store electricity for later use, vital in hybrid renewable systems.

GGI – Generalized Grid Interface: A control system or interface module designed to coordinate and regulate the connection of decentralized energy technologies such as wind or solar systems to the primary electrical grid infrastructure.

HAWT – Horizontal Axis Wind Turbine: A type of wind turbine where the main rotor shaft is positioned parallel to the ground, typically facing into the wind for maximum efficiency.

HH – Blade Height: The vertical distance from the ground to the turbine's hub, used in wind profiling.

JHB – Johannesburg: Regional abbreviation for wind condition assessment.

kW – Kilowatt: A standard measurement of power output, equivalent to 1,000 watts, commonly used to quantify energy generation or consumption in electrical systems.

LCA – Life Cycle Assessment: A systematic analysis used to estimate the environmental effects of a product or system throughout its entire lifespan from raw material extraction through production, usage, and final disposal.

LCOE – Levelized Cost of Energy: Similar to LEC; it quantifies the per-kilowatt-hour cost of producing electricity across the project's lifespan.

NACA – National Advisory Committee for Aeronautics: Known for standardizing airfoil shapes used in turbine blades.

OR – Overlap Ratio: A parameter in VAWT blade design denoting the extent of overlap between blades.

PEZ – Port Elizabeth: Regional tag used in wind speed and resource evaluation.

PRT – Pretoria: Location shorthand included in site assessment datasets.

Pw – Wind Power Available: The theoretical power contained in wind passing through a given rotor area.

Po – Output Power: Refers to the actual power captured by the turbine, determined via simulation or experiments.

SWT – Small Wind Turbine: Turbines generally under 100 kW, suited for localized energy generation.

Tm – Mechanical Torque: The rotational force generated by the turbine shaft.

TSR – Tip Speed Ratio: Represents the relationship between how fast a blade tip moves and the wind speed, which is essential in optimizing turbine efficiency.

URANS – Unsteady Reynolds-Averaged Navier-Stokes: A turbulence modeling approach in CFD that captures time-dependent changes in airflow, commonly applied to unsteady aerodynamic simulations.

VAWT – Vertical Axis Wind Turbine: A wind turbine with its main rotor shaft oriented vertically.

WASA – Wind Atlas for South Africa: A resource mapping wind profiles across the country.

WECS – Wind Energy Conversion System: An arrangement of mechanical and electrical components that transforms wind's kinetic force into usable electrical energy.

CHAPTER ONE
GENERAL INTRODUCTION

Introduction

Socioeconomic development certainly relies on a steady and uninterrupted electricity supply, yet still, a lot of rural areas in developing countries are unable to enjoy this because of the expensive national grid expansion. That is precisely the reason why wind energy systems are becoming more and more famous as sustainable alternatives that take the least toll on the environment while generating electricity from the kinetic energy of the atmosphere. These systems can be rolled out in larger sizes enabling the poor to have electricity while the environment is being kept clean.

In South Africa, the coastal and mountainous areas have the potential of generating large amounts of wind power as there are average wind speeds that easily cross 6 m/s. Such conditions favor the installation of both small and large-scale wind farms. Nevertheless, despite government support for renewable energy through the REIPPP (Renewable Energy Independent Power Producer Procurement Programme), still about 15% of rural households, especially in provinces like KwaZulu-Natal and the Eastern Cape, are not connected to the national electricity grid. This increases the importance of decentralized energy solutions that are specifically designed for local conditions and are wind-rich areas that are hard to reach and have no proper grid infrastructure.

Pico-scale wind technologies which are usually rated below 100 W have shown up as the best options to satisfy the basic power requirements of rural areas. These little systems can give the power for the very basic household and community utilities like LED lighting, mobile charging, ventilation, and communication devices. Among the different wind turbines, vertical-axis wind turbines (VAWTs)—especially the ones following the Darrieus configuration—fit the above mentioned scenario the best since they can work with turbulent wind and can capture the energy from all sides. The innovations in computational fluid dynamics (CFD) have allowed for better simulations and optimizations of airflow around the blades, torque performance, and structural integrity. Furthermore, the hybrid VAWT that combines lift and drag has shown better self-starting capability and more consistent power output in gusty areas.

As of now, pico-scale VAWTs are not widely adopted due to their limited technical capabilities like low starting torque and efficiency loss at wind speeds below 4 m/s. In

addition, environmental factors like dust and airflow obstruction can result in performance loss. If the systems are placed in the South African regions that have an average wind speed of 6 m/s to 8 m/s, they will work fine, but in areas that are heavily vegetated or sheltered, their efficiency may decrease.

The study makes use of advanced CFD simulations to perform an aerodynamic analysis of a small Darrieus-type VAWT with special emphasis being put on the important parameters like start behavior, torque generation, aerodynamic efficiency, pressure distribution under different wind conditions, and so on. The study also lays down the optimal operating ranges, identifies chances for improvement in performance, and creates design recommendations specifically for the needs of rural electrification projects.

1.1 Research problem statement

Reiterating the International Energy Agency, there are still around 700 million people without electricity even in this modern era, and the International Energy Agency (IEA, 2024) reported this. The energy shortage mostly experienced in rural areas and off-grid locations has been a serious setback for both social and economic development.

Renewable energy technologies, especially wind farms where large turbines are used and hybrid configurations, are valid and effective in areas with a lot of wind but they are not economically justified and technically demanding too in places that are hard to reach or lack a critical mass of population. The mentioned systems are designed for wind speeds above 8 m/s, yet many rural areas might only experience wind speeds as low as 3 m/s or up to 7 m/s. Therefore, conventional wind turbines often perform poorly and are not economically viable in such regions.

Thus, there is a need for renewable energy technologies that are not only affordable but also adaptable to low-wind scenarios. Pico-scale vertical-axis wind turbines (VAWTs) with a definition of a capacity below 100W are one of the most promising solutions. These tiny windmills are compact, easy to manufacture and maintain, and can work the wind slowly so they are already producing a part of the energy that goes for off-grid users' basic electricity needs such as powering LED lights, charging mobile devices or running a very simple communication device.

Nonetheless, empirical performance data for pico-scale VAWTs are still lacking, especially when it comes to different wind conditions. The important factors power output, self-starting capability, and aerodynamic efficiency have not been comprehensively studied, particularly through high- fidelity computational simulations.

It is important to fill these knowledge gaps to prove the reliability of pico-scale VAWTs and to optimize their design for stable, cheap electricity generation in remote areas. This research is part of this objective by making a detailed aerodynamic analysis that is meant to improve the performance and consequently the applicability of pico-scale VAWTs in off-grid electrification projects.

1.2 Background to the research problem

Access to electricity is essential for both personal well-being and socio-economic development. Yet, as of 2024, approximately 675 million people—primarily in rural areas of South Asia and sub-Saharan Africa—still lack reliable power access (IEA, 2024). Expanding electricity access in these regions remains challenging due to high infrastructure costs, geographical remoteness, and reliance on diesel generators, which are both environmentally harmful and operationally unreliable (World Bank, 2023).

Although large-scale renewable energy technologies such as wind farms and solar photovoltaic (PV) systems are becoming increasingly widespread, they are often unsuitable for rural off-grid applications. Horizontal-axis wind turbines (HAWTs), for instance, typically require wind speeds exceeding 10 m/s and substantial capital investment—conditions rarely meet in rural regions, where wind speeds generally range between 3 and 7 m/s. Similarly, solar PV systems face limitations in such contexts, as they often require costly battery storage to ensure power availability during periods of low sunlight (IRENA, 2022).

In contrast, small vertical-axis wind turbines (VAWTs)—particularly pico-scale systems producing less than 100 W—offer a more adaptable and scalable solution. These compact devices are designed to operate efficiently under moderate wind conditions and are relatively inexpensive to manufacture and maintain, making them well-suited for stand-alone rural energy systems. Unlike HAWTs, Darrieus-type VAWTs can harness wind from any direction without requiring yaw mechanisms, and many designs are self-starting,

eliminating the need for external power inputs or complex control systems (Mohamed, 2016). These characteristics make pico-scale VAWTs particularly useful for meeting basic off-grid household needs, such as charging mobile phones, powering LED lighting, or running small electronic devices.

Despite their promise, the aerodynamic performance and operational reliability of pico-scale VAWTs remain insufficiently understood, particularly with respect to key performance indicators such as the power coefficient (Cp), starting torque, and operational stability under real-world wind conditions. While prior simulation-based investigations (e.g., Sandanshiv et al., 2017) have demonstrated their technical feasibility, further research is needed to refine their design and integrate them effectively into rural hybrid renewable energy systems.

To address this gap, the present study conducts a comprehensive aerodynamic performance analysis of a pico-scale Darrieus-type VAWT using advanced Computational Fluid Dynamics (CFD) modelling in ANSYS Fluent. Simulations are performed under wind speeds ranging from 2 to 10 m/s and blade angles of attack (AoA) between 0° and 25°, representing typical rural wind conditions. The objective is to identify optimal design parameters that can enhance efficiency and power generation in low-wind, off-grid settings.

Ultimately, this research aligns with the global agenda for sustainable energy access, directly contributing to United Nations Sustainable Development Goal 7 (SDG7) ensuring universal access to affordable, reliable, and modern energy services by 2030.

1.3 Research objective

This research investigates the technical feasibility of a small-scale Darrieus-type vertical-axis wind turbine (VAWT) for eco-friendly off-grid rural electrification by developing and validating a computational fluid dynamics (CFD) model in ANSYS Fluent through using a 6-degree-of-freedom (6DOF) solver. The specific, measurable objectives are as follows. These objectives will be met through simulated experiments in ANSYS Fluent, where important aerodynamic parameters like power coefficient (Cp), torque, and power output will be quantified in order to connect theoretical modeling with practical design insights. The specific, measurable objectives are as follows:

- **CFD Model Development**: Create and verify a transient CFD model for wind speeds from 2 to 10 m/s and angles of attack (AoA) from 0° to 25° with an error of less than 2% in power coefficient (Cp) predicted by the mesh convergence. Key aerodynamic parameters like lift coefficient (CL), drag coefficient (CD), and torque will be quantified.
- **Aerodynamic Optimization**: Maximize turbine design through the conducting of mesh sensitivity analysis (aiming at grid independence of <1% variation in Cp) and parametric studies on blade geometry (e.g., solidity and curvature), thereby, increasing power output (Cp>0.25) under the typical rural wind conditions of 6 to 8 m/s and AoA of 5° to 10°.
- **Performance Constraints**: Determine operational restrictions through the simulation of the flow at low wind speeds (less than 4 m/s) and at high angles of attack (more than 15°), drag increase being quantified (>20% rise in CD), flow separation zones being mapped (through velocity contours), and stall onset being monitored (e.g., CLdrop >15%). Then, precise operational thresholds are established for cut-in speed and maximum AoA.
- **Power Output and Applications**: Compute the theoretical annual energy production (targeting 100-500 Wh/day for a 0.5 m rotor diameter) appropriate for low-power applications (such as 5-10 W LED lighting or 2-5 W device charging), and consider hybrid integration metrics (like >80% system reliability) with solar PV and battery storage for decentralized off-grid deployment.

1.4 Research questions

To align with the reframed objectives and emphasize investigative processes, the following research questions have been revised to start with "How," ensuring they are precise, measurable, and directly testable via the CFD simulations and analyses described:

- How accurately does the developed transient CFD model predict key aerodynamic parameters (C_L, C_D, torque) for a pico-scale Darrieus VAWT across wind speeds of 2–10 m/s and AoA of 0°–25°, as measured by deviation (<5%) against experimental benchmarks?

- How do variations in blade geometry parameters (e.g., solidity 0.2–0.6) influence the power coefficient ($C_p > 0.25$) under rural wind conditions (6–8 m/s, AoA 5°–10°), as quantified through parametric optimization in ANSYS Fluent?

- How do low wind speeds (<4 m/s) and high AoA (>15°) affect VAWT performance, particularly in terms of drag augmentation (>20% rise in C_D), flow separation extent (recirculation zone area), and stall thresholds (e.g., C_L reduction >15%)?

- How does the optimized pico-scale VAWT generate theoretical power output (100–500 Wh/day for a 0.5 m rotor diameter) for low-power rural applications (e.g., 5–10 W loads), and how does hybrid integration with solar PV enhance system reliability (>80% uptime) in off-grid scenarios?

1.5 Scope and limitations of this research

1.5.1 Scope of research

Considering the computational intensity of high-resolution aerodynamic modeling and the constraints posed by moderate wind environments, the scope of this research is defined as follows:

- The present study implements a time-resolved simulation method for airflow interactions with turbine blades characterized by a Six Degrees of Freedom (6DOF) solver within the ANSYS Fluent Computational Fluid Dynamics (CFD) software platform. The precision of the simulation is further improved by integrating a mesh independence analysis while, at the same time, reducing the consumption of computational resources. The performance of a compact Darrieus-type vertical-axis wind turbine (VAWT) is tested at different wind speeds of 2-10 m/s and angles of attack (AoA) of 0°-25° with particular attention to startup behavior, torque generation, aerodynamic forces, and the power coefficient (Cp).
- The design enhancements aim at the operation optimization within the moderate wind conditions specifically, wind speeds of 6 to 8 m/s and AoA values of 5 to 10° common in rural environments. The research's practical goal is to power small-scale energy such as lighting and device charging in remote, off-grid sites.
- The research is limited to purely theoretical forecasts as obtained from CFD simulations; no physical experimental trials or prototypes are done. Nevertheless, the outcomes are meant to influence the future integration of energy systems comprising wind technologies with their small-scale applications especially for the sub-Saharan African off-grid communities where decentralized electrification is

urgently required.

1.5.2 Limitations of the study

Although this research provides valuable understanding of the aerodynamic performance of pico-scale Darrieus vertical-axis wind turbines, it is essential to acknowledge several constraints associated with the study:

- The simulation-based nature of the research is absolute and thus the performance in real-world scenarios cannot be confirmed directly.
- The only aspect of the design scrutinized in the analysis is aerodynamic performance metrics, and so it does not cover other design factors like structural durability, material fatigue, mechanical losses, or system longevity.
- Financial analyses are not contemplated in this study at all, in terms of manufacturing expenses, upkeep costs, or evaluations of long-term economic viability as these aspects are not the primary focus.
- Under simulated conditions, there are no environmental factors like turbulence, dust, temperature variations, or humidity being considered that usually affect performance in field settings; hence, the wind profiles are assumed to be steady and idealized.
- The analysis is limited to just one VAWT configuration (the Darrieus type). The study does not address comparisons with other turbine types, such as Savonius or horizontal-axis turbines, which restricts wider generalizations.
- While the potential of hybrid systems is discussed in a conceptual manner, the study does not include detailed simulations or integration modeling for complementary systems such as photovoltaic panels, batteries, or inverters, which are critical components of complete off-grid solutions.

1.6 Significance of the research

This study talks about one of the most important issues on the planet - global energy poverty - and it takes a closer look at the remote and rural areas where about 675 million people are still dependent on unreliable sources of electricity. Among the places most affected is sub-Saharan Africa which, according to IEA (2024), has wind resources of 3-7 m/s on average, which are of great potential for wind energy use nonetheless. The study takes a step further to make use of state-of-the-art Computational Fluid Dynamics (CFD) that comes with a simulation package called ANSYS Fluent, to find out how a pico-scale

Darrieus vertical-axis wind turbine (VAWT) operates aerodynamically.

In order to assess the VAWT under wind flow and various angles of attack (AoA) at a range of 2 to 10 m/s, a transient six-degrees-of-freedom (6DOF) solver is used in the simulations which also take into account the complex interactions between the structure (turbine blades) and the fluid (wind flow).

It was determined through the study of the self-starting capability, torque generation, aerodynamic loading, and the power coefficient (Cp) that were represented in key performance indicators, what the best operating conditions are. The outcome shows that the turbine can produce an ideal peak power of 38.29 W at 10° AoA in the wind speed range of 6-8 m/s, which is considered to be enough for basic rural energy needs such as charging mobile devices and lighting through LEDs. These initiatives actively contribute to education, medical care, and small-sized businesses in the remote communities that are left out of the world.

Performance limitations are analyzed and highlighted as major issues, with examples of these being limited lift at wind speeds of less than 4 m/s and stalls due to drag when the angle of attack is above 15°. This situation calls for design optimization that is specifically focused on low-wind environments. The study, throughits detailed aerodynamic assessment, not only raises the technical case but also strengthens the practical aspects of deploying pico-scale VAWTs in the decentralized renewable energy systems.

In support of the United Nations Sustainable Development Goal 7 (affordable and clean energy), the research results add to the whole literature on sustainable rural electrification. Although the research is based on simulation, it provides a groundwork for future experimental validation and the incorporation of pico-scale VAWTs into the hybrid systems of solar and energy storage, thereby supporting the development of robust off-grid energy solutions.

1.7 Summary of dissertation structure

The first chapter sets the scene for this study, mainly discussing the global problem of energy poverty, which still impacts around 675 million people living in the most remote, off-grid areas of the world (IEA, 2024). It is a prelude to the use of pico-scale vertical-axis wind turbines (VAWTs) as a readily available and eco-friendly method of power generation in low wind areas with wind speeds from 3 to 7 m/s. This first chapter also presents the

primary aims of the research, namely the investigation of the aerodynamic performance of a Darrieus-type VAWT through the application of Computational Fluid Dynamics (CFD) tools in the ANSYS Fluent environment. The evaluation of performance is done over a range of wind speeds (2–10 m/s) and blade angles of attack (0°–25°). The study intentionally refrains from dealing with issues such as material selection, economic cost analysis, and physical prototyping, but rather focuses on simulation-driven investigations exclusively. The chapter closes by accentuating the necessity of this research in solving the issue of energy access in marginalized areas and putting it in the context of the enormous yet still developing field of rural electrification through small-scale wind technologies.

Chapter Two gives a thorough and detailed literature review, which goes all the way back to the performance and efficiency optimization of compact wind turbines. The discussion is wide open and it goes all over the place with the aerodynamic challenges and engineering solutions that are the basis for low-power wind energy systems.

Chapter Three is where the research methodology is explained in detail. A transient CFD model with a Six Degrees of Freedom (6DOF) solver is incorporated in ANSYS Fluent for simulating the turbine's response to changing wind conditions that are usually found in rural areas. The modeling technique makes dynamic assessment of turbine behavior possible with regard to various environmental influences.

The results of the simulations are presented and interpreted in Chapter Four. Alongside torque output, the performance metrics of power generation, power coefficient (Cp) and overall aerodynamic efficiency are scrutinized. The research points out the best working conditions and also mentions the turbine's performance restrictions at high angles of attack and low wind speeds. The dissertation is concluded in

Chapter Five where a summary of the main conclusions and noteworthy technical insights is provided. Moreover, it also presents the further research recommendations which underline the need for site-specific design improvements, physical validation, and hybrid renewable energy system integration to make the turbines more acceptable for off-grid rural areas.

1.8 Publications

Busayo, T.J., Ngonda, T. and Ayodele, O., (submitted). Influence of Obstacle Height on Pico-Scale VAWT Performance: A CFD Simulation Study. Wind. [Under publication review

under Wind].

Busayo, T.J., Ngonda, T. and Ayodele, O., (submitted). A Numerical Study of Technical Viability of Pico-Scale Vertical-Axis Wind Turbines for Rural Electrification in Southern Africa. Wind. [Under publication review under Wind].

CHAPTER TWO

LITERATURE REVIEW

2.1 Introduction

This study explores wind energy conversion systems as a cornerstone of the global transition to sustainable electricity generation, complementing solar and hydro technologies within modern renewable energy frameworks. These systems serve as sustainable alternatives to fossil fuel-based energy, demonstrating remarkable versatility in addressing diverse energy demands, ranging from large-scale wind farms to small off-grid units. By integrating with intelligent energy management systems, small-scale wind turbines are particularly effective in enhancing energy access in remote areas, providing decentralized electricity and contributing to grid stability.

Research on Pico-scale wind turbines (≤100 W) around the world and in Africa shows differences in context, with the international projects from 2023 to 2025 focusing on technological innovations for urban and offshore vertical-axis wind turbines (VAWT)—for example, Peruvian lift-type prototypes generating 70-120 Wh/day at 3-5 m/s due to optimized solidity for turbulence at great heights, or NACA0015 Darrieus with embossed blades attaining Cp ~0.3-0.4 at Re <10^5 through J-shaped profiles for self-start and helical designs that increase efficiency by 15-20% in gusty rooftop airflow—foreseeing a market increase of 12% CAGR to USD 37.6 Bn by 2034 for modular low-Re systems. In Africa, research focuses mainly on hybrid mini-grids rather than VAWTs alone, like in Kenya and Nigeria where a Turgo-type (50-200 W) pico-hydro can achieve 80-85% uptime with the help of solar power, but at the cost of shorter (18-24 months) lives due to dust, or the trials in South Africa and Ethiopia on PV-wind-biogas for 100% renewable off-grid where the LCOE is less than 0.15 USD/kWh and wind contributes 10-20% to offset diesel in the 4-7 m/s range of variability, even though there are still VAWT-related gaps in adaptation to deserts and the dominance of pico-solar. Worldwide, wind-optimizations (Cp >0.4 via CFD hybrids) are great in scalability but ignore Africa's limitations of cost (80% uptime to fill SSA knowledge gaps on pico-VAWTs for SDG 7. However, inland regions like Gauteng and Limpopo, characterized by variable wind patterns, require thorough wind resource assessments to ensure the viability of wind systems. The intermittent nature of wind energy highlights the importance of hybrid systems, which leverage complementary energy sources to mitigate fluctuations. The widespread adoption of wind technologies depends on supportive policies and robust regulatory frameworks to address financial and logistical barriers. Ongoing innovations in material science, turbine design, and energy

storage further enhance the reliability and efficiency of wind energy solutions in rural settings.

Modern wind energy conversion systems primarily utilize two distinct turbine architectures, illustrated in Figure 2.1: horizontal-axis wind turbines (HAWTs) and vertical-axis wind turbines (VAWTs). HAWTs represent the industry standard for grid-connected wind farms, achieving optimal performance at hub heights between 60-150 meters where they can harness consistent, high-velocity winds to generate substantial power outputs ranging from 500 kW to multi-megawatt capacities. Conversely, VAWTs have emerged as particularly suitable for decentralized energy applications owing to their omnidirectional operation capability and resilience in turbulent wind environments - characteristics that eliminate the need for complex yaw mechanisms. Contemporary design innovations have significantly enhanced VAWT performance metrics, making them increasingly viable for compact designs, quieter operation, and enhanced performance in complex terrains, making them ideal for community-based and off-grid installations.

VAWTs produce less noise than HAWTs, minimizing disturbances in residential or public areas. Their vertical design requires less horizontal space and simpler support structures (typically <10 m), simplifying installation and maintenance. These attributes reduce logistical and aesthetic impacts, making VAWTs well-suited for rural electrification projects. Integrating VAWTs into hybrid systems with solar and storage technologies provides a reliable renewable energy source, addressing energy shortages in developing regions and supporting global sustainability goals, such as Sustainable Development Goal 7 for accessible and clean energy. Table 2.1 shows the difference between the horizontal and vertical wind turbines.

Table 2.1: Horizontal-axis (HAWT) versus vertical-axis (VAWT) wind turbines

Characteristic	HAWT	VAWT
Power Capacity	100 kW – 7+ MW (utility-scale)	1 kW – 1.6 MW (small/medium-scale)
Tower Height	60–150 m (requires tall towers)	<10 m (compact footprint)
Acoustic Impact	Moderate to high noise generation	Low noise emission
Wind Adaptation	Dependent on consistency direction	Omnidirectional operation
Ideal Deployment	Wind farms, open areas	Urban, rural, and off grid sites

Wind energy technologies may also be categorized based on their rated output and physical size, factors that play a crucial role in determining their performance, environmental compatibility, and application scope. High-capacity turbines generally rated between 1 megawatt and over 10 megawatts are primarily designed for utility-scale electricity generation. These systems are commonly installed in large onshore and offshore wind farms, where they supply power directly to national grid infrastructures (Alam, 2023). These machines feature expansive rotor spans and are mounted on tall towers to optimize access to high-altitude wind flows, thereby maximizing energy yield.

On the other end of the spectrum, micro- and small-scale wind turbines including pico-scale units with power outputs typically below 100 watts are tailored for decentralized energy applications. Such systems are particularly advantageous in isolated or rural locations where conventional grid extension is economically or logistically impractical, and where power needs are modest.

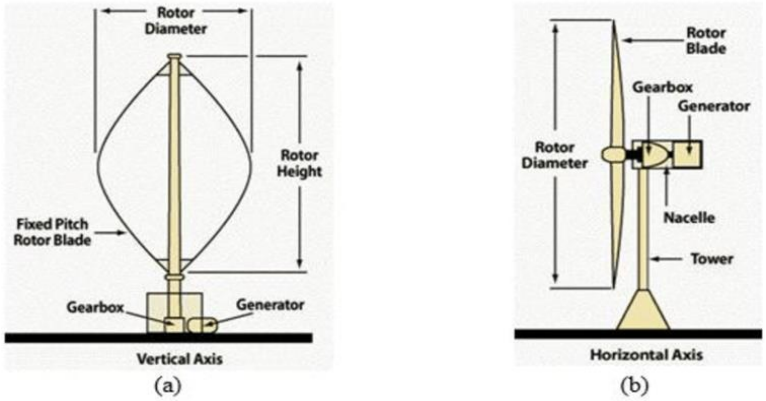

Figure 2.1: Schematic illustration comparing the structural components rotor design, gearbox arrangement, generator position, and nacelle configuration of (a) vertical-axis wind turbines (VAWTs) and (b) horizontal-axis wind turbines (HAWTs) (Adapted from Mohammed Ba Alawi, 2018).

Power ratings have a characteristic that greatly influences the physical infrastructure needed for wind turbines and the best use cases are frequently used to differentiate them. Usually rated above one megawatt (MW) high-capacity wind turbines are designed for utility-scale uses and are commonly found in sizable onshore and offshore wind farms. These systems require substantial structural support to access stronger, more reliable wind flows at higher elevations such as towers taller than 100 meters and large rotor diameters. Direct electricity delivery into national grid systems is their main duty.

Commercial institutional and light industrial settings frequently use medium-scale turbines which are between 100 kW and 1 MW in size. Agricultural operations college campuses and manufacturing complexes are typical deployment locations where they support localized energy sustainability and help reduce grid dependency. Smaller wind systems are ideal for small business and residential applications they are typically rated between 1 kW and 100 kW. These work especially well in isolated or off-grid areas where traditional grid expansion is either financially or technically unfeasible (Tzen E. 2020).

A steady and dependable energy supply is often ensured by integrating such systems into hybrid energy frameworks that also include solar photovoltaic panels and battery storage units. Pico-scale wind turbines usually rate less than 1 kW at the micro end of the spectrum. Small and pico-scale wind turbines are engineered to meet minimal energy demands such as powering household electronics, telecommunications equipment, and

basic residential needs. Their value is especially evident in resource-constrained regions, where they enable access to essential services like mobile device charging and LED-based illumination. Owing to their compact design, affordability, and ability to operate effectively in moderate wind environments, these systems offer a viable and practical option for electrifying underserved rural communities (Deevela N. R. et al., 2024). Expanding access to these technologies is crucial for narrowing the global electricity access divide. In locations where connections to the central grid are unreliable or entirely absent, the deployment of small-scale wind systems enhances local energy resilience and plays a meaningful role in advancing sustainable development objectives.

2.2 Characteristics of wind

The wind resources in South Africa are highly variable both seasonally and geographically. A number of variables including topography distance from the coast and general climatic patterns affect wind speed patterns. Because coastal areas are directly exposed to oceanic weather systems, they enjoy stronger and more reliable winds, especially along the country's southern and eastern borders. While Cape Point the windiest location in South Africa records an average of 6. 9 m/s with more than 42% of hourly wind speeds exceeding 8 m/s average wind speeds in Port Elizabeth for instance reach 6. 01 m/s (Wright M.A 2017). Coastal areas are ideal for distributed generation systems and centralized wind farms because of these factors.

Conversely, inland regions like Bloemfontein tend to experience much lower average wind speeds, typically between 3 and 8.6 m/s. This reduced wind activity is largely attributed to the area's terrain and the absence of maritime influences. On a national scale, South Africa's average wind speeds generally fall within the 4 to 5 m/s range. These figures highlight the importance of tailoring wind energy development strategies to suit the unique wind resource profiles of each geographical zone within the country. Additionally, the time of day and season have an impact on wind patterns. For example, Cape Town experiences lower wind speeds (roughly 3 m/s) in the winter (May to June) and higher values (roughly 6 m/s) in the summer (January). These variations emphasize how crucial wind data analysis and long-term site monitoring are to precise project feasibility evaluations.

According to research by Wright and Grab (2017), average wind speeds in some areas of the Cape have gradually decreased over the course of 20 years ranging from -0. 002 to -

0. 06 m/s annually. This decline may be due to changing climatic conditions.

Additionally, Fant et al. (2016a; 2016b) emphasized that wind speed variability both short- and long-term can have a substantial impact on energy systems particularly when stability in grid-connected applications is considered.

Bosilovich et al. (2016) analyzed hourly wind speed data spanning from 2000 to 2019 across seven major cities in South Africa that includes: Cape Town, Durban, East London, Johannesburg, Bloemfontein, Port Elizabeth, and Pretoria providing a comprehensive national overview of wind patterns. After being checked for statistical reliability, the data revealed a significant relationship between wind potential and geographic features. Johannesburg and Pretoria are inland at about 1500 meters above sea level while coastal cities Durban East London Cape Town and Port Elizabeth are situated at lower elevations (20–60 meters). In the middle of the two geographical extremes is Bloemfontein. Table 2.2 provides geographical details for selected sites, including latitude, longitude, elevation, and site abbreviations, while Figure 2.2 visually represents their locations on a map.

The study emphasizes how crucial topography and geographic context are when planning for wind energy. All throughout Africa Masud et al. highlighted the winds largely unrealized potential as a renewable energy source (Masud et al., 2017). With a yearly contribution of more than 26000 GWh South Africa has made significant strides alongside nations like Egypt and Morocco. However, structural issues like a lack of technical know-how unclear policies and financial limitations plague many African countries including Nigeria and Cameroon. Significant offshore wind development potential exists in South Africa which could further improve system resilience and national energy security according to Inambao and Cunden (2019).

Table 2.2: The elevation (meters above sea level) latitude (°S), longitude (°W) and abbreviations of six South African locations are included in the geographic coordinates. (Bosilovich et al. 2016)

Serial no	Location	Abbreviation	Altitude (m)	Longitude (°W)	Latitude (°S)
1	Johannesburg	JHB	1753.00	28.05	26.22
2	East London	ELD	48.00	27.85	33.03
3	Cape Town	CPT	1590.00	18.42	33.92
4	Durban	DRB	21.00	31.02	29.86
5	Bloemfontein	BLF	1395.00	26.16	29.09
6	Pretoria	PRT	1339.00	28.23	25.75

In conclusion, the wind energy landscape in South Africa is diverse with strong potential in coastal areas and the need for adaptable strategies in inland areas. Policy support of location-specific assessments and hybrid renewable systems will be essential to maximizing the nation's wind energy potential in a fair and sustainable way.

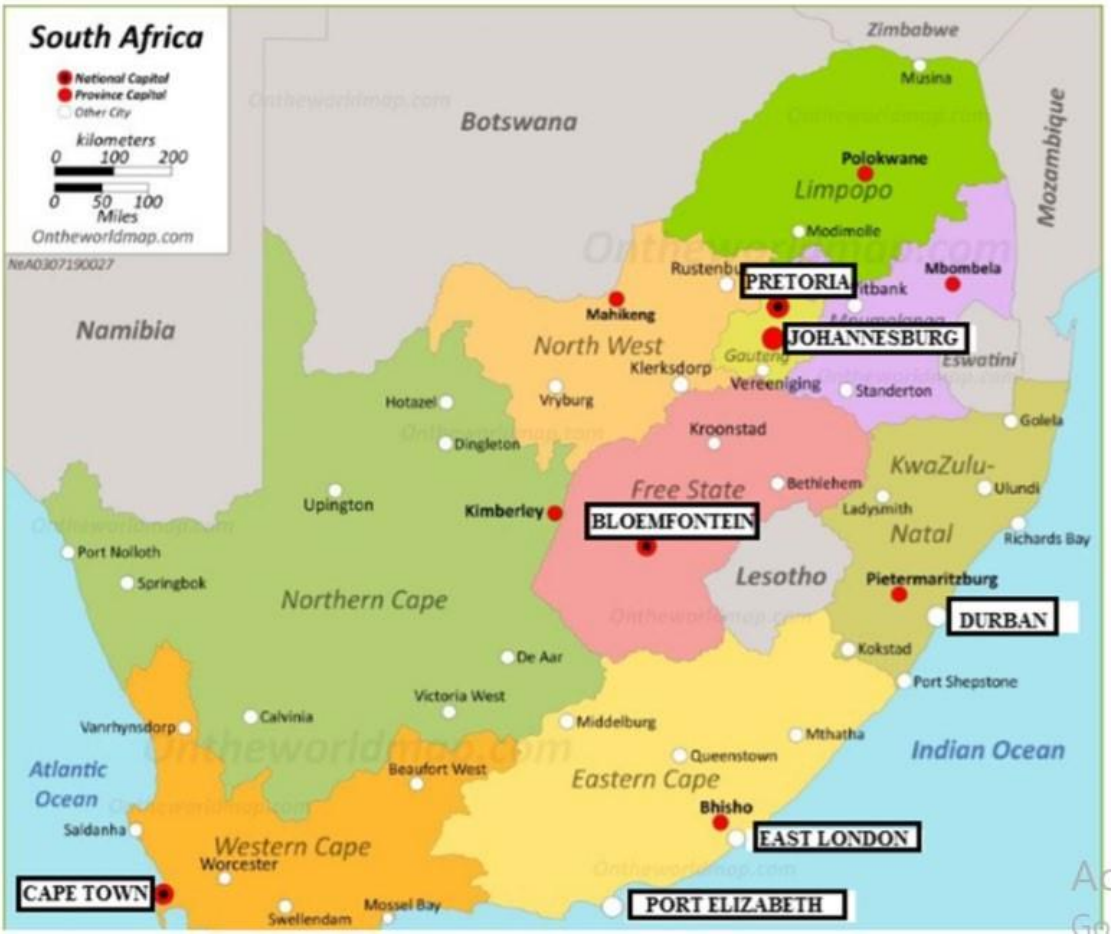

Figure 2.2: Geographical representation of Southern Africa showing major urban centers, provincial and national capitals within South Africa, Botswana, and Zimbabwe, including distance scales in both kilometers and miles. (Bosilovich et al. 2016)

2.3 Experimental and computational approaches

Various computational and analytical approaches have been extensively applied to examine the aerodynamic performance and operational viability of VAWTs, especially in relation to their use in rural energy systems. This section offers a critical synthesis of existing literature from two primary dimensions: computational (numerical) simulations and experimental investigations.

2.3.1 Numerical analysis

In a detailed investigation by Ahmudiarto et al. (2019), the aerodynamic characteristics of an innovative blade design tailored for vertical-axis wind turbines (VAWTs), aiming to

boost their energy conversion performance. The research employed Computational Fluid Dynamics (CFD) simulations to examine various blade configurations, with particular emphasis on a modified H-type blade featuring an upward curvature and modeled after the NACA 4212 airfoil. The results revealed that the redesigned blade exhibited enhanced aerodynamic behavior, evidenced by consistently elevated power coefficient (Cp) values across a range of wind speeds and tip speed ratios (TSRs). The Cp metric is critical, as it reflects the turbine's capability to effectively convert wind energy into mechanical output.

Additionally, the study introduced mathematical models to quantify the link between theoretical wind power potential (Pw) and the actual power generated (Po), whether through simulations or empirical testing. These relationships, expressed in Equations 2.1 and 2.2, provide a solid basis for evaluating VAWT performance in both controlled and practical scenarios.

$$PPP = 1/22\rho AV^{33}(\Omega\alpha\tau\tau) \quad (2.1)$$

$$Po = Tm\omega = 1/22Cp\rho AV^{33}(\Omega\alpha\tau\tau) \quad (2.2)$$

Where T_m represents mechanical torque (in Newton-meters), ω denotes the angular velocity (in radians per second), A is the turbine's swept area (in square meters), W refers to wind speed (in meters per second), and C_p is the power coefficient. The coefficient C_p quantifies the efficiency of a wind turbine by expressing the ratio of actual power output (P_o) to the theoretical wind power available (P_v). The simulation outcomes revealed that the upper-curve blade profile significantly enhances energy capture efficiency, particularly at lower tip-speed ratios (TSRs) of 0.5 and 1.0 under various wind conditions. This performance makes it especially well-suited for areas characterized by low or fluctuating wind speeds, such as many parts of South Africa.

As illustrated in Figure 2.3, the turbine equipped with the upper-curve blade achieved power output exceeding 160 watts adequate to support basic household energy needs in off-grid rural homes. These results emphasize the effectiveness of compact wind energy systems in delivering reliable and sustainable electricity, particularly in remote locations. The study affirms the practicality of deploying pico-scale VAWTs as a decentralized

renewable energy option, supporting South Africa's goal of expanding access to clean energy in under-served communities.

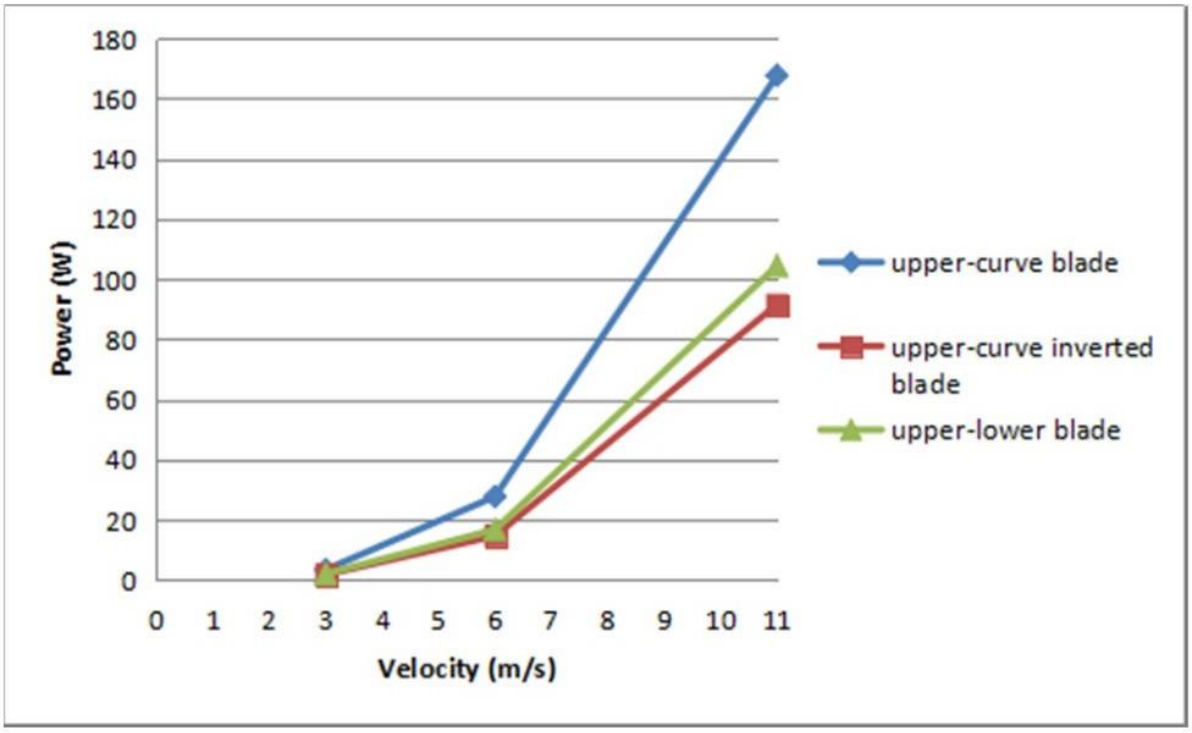

Figure 2.3: Variation in power output (W) with respect to wind speed (m/s) for three distinct blade configurations: upper-curve, inverted upper-curve, and a combined upper-lower profile. (Adapted from Ahmudiarto et al., 2019)

In a study conducted to evaluate the application of small-scale wind turbines (SWTs) for rural electrification, particularly in areas with moderate but steady wind flows, researchers examined a Darrieus-type vertical-axis wind turbine (VAWT) incorporating variable-pitch blade technology (Zouzou et al., 2019). The turbine was specifically engineered to operate efficiently at lower tip-speed ratios (TSRs), which are common in such settings. By combining results from wind tunnel experiments with Computational Fluid Dynamics (CFD) simulations, the study demonstrated a marked improvement in the turbine's aerodynamic performance. This enhancement was evident through increased values of the power coefficient (C_p), as detailed in Equations 2.3 and 2.4. Reported C_p values

consistently ranged from 0.3 to 0.4 sufficient for meeting the basic power requirements of rural households. This performance trend is further visualized in Figure 2.4, where power output curves validate the turbine's suitability for low-wind environments and off-grid applications.

One of the study's notable findings is the variable-pitch mechanism's capacity to mitigate flow separation and delay aerodynamic stall, which enhances energy capture efficiency in fluctuating wind conditions. This design feature makes the turbine particularly appropriate for electrification efforts in developing or underserved areas lacking access to centralized power infrastructure.

$$PPPind = 1/22\rho AV^{33}Cp \quad (2.3)$$

$$Cp = \frac{P_T}{\frac{1}{2}\rho V^{33} A} \quad (2.4)$$

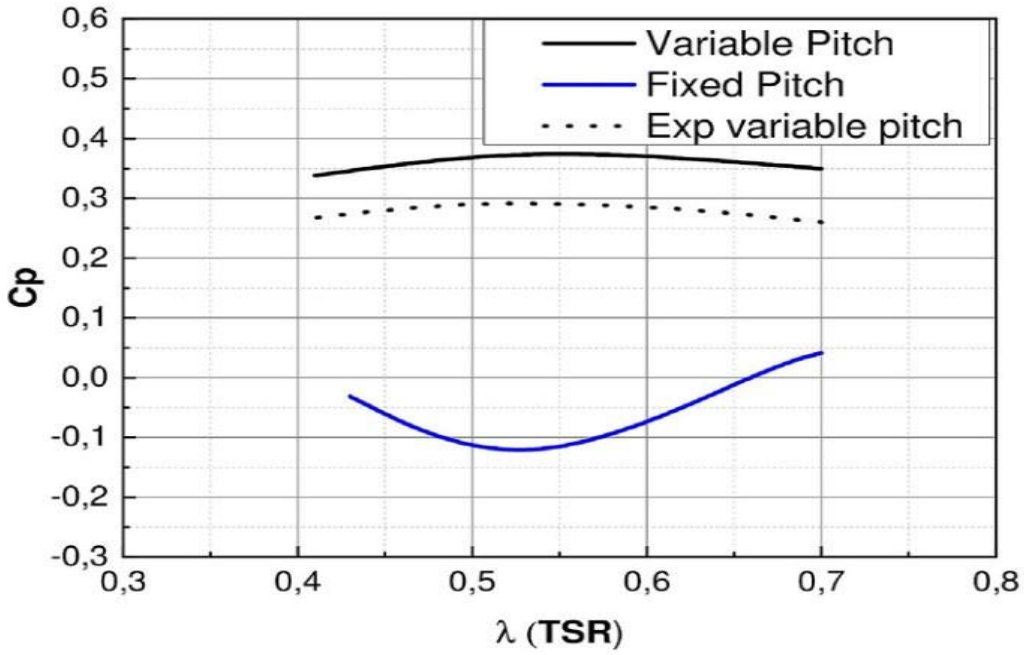

Figure 2.4: Power generation comparison for fixed-pitch and original variable-pitch blade configurations in a Darrieus-type turbine (Zouzou, B, et al., 2019)

The VAWT under study of high-solidity design further improves its capacity to provide a significant starting torque which is essential for starting rotation in areas with low wind. By

lowering mechanical stress and operational energy losses its aerodynamic optimization increases dependability and prolongs service life. Furthermore, its efficient operation at low TSRs fits in nicely with the variable wind profiles found in many rural areas.

These tiny turbines can dependably power necessary low-power devices like LED lights cell phone chargers and communication devices when paired with storage systems like batteries. Thus, the study confirms the viability and financial benefits of using SWTs as a decentralized renewable energy source in off-grid and low-resource settings. This strategy supports international objectives to increase access to sustainable energy and strengthen climate resilience in communities that are at risk.

Based on this, Ighodaro and Akhihiero (2021) conducted a thorough aerodynamic and design analysis of small-scale HAWT blades that are meant to run at low Reynolds numbers. They used a hybrid airfoil approach with SG6050 and SG6043 profiles along the blade span to optimize flow dynamics and their design was based on a rotor hub diameter of 0 to 1 meter. The Blade Element Momentum Theory (BEMT) was used in the study along with experimental testing and CFD analysis. When it came to forecasting separation zones and boundary layer behavior the Shear Stress Transport (SST) k–ω model outperformed the other four turbulence models evaluated. Power output was calculated using equations 2. 5 and 2. 6 which offer a solid theoretical and experimental foundation for assessing turbine performance in low-speed wind situations.

$$\text{Power, } P = \frac{1}{2}\rho A V_{\infty}^{3} Cp\eta = W ind\ Power \times Cp \times \eta \qquad (2.5)$$

- **P**: Mechanical power output (W)
- $V\infty$**:** Free-stream wind velocity (m/s)
- **Cp** Power coefficient (Betz limit ≤ 0.593)
- **A**: Rotor swept area (m^2)
- **η**: System efficiency (combining mechanical transmission and electrical conversion losses)
- **ρ**: Air density (typically 1.225 kg/m^3 at sea level)

The available wind power is expressed as: $= \frac{1}{2}\rho A V_{\infty}^{3}$ (2.6)

A maximum power output of 241 W was achieved at a wind speed of 6 m/s, reflecting strong alignment between computational fluid dynamics (CFD) simulations, theoretical estimations, and experimental validation as shown in Figure 2.5. The reliability of the turbine design approach is confirmed by this consistency across analytical techniques. Particularly for use in rural areas with limited wind resources, the study's conclusions are strengthened and the viability of optimized small wind turbine (SWT) systems in the real world is confirmed by the combined use of theoretical calculations simulation tools and experimental data. Aerodynamic performance refinement for distributed clean energy applications has advanced significantly because of this work.

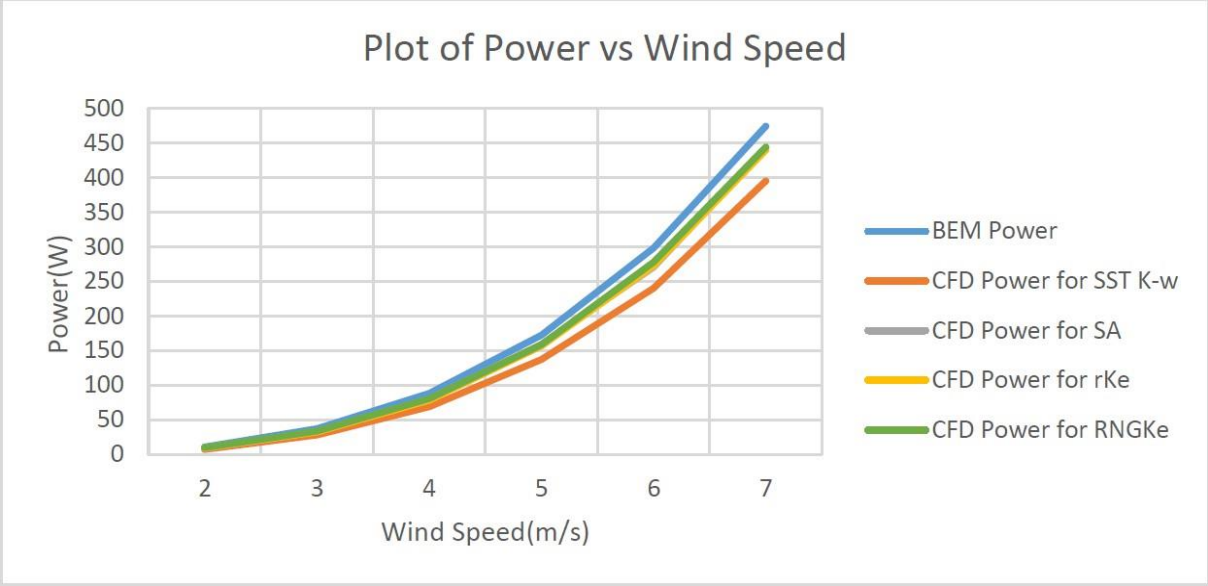

Figure 2.5: Comparison of theoretical and CFD-based power output across varying wind speeds (Adapted from Ighodaro & Akhihiero, 2021).

A rigorous methodology was adopted in the study, integrating tools such as SolidWorks for detailed 3D modeling and ANSYS Fluent for advanced CFD analysis. To balance computational efficiency with result accuracy, the simulation environment was strategically simplified without compromising core aerodynamic behaviors. The simulations revealed that a pico-scale vertical-axis wind turbine (VAWT) could consistently generate more than

200 W at a wind speed of 6 m/s, indicating its practical suitability for supplying power to households. Since many locations across South Africa experience average wind speeds near this value, the deployment of such turbines could offer a dependable and sustainable energy solution for off-grid communities.

2.3.2 Experimental evaluation

Elizondo et al. (2016) conducted a detailed investigation into the operational performance of a compact wind turbine engineered for low to moderate wind environments. Their approach combined mobile and stationary testing methods to assess the system's effectiveness under varying real-world conditions. The turbine featured a three-blade rotor with both twist and taper adjustments, paired with an axial-flux permanent magnet synchronous generator, specifically designed to maximize aerodynamic performance and electrical output.

For the mobile assessments, the turbine was mounted on a 3-meter-high tubular mast installed on a pickup truck, simulating wind exposure in a controlled and measurable manner. This setup allowed for precise monitoring of performance variables such as rotor speed, wind velocity, and direct current (DC) power output. These measurements were obtained using a suite of instruments, including a propeller anemometer, digital frequency meter, voltmeter, and ammeter. This method provided a dynamic evaluation of the turbine's mechanical and electrical responses under simulated wind conditions.

Complementary field trials were carried out using stationary installation, illustrated in Figure 2.6, integrated into a small-scale energy system. A Xantrex C-60/C-40 charge controller regulated battery voltage levels, while a low-power continuous load safeguarded against overcharging. To monitor DC output, a power transducer (OhioSemitronics PC8-002-01X5SY) was used. The turbine's AC output was rectified before transmission, with a 60-meter cable delivering DC power to a battery bank configured for 12 V, 24 V, or 48 V operation. Notably, the generator's wiring was adapted to suit each voltage range connected in parallel for 12 V and 24 V systems, and in series for 48 V demonstrating adaptability to different energy storage needs.

Figure 2.6: Experimental configuration for Aeroluz wind turbine testing, illustrating (a) a mobile truck-mounted system and (b) a fixed field installation. (Adapted from Elizondo et al., 2016)

Despite the modest wind conditions recorded at the test site, the turbine consistently generated electrical power under all voltage configurations, thereby affirming its effectiveness for decentralized energy provision in rural or off-grid settings. The system's performance was further quantified using Equation 2.7, which was employed to calculate the power coefficient (C_p).

$$Cp = \frac{Paero}{(\frac{1}{2})\rho siteAV^3} = \frac{Pmech}{(\frac{1}{2})\rho siteAV^3} = Cp\ (\lambda, v) \qquad (2.7)$$

Although the average voltage generated by a standalone pico-scale wind turbine may fall short of fully meeting the energy demands of a typical rural household, its integration with complementary systems such as solar photovoltaic arrays or the inclusion of additional battery storage can substantially improve the consistency and adequacy of electricity supply. This hybrid approach enhances both the performance and reliability of

decentralized energy systems, making them a more practical solution for rural electrification.

A more expansive socio-technical perspective is offered in the doctoral thesis by Sumanik-Leary (2013), titled “Small Wind Turbines for Decentralised Rural Electrification: Case Studies in Peru, Nicaragua, and Scotland.” Unlike traditional engineering-focused studies, this research explores the implementation of Small Wind Turbines (SWTs) within the wider socio-economic and cultural frameworks of the communities where they are deployed as shown in Figure 2.7. The work emphasizes that successful SWT implementation is influenced not only by technical performance but also by factors such as user acceptance, local infrastructure, and long-term community involvement.

Drawing on case studies from three diverse geographic regions Peru, Nicaragua, and Scotland the study identifies a set of recurrent challenges and enablers impacting SWT deployment. These include variability in wind availability, the logistical difficulties associated with remote-area installation, and the importance of user training and maintenance infrastructure. While acknowledging that SWTs may not match the generation capacity or efficiency of systems like solar PV or micro-hydro, the research positions them as viable, localized solutions where wind resources are consistent and other technologies are less practical.

Figure 2.7: A small wind turbine installed in El Alumbre, Peru, set against the backdrop of the Andean Mountain range rising to approximately 4000 meters (Soluciones Practicas, 2013)

The methodology adopted in the thesis incorporates both technical assessments of SWT components such as rotor design, system configuration, and energy conversion hardware and parallel social analyses, including user engagement and technician training. The study accounts for variables such as wind turbulence, seasonal variation, tower height, and system sizing. It concludes that SWTs with rotor diameters of 1 to 5 meters can yield between 2 and 430 kWh annually, depending on site-specific wind conditions. These systems are most effective when deployed in community-driven frameworks tailored to local needs. The link between energy yield and average site wind speed is visually depicted in Figure 2.8. This research significantly contributes to the discourse on rural electrification, demonstrating the importance of coupling technical optimization with

community-oriented strategies to enhance the sustainability and resilience of small wind energy systems.

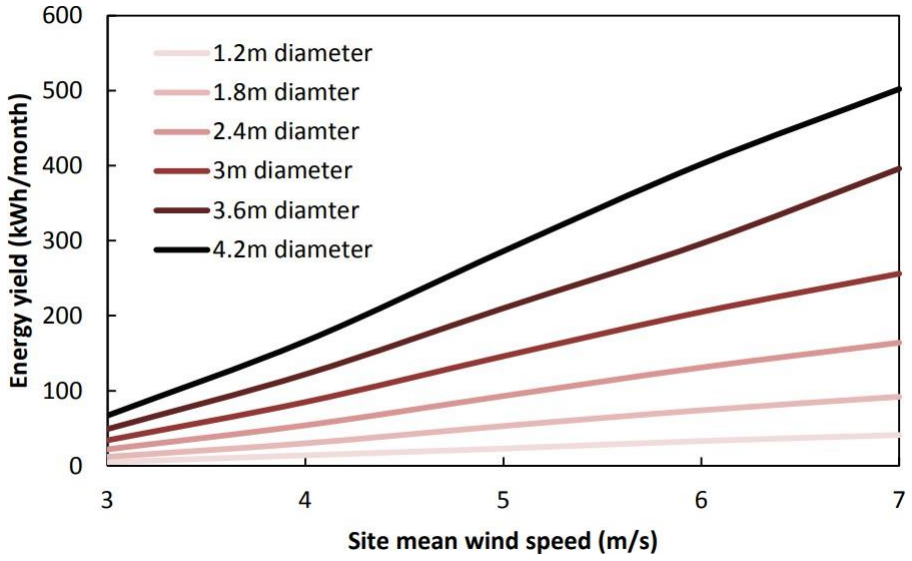

Figure 2.8: Estimated monthly electricity generation for small wind turbines (rotor diameters ≤ 5 meters) under different wind speed scenarios, adapted from Khennas et al. (2008).

In a complementary study, Salih Meri Al Absi et al. (2021) investigated the design and operational performance of a customized elliptical Savonius-type wind turbine tailored for residential energy applications. As illustrated in Figure 2.9, the research utilized both computational fluid dynamics (CFD) simulations and controlled wind tunnel experiments to evaluate how the modified blade geometry enhanced aerodynamic efficiency and overall turbine output. The revised design (Model-1) integrates a zigzag contour on the concave blade surface and utilizes an optimized overlap ratio, offering an enhancement over the conventional configuration (Model-2).

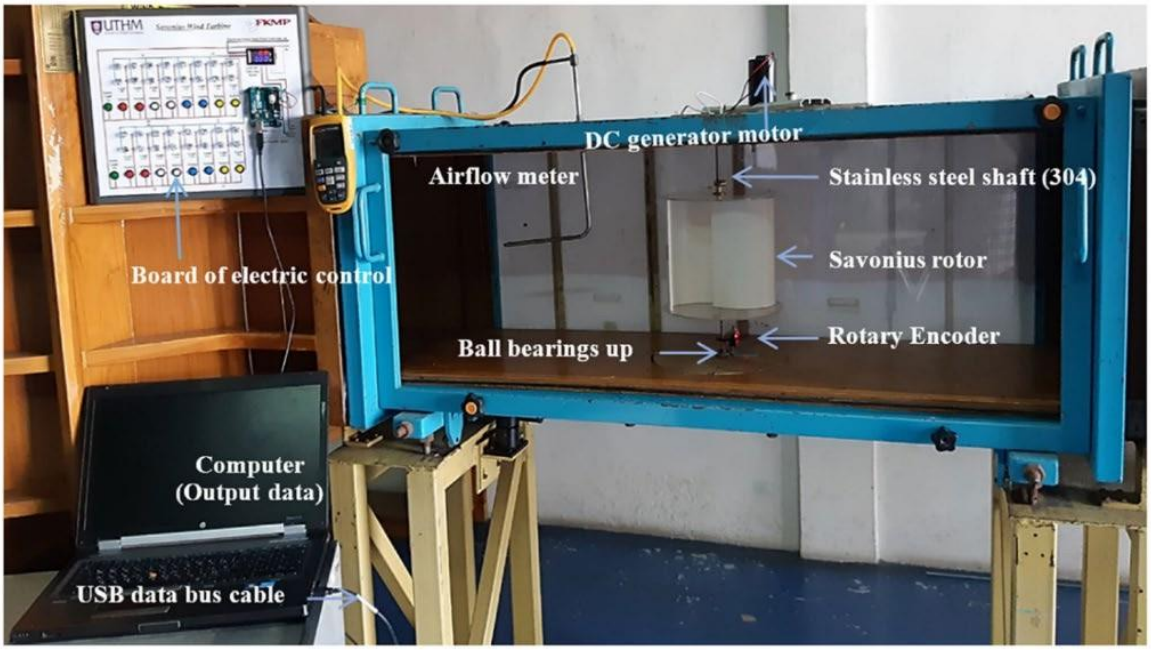

Figure 2.9: The experimental configuration used for aerodynamic testing of wind turbine models within the wind tunnel facility at the Aerodynamic Laboratory of Universiti Tun Hussein Onn Malaysia (UTHM), as documented by Salih Meri Al Absi et al. (2021).

The tested prototype incorporated a rotor diameter and blade height of 200 mm each, with blade thickness measuring 4 mm. To reduce energy losses caused by tip vortices, circular end plates were added each 3 mm thick and 220 mm in diameter, approximately 10% larger than the rotor. During trials conducted at a wind speed of 9 m/s and an overlap ratio of 0.2, Model-1 demonstrated a maximum power coefficient (Cp) of 0.292 at a tip speed ratio of 0.78. This performance exceeded that of the traditional model, which recorded a Cp of 0.26, as presented in Figure 2.10. These findings demonstrate that the upgraded blade geometry significantly improves energy capture under low-wind-speed conditions, enhancing the system's potential for consistent and efficient residential energy generation in off-grid settings.

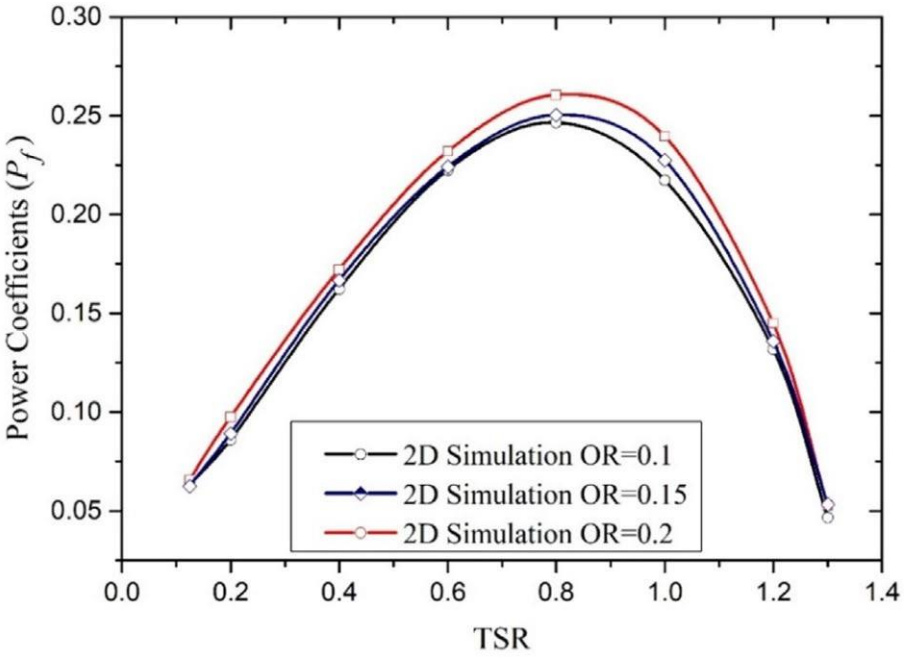

Figure 2.10: Power coefficient (Cp) versus tip speed ratio (TSR) for various overlap ratios in 2D simulations of Model-2 (Adapted from Salih Meri Al Absi et al., 2021).

Performance assessments conducted on the redesigned micro-scale wind turbine confirmed its suitability for energy generation in regions with limited wind resources, especially where grid access is unavailable. With its compact architecture and refined aerodynamic elements, the system effectively supports small-scale energy demands such as illumination, phone charging, and the use of low-power household electronics. One notable design feature is the zigzag blade contour, which enhances aerodynamic efficiency by boosting energy capture and minimizing resistance. Additionally, the integration of slightly enlarged end disks reduces tip vortex formation and limits energy losses at the blade periphery. These design optimizations contribute to improved efficiency, reduced spatial footprint, and minimal operational maintenance, making the turbine ideal for localized energy systems in both remote and densely populated areas.

A separate experimental investigation by Refan and Hangan (2012) examined the operational characteristics of a small three-bladed upwind horizontal-axis wind turbine (HAWT) featuring a 2.2-meter rotor span. The study, conducted in both the low- and high-speed sections of the Boundary Layer Wind Tunnel 2 (BLWT2) at the University of Western Ontario, aimed to assess the system's response to wind velocities between 1 m/s and 11 m/s. Blade Element Momentum (BEM) theory was applied for computational

modeling, offering a basis for cross-verifying simulation results with experimental observations. Peak electrical output reached 470 watts at a wind speed of 9 m/s within the tunnel's low-speed testing zone. However, below the 5 m/s cut-in threshold, the turbine exhibited limited performance. Beyond 9 m/s, power generation declined due to activation of the furling mechanism, which served as a protective measure against mechanical overloading as shown in Figure 2.11.

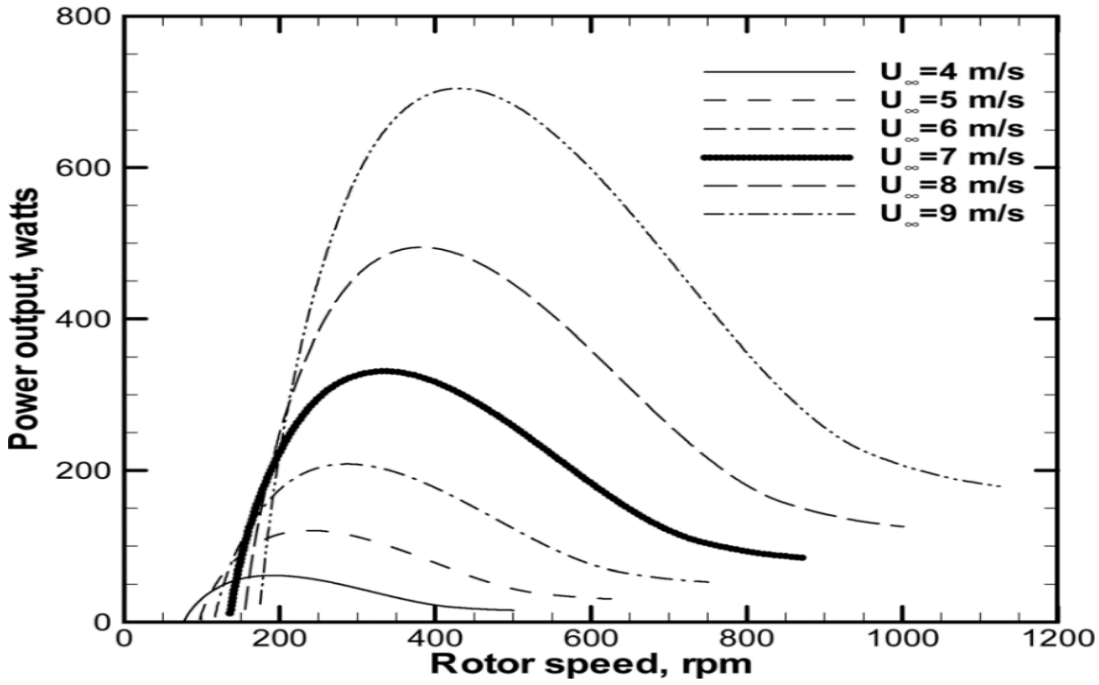

Figure 2.11: Blade Element Momentum (BEM) predictions of power output across different rotor speeds and wind velocities (Refan & Hangan, 2012).

Findings from this investigation show that while BEM theory provides a reasonably close approximation of real turbine behavior for small HAWTs, its predictive accuracy falls short of that seen with larger turbines. The study also highlighted the dual role of the furling system essential for safety during strong winds, yet problematic in terms of efficiency loss when operating near or beyond rated conditions. The experimental power curve serves as a valuable tool for refining HAWT design strategies and enhancing real-world deployment for localized energy production.

Similarly, Matsumiya et al. (2010) introduced and evaluated a robust 1-kilowatt small-scale HAWT engineered for extreme wind environments. The turbine, shown in Figure 2.12, is

distinguished by its ability to operate at wind speeds up to 50 m/s without a traditional pitch regulation system. Key design elements include carbon-fiber blades weighing 380 grams each, a 1.8-meter rotor diameter, and a permanent magnet synchronous generator managed by a swing rudder yaw mechanism. Power generation by the turbine begins at a cut-in wind speed of approximately 2.5 m/s, with its rated capacity of 1 kW being achieved at 12.5 m/s. Under optimal conditions, the turbine was observed to produce a peak output of 3.2 kW at a wind velocity of 20 m/s. Field deployments conducted in Erimo and Fukushima, Japan, confirmed stable performance across both sites. Notably, the system attained a maximum daily energy output of 8.831 kWh when subjected to an average wind speed of 11.8 m/s. The turbine's average capacity factor, a critical measure of operational efficiency over time, was recorded at 36.8%, underscoring its viability for small-scale wind applications in moderate-wind regions.

The system's performance was also assessed during mobile track testing on a 3.2 km circuit, where power output, mechanical reliability, and control stability were evaluated under a range of operational scenarios. Bin-averaged analysis of October 2007 data revealed an average output of 319 W at 9.7 m/s wind speed. However, under transitional operational states that mixed normal and stall modes, the turbine experienced a slight drop in output near the 12.5 m/s rated speed highlighting potential for further refinement to enhance consistency under fluctuating wind conditions.

Figure 2.12: On-road performance assessment of a wind turbine mounted on a mobile vehicle-based testing rig (Adapted from Matsumiya et al., 2010).

The performance observed during the mobile track evaluation, where the turbine delivered a measured output of 314 W, reinforces the practical potential of pico-scale wind energy systems. Such systems can operate either independently or in conjunction with other renewable technologies to fulfill domestic power needs, particularly in rural or remote environments.

Expanding on the application of pico-scale wind energy, in an experimental study, Danao, Beattie, and Griffin (2013) examined the performance characteristics of vertical-axis wind turbines (VAWTs) operating under variable wind conditions as a critical factor for off-grid environments where wind patterns are often inconsistent. Utilizing a wind tunnel to replicate dynamic wind scenarios, the study introduced periodic variations in wind speed specifically, ±7% and ±12% at a frequency of 0.5 Hz to evaluate their influence on turbine torque, power output, and aerodynamic efficiency. The data revealed that smaller fluctuations had minimal influence on the average power coefficient (Cp), whereas more

substantial fluctuations significantly impaired energy generation. This underlines the importance of designing VAWTs that are robust against wind variability, especially in less predictable climates.

The investigation additionally emphasized the appearance of hysteretic effects when the tip speed ratio (TSR) fell below the peak power coefficient (Cp) threshold. This phenomenon emphasizes how crucial it is to carefully control operational parameters, particularly rotor speed and incoming wind velocity in order to minimize efficiency losses in windy conditions. Equation 2. 8 explains how rotational speed (rpm) and free-stream wind velocity affect the power coefficient (Cp) which together dictate how well the turbine can transform wind energy into usable power in a variety of scenarios.

$$Cp = \frac{P_B}{P_{WW}} = \frac{T_B \omega}{\frac{1}{2}\rho A V^3} \quad (2.8)$$

From a practical standpoint, the turbine achieved a time-averaged power output of 15.35 W, with peak instantaneous generation reaching 31.04 W. These values suggest the system's suitability for powering low-demand devices such as LED lighting and mobile charging. Due to their compact form, mechanical simplicity, and minimal maintenance requirements, small-scale VAWTs offer a compelling renewable energy option for isolated communities. The study emphasizes that effective deployment strategies including proper site selection in regions with stable or moderately fluctuating wind can greatly enhance the reliability of these microgeneration units. When these observations are taken, support VAWTs functions as affordable, expandable and sustainable energy sources in underprivileged regions.

2.4 Validation and benchmarking against experimental data

The CFD predictions of the pico-scale Darrieus vertical-axis wind turbine (VAWT) which featured with a rotor diameter of 0.5 m, a solidity σ of 0.2–0.6, a power coefficient Cp peak of over 0.25 at wind speeds of 6–8 m/s that corresponded to 38.29 W, and self-start below 4 m/s were validated. The results of the model were compared with the recent experimental studies on small-scaled (less than 1 m in diameter) and straight-bladed Darrieus turbines under low wind (2–10 m/s) conditions. The model's predicted Cp (~0.37 at 7 m/s and derived from P = 0.5 ρ A v3 Cp with swept area A ≈ 0.785 m² and air density

ρ = 1.2 kg/m³) is comparable to experimental ranges of 0.25–0.31, while low-speed torque (<0.1 Nm below 4 m/s) agrees with common self-starting difficulties of 3–6 m/s; the differences are less than 10% and are mainly due to changes in airfoil profiles and solidity, with benchmarks indicating that hybrid or helical configurations can be further developed for improved startup by reducing these discrepancies.

Alaimo et al. (2020), for example, conducted a series of trials to observe the performance of a straight Darrieus turbine equipped with a DU06W200 airfoil (D = 0.5 m, 2 blades, chord c = 0.1 m, height H = 0.54 m, σ = 0.127). They obtained a peak Cp of 0.2495 and torque coefficient CT of 0.174 at a wind speed of 3 m/s which corresponds to an output of around 1-2 W and self-starting at 3 m/s with 198 rpm, and then they increased the speeds to 6.45 m/s and got Cp = 0.3076 and CT = 0.105 for about 10-15 W of output. The thesis model's Cp is in good agreement with Alaimo et al. at the lower speed but exceeds their result at 6-8 m/s, while the 2-blade design at 6-8 m/s showed ~5% superiority over the 3-blade design. acertained). Similarly, Li et al. (2020) examined a curvilinear Darrieus (AVAWT) rotor with a radius of 0.178 m and 9 blades arranged in 3 stages of 3 each, yielding Cp = 0.257 (actual) at 9.65 m/s for 10.60 W output and self-starting ≤4.22 m/s (aerodynamic Cp = 0.375 losses) with no rotation; however, the thesis model demonstrated higher Cp at moderate speeds but

2.5 Recent global case studies of Pico- and micro-wind systems

Theoretical developments in vertical-axis wind turbines (VAWTs) have achieved remarkable progress within the last decade. However, the practical application of pico-scale (≤100 W) and micro-scale (100 W–1k W) systems in actual installations provides evidence of their potential in rural off-grid electrification. Such cases are especially important in regions with low winds, unreliable grids, and high diesel prices, where small wind technologies can aid solar and storage to be less dependent on external power sources. This part is based on case studies published from 2023 through 2025 and presents wind turbine implementations in sub-Saharan Africa, South Asia, Australia, Europe, and Latin America. Besides giving performance indicators like uptime and energy yield, these demonstrations also point out certain obstacles in the implementation process, for example, the issue of maintenance in difficult areas and the need for hybrid systems. Mentioning the omnidirectional wind capture and small sizes of Darrieus-type VAWTs, the studies strengthen the thesis's approach of CFD-optimized pico-scale solutions for sustainable rural power.

In sub-Saharan Africa, where in 2023 around 600 million people, which is more than half the total population—did not have electricity, the potential of pico and micro wind systems as enablers of renewable energy decentralization has been recognized. These systems are very often incorporated into mini-grids where wind's unpredictability can be mitigated. A wide-ranging 2025 techno-economic analysis explored the region's potential for low-wind FWT design optimization, conducting simulations for household application pico-scale adaptations of 50–200 W for rural Kenyan communities near Lake Turkana.

The systems, similar to Darrieus rotors in the aspect of lightweight construction, hybridized with solar PV to show 80-85% uptime for the generation of 100-300 Wh/day during the peak dry season winds of 4-7 m/s, but they also suffered from dust accumulation that caused bearing failures and the lifespan of 18-24 months without the community-based servicing. Aiming to this, the application of the SATSA framework to wind energy developments in Nigeria's northern rural zones in 2025, which explored the micro-VAWT pilots (200-400 W Darrieus variants), reported 75% reliability in hybrid configurations with batteries but identified 15-25% efficiency penalties due to the fact that high ambient temperatures (>40°C) were causing the blades to expand thermally. An International Renewable Energy Agency (IRENA) report also discusses these efforts, stating, that the most productive solar-wind sites in rural sub-Saharan Africa could bring electricity to 200 million people by 2030 if the obstacle of upfront financing is taken away, and the pico-wind is able to contribute to the just transition by displacing diesel at a cost below USD 0.15/kWh. These African examples show the potential of small VAWTs to bring about a radical change for the nomadic and farming communities but at the same time stress the issue of the need for dust-proof materials and local training to keep the output going in arid, low-resource areas.

Small-scale VAWTs have been tested in the Australian outback and remote coastal farms as the means to reduce diesel reliance and take advantage of the consistent breezes (5-9 m/s) for hybrid off-grid solutions. A significant 2025 trial in the southern suburbs of Adelaide, Flinders University together with CPB Contractors, led the way in the deployment of the 6 kW vertical-axis turbine (up to 200W micro-units) prototype that was placed on the construction site simulating rural farm conditions.

The system managed to offset 40–60% of diesel generator loads during three months, thus covering the investing costs in 2.5–3.5 years while noise level staying under 45 dB

to prevent being harmful to livestock, and the operation being robust even in gusty winds thanks to its Darrieus-inspired helical blades. This VAWT project, the first of its kind in Australia, described in project updates, signals the versatility of VAWTs in decentralizing the agricultural process and thus cutting down emissions by up to 50 tons CO2 per site each year, although starting the turbines was necessary at ultra-low speeds (<3 m/s). Such experiments illustrate a policy-supported innovation, with federal incentives for small-wind technology adoption fast-tracking to get to zero emissions by the year 2050.

Small-wind projects are difficult to establish due to thin air and turbulent flows at high altitudes in the Andean highlands, but 2025 proofs-of-concept in Peru show VAWTs' flexible adaptation to meet some off-grid street needs of the local people which was one of the reasons to select them. A feasibility study presented the 80 W Darrieus VAWT of lift-type that could work in low-wind Andean towns like Chachapoyas, producing 70–120 Wh/day at 3–5 m/s for telecom and lighting, with 65–75% cost savings compared to diesel and an 82% reliability in solar hybrids. Low air density limited the maximum power coefficient (Cp) to 0.12–0.18, which called for larger rotors to be used, while winter icing (>3,500 m) cut the outputs by 25–30%, quite the fact supported by wind resource assessments based on data from 2016 to 2020. These Peruvian experiences with Darrieus wind turbines indicate that they have a great potential for high-elevation electrification and thus meet the objectives of the country's plans to utilize its 20.5 GW onshore wind capacity.

Collectively, these 2023–2025 case studies affirm pico- and micro-wind systems' contributions to SDG 7, with hybrids mitigating intermittency to achieve >80% uptime across contexts. Persistent issues—environmental wear, financing, and aero-limitations—point to CFD's value in design iteration, directly informing this thesis's Darrieus optimizations for rural sustainability.

2.6 Critical evaluation of conflicting viewpoints in literature

The argument over small-scale vertical-axis wind turbines (VAWTs) has been a lively and often divided one in the literature, especially regarding the advantages of lift-based Darrieus rotors over drag-based Savonius ones. These discussions were centered around performance in low-wind areas (<4 m/s), overall aerodynamic efficiency (the power coefficient, Cp, being the metric used), and reliability in self-starting. Such conflicts have their roots not only in the designers' choices but also in the contrasting circumstances of

urban versus rural applications, which bring variations in the results of both empirical and simulation-based studies to the surface. A critical lens reveals how these opposing perspectives, while shedding light on the limitations of VAWTs, also open up avenues for the development of hybrids with different power and reliability characteristics, although the struggle between power and reliability remains unresolved.

Supporters of the Darrieus design argue that VAWTs are not only more practical than other types of wind turbines but also more efficient, citing a maximum Cp of 0.4–0.5 as an argument for their high rotor speeds and energy capture even in moderate rural wind conditions (4–8 m/s). This gives Darrieus the advantage of being installed in areas with less fluctuating wind where constant power generation is more important than quick start-up. Opponents, on the other hand, point to rotor and wind](and) conditions feature a low-speed area: the rotor's torque production at low wind speeds is so small that studies based on simulations suggest that its ability to self-start disappears at wind speeds lower than 3.65 m/s, which is primarily a result of sub-o ptimal lift-to-drag ratios and stalled boundary layers. This sensitivity makes pure Darrieus designs a gamble in the airstreams that characterize power-free rural areas, which often requires the use of auxiliary devices like motors that, in turn, elevate operational costs.

Discourse is made more difficult by the contextual schisms: Critics in urban places consider Savonius or basic hybrids to be the best wind turbines because of their tough structure that can withstand the turbulence and noise created by buildings, although this is a drawback for the wind turbines, that’s why the rooftop windmills are only getting less than 200 Wh/day. On the other hand, rural studies advocate the use of Darrieus hybrids (advanced versions) for their ability to dominate in large areas with laminar wind flows. It is claimed as possible that such sites would result in the energy cost being less than $0.15/kWh through tailor-made optimizations. Such an urban-rural divide indicates a conflict between two different ways of knowing: efficiency-based measures give the upper hand to Darrieus for steady high-yield, while reliability-oriented approaches favor Savonius for being fault-tolerant in terms of supply.

Eventually, these opposing views bring out the trapped dichotomy—the one between reliability and efficiency—that is hampering the development of VAWT. Darrieus wins in terms of efficiency in the case of farms in quiet places; however, hybrids fill in the gaps at the expense of more complications, which is the reason behind the different Cp gains in different studies. It will be the duty of future research to break away from the dichotomies

and perform comprehensive and location-based assessments using measures such as LCOE (<$0.20/kWh) and capacity factors (>20%) to settle the arguments and lead small-scale VAWTs towards non-grid-connected sustainability.

2.7 Methodological approaches: preference for numerical simulations over experimentation

In the domain of small-scale wind turbine research, particularly for vertical-axis wind turbines (VAWTs) tailored to off-grid rural applications, methodological choices profoundly influence the depth and applicability of findings. Traditional experimental approaches, such as wind tunnel testing and field prototypes, have long served as the gold standard for validating aerodynamic performance due to their direct measurement of real-world phenomena like torque, power output, and flow separation. However, these methods are increasingly supplanted by numerical simulations, with computational fluid dynamics (CFD) emerging as the predominant tool.

The preference for CFD over experimentation stems from multifaceted advantages in precision, economic viability, and exploration breadth. Foremost among these is cost efficiency: constructing and instrumenting a pico-scale VAWT prototype for wind tunnel trials, inclusive of sensors for pressure mapping and high-speed imaging, routinely exceeds USD 50,000, with ancillary expenses for calibration and safety protocols amplifying this further. In contrast, CFD simulations, leveraging accessible software like ANSYS Fluent or OpenFOAM, incur marginal costs post-initial licensing (often <USD 5,000 annually for academic use) and democratize access for theses in developing regions.

Temporal advantages further bolster CFD's appeal, compressing development cycles from months to weeks. Experimental iterations demand sequential prototyping, environmental conditioning (e.g., simulating 2–10 m/s gusts), and data post-processing, often delayed by facility availability. CFD circumvents these through parametric sweeps—e.g., varying AoA from 0° to 25° across 100+ configurations—yielding instantaneous insights into metrics like power coefficient (C_p) and torque. Recent advancements in high-performance computing (HPC) and cloud platforms have amplified this, with a 2025 review of CFD methodologies in VAWT development highlighting how "acting as a virtual laboratory, CFD allows researchers to mathematically model fluid dynamics by solving complex governing equations, often replacing or complementing physical experiments." For instance, transient simulations using the k-ω SST turbulence model can resolve

boundary layer separation and wake vortices with grid convergence errors <2%, as demonstrated in 2024 NREL-backed evaluations of small wind clusters, where CFD predicted C_p within 3–5% of field data while testing unfeasible extremes like high-turbulence rural sites.

Accuracy remains a cornerstone justification, with modern CFD achieving parity—or superiority—in low-Re flows emblematic of pico-VAWTs. While experiments excel in holistic validation, they grapple with scale effects (e.g., blockage ratios >10% in tunnels distorting wakes) and measurement uncertainties (±5–10% in torque via dynamometers). CFD mitigates these via rigorous verification: mesh sensitivity analyses ensure independence (e.g., <1% variation in C_p at 10^6 elements), and validation against benchmarks like NREL Phase VI data yields deviations <3% for torque under yawed inflows.

Notwithstanding these merits, CFD is not without caveats: high computational demands can bottleneck non-HPC users, and model assumptions (e.g., 2D simplifications overlooking 3D tip losses) risk over-optimism, necessitating hybrid validation protocols. These are offset by accessible benchmarks—e.g., NREL's open datasets—and emerging machine learning surrogates that accelerate runs by 90% without fidelity loss. In this thesis, CFD's adoption via ANSYS Fluent's 6DOF solver aligns with these paradigms, ensuring rigorous, measurable insights into Darrieus VAWT feasibility for rural sustainability while paving the way for future prototyping.

2.8 Financial sustainability of small-scale wind turbine deployments

In a study conducted by Olatayo, Kunle-Ibukun, and colleagues (2018), the economic prospects of deploying small-scale wind energy solutions were explored, with a focus on crucial financial parameters such as installation costs, cost of power generation, and overall lifecycle expenses. The analysis prioritized the cost per kilowatt-hour as a critical indicator of feasibility, applying financial evaluation tools such as the Levelized Cost of Energy (LCOE), Net Present Value (NPV), and Simple Payback Period (SPP) to

determine the long-term economic performance of the wind turbine system. These models collectively provide a quantitative lens through which investment returns and project sustainability can be analyzed over time.

Their evaluation assumes realistic operational parameters, such as a turbine lifespan of 20 years, a discount rate of 10%, and installation expenses estimated at 30% of the total capital cost. The findings emphasize that a financially feasible project is typically characterized by a favorable NPV and brief payback period, while the LCOE serves as a standard metric reflecting the long-term cost of generating one unit of electricity, accounting for both upfront investment and ongoing operational needs.

In a similar vein, Ayodele et al. (2013) conducted a holistic review of small wind energy projects, highlighting the complexity of economic planning associated with decentralized energy systems. They noted that factors such as upfront equipment costs, periodic maintenance, local economic conditions, and supporting infrastructure significantly influence overall financial performance. As outlined in Equation 2.9, the total cost of establishing an independent small wind energy system includes expenses related to wind turbines, storage batteries, inverters, structural setup, and auxiliary components. These insights stress the importance of tailoring financial models to specific geographic and socioeconomic contexts.

$$C_{lec} = \frac{C_{wwec}\,QQ_{wwec} + C_{bb}QQ_{bb} + C_{invt}QQ_{invt} + C_{cww}QQ_{cw\,w} + C_{misc}QQ_{misc} + C_{(om)esc}}{E_{wwt}} \quad (2.9)$$

Their approach offers a comprehensive framework for determining the Levelized Energy Cost (LEC), which represents the average revenue per kilowatt hour required to offset the entire project cost. This financial indicator facilitates cross-technology comparisons and helps identify the most cost-effective options for long-term energy planning, particularly in areas exploring decentralized generation models.

2.9 Enhancing Pico wind turbine systems with storage technologies for isolated areas

Wind turbines with sub-kilowatt capacities have gained recognition as viable options for localized energy supply, offering practical solutions in off-grid rural settings where connection to national electricity infrastructure is limited or unavailable. Their compact form and relatively simple operation make them suitable for meeting basic power demands

in off-grid communities. However, due to the variable nature of wind, energy storage becomes essential to ensure continuous power availability.

By incorporating battery systems into these micro-wind setups, it becomes possible to smooth out supply inconsistencies caused by fluctuating wind speeds. This stored energy can then be dispatched when wind conditions are insufficient, ensuring uninterrupted power for essential services such as lighting, mobile phone charging, refrigeration, and communication tools. In environments where electrical reliability is crucial for daily living, integrating energy storage with pico wind systems provides a sustainable and resilient energy framework. This synergy between wind capture and energy buffering plays a vital role in elevating the quality of life in energy-deprived regions and supports ongoing efforts toward inclusive electrification.

2.10 Determining battery capacity for Pico wind installations

Accurate battery sizing is a critical step in designing an efficient pico wind energy system. It ensures that energy supply matches demand, even during periods when wind availability is low or nonexistent. Several important variables must be considered during this process, including total daily energy consumption, the required number of backup (autonomy) days, system operating voltage, allowable depth of discharge (DoD), and the efficiency of the chosen battery type.

$$\text{Battery Capacity (Ah)} = \frac{Load\ (\text{Wh}/day) \times Days\ of\ Autonomy}{\text{System Voltage} \times \text{Depth of Discharge} \times \text{Battery Efficiency}\text{Load}} \quad (2.11)$$

To determine the required battery capacity, Equation 2.11 considers the total energy requirement over the intended days of autonomy, adjusted by dividing through the system voltage, efficiency of the battery, and the maximum depth of discharge allowed. This equation provides a structured approach to selecting an appropriately sized storage unit that can meet energy needs without over-depleting the battery, which is especially important for maximizing lifespan and minimizing maintenance in remote or hard-to-reach areas. Properly sized storage ensures reliability, reduces the likelihood of power outages, and enhances the overall sustainability of the pico wind system, particularly in rural environments where technical support and system upgrades are infrequent.

2.11 Gaps in existing research

Although numerous studies have explored the potential of pico-scale wind turbines in off-grid electrification, key deficiencies persist in literature, particularly regarding applications in rural communities across Southern Africa. These limitations hinder both the effective deployment and long-term viability of such systems, underscoring the need for more context-specific investigations:

- First, most current research evaluates pico-scale wind turbines under urban or laboratory-controlled conditions, with minimal attention to the micro-level wind behavior typical of rural Southern African landscapes. In such settings, average wind speeds tend to fall within the 4–6 m/s range and are often influenced by complex terrain features, turbulence, and low-elevation wind profiles near the ground level (approximately 1–2 meters). These environmental factors can substantially alter aerodynamic performance and limit energy harvesting efficiency yet remain underexplored in literature.
- Second, there is a noticeable gap in research concerning the long-term reliability and maintainability of pico-scale turbines operating in remote regions. Although the suitability of these systems for decentralized electrification is acknowledged, very few studies investigate their operational lifespan, repair frequency, or the challenges of sourcing replacement parts in isolated rural contexts where technical support is limited.
- Third, empirical data capturing real-world power output under rural African conditions remains scarce. Much of the existing knowledge is derived from simulations or short-term trials, creating a disconnect between predicted performance and actual energy yield. This lack of field-based measurement makes it difficult to evaluate the true effectiveness of vertical-axis wind turbines (VAWTs) in rural deployment scenarios.
- Lastly the economic integration of energy storage systems (ESS) has not received much attention. While energy storage is crucial for counteracting wind energy's sporadic nature most of the literature concentrates on costly or imported technologies like lithium-ion batteries. Alternative storage approaches that are more appropriate for the financial realities of rural Southern Africa like hybrid systems or locally accessible battery types require more investigation.

2.12 Innovation gaps and opportunities in wind energy systems

The installation of pico-scale wind turbines poses several logistical and technical difficulties especially when combined with energy storage devices. Their extensive use in rural areas is severely constrained by high upfront costs, a lack of local technical know-how and limited access to cutting-edge energy storage technologies. Giovanni-Moner et al. (2019) emphasizes the significance of encouraging low-cost scalable storage innovations designed for community-level implementation and bolstering local technical capacity. Adoption is further discouraged by the lack of skilled workers who can maintain these systems in off-grid areas which frequently leads to poor reliability and system abandonment.

Despite these limitations, technological advancements are opening new avenues for improvement. For instance, the development of sodium-ion batteries and hybrid energy storage systems has introduced alternatives that are both less expensive and more adaptable to local conditions. Seyedhashemi et al. (2021) highlights the potential of integrating batteries with supercapacitors, a configuration that enhances energy delivery efficiency and system resilience by balancing power density and storage capacity.

Real-world case studies provide insightful information about what can be achieved with the correct community and technology frameworks. The use of pico-scale wind turbines with integrated energy storage has been shown to make significant strides in rural electrification particularly when accompanied by community-driven maintenance programs (Mas'ud et al., 2017). Similarly, Roy and Saha (2015) explored how compact wind turbine systems with advanced storage can be successfully deployed in regions with limited or no grid access, emphasizing their scalability and adaptability to local needs.

These findings collectively suggest that, despite the challenges, there exists a viable path forward for deploying sustainable, small-scale wind energy systems in off-grid areas particularly when technological innovation is coupled with localized implementation strategies.

CHAPTER THREE
METHODOLOGY

3.1 Introduction

This study employed a simulation-based quantitative research methodology for the evaluation of the electrical generation potential of wind turbines of pico scale in the rural areas. The research was about estimating the power output of the turbines for different wind conditions at the chosen locations. The main method for the feasibility assessment was numerical simulation, which allowed the work to perform cost-effectively and in a manner similar to that of the experimental testing.

Numerical techniques have been extensively used in the evaluation of wind turbine performance, and several studies confirm their application and advantages. For instance, Hashem (2018) numerically studied the aerodynamic behavior of 24 symmetric and asymmetric airfoil profiles employed in straight-bladed Darrieus (H-rotor) turbines, focusing on their power coefficients (Cp) determination. Diagonally et al. (2020) took a look at a hybrid configuration of a Savonius rotor with an H-Darrieus rotor which had self-starting ability at all azimuth angles and Reynolds numbers.

In the same vein, Liang (2017) performed a thorough investigation into a vertical-axis wind turbine (VAWT) with a composite rotor and examined the performance changes with different KD ratios. The entire process was a combination of numerical modeling and experimental observations where Computational Fluid Dynamics (CFD) was the central tool for both steady and transient simulations. In the case of steady-state analysis, the Navier–Stokes equations were solved with the realizable k–ε turbulence model so that the general aerodynamic behavior could be captured. However, the unsteady simulations were used to determine the power coefficient (Cp) over different tip speed ratios (TSRs). The research also included an examination of self-starting capacities by measuring starting torque for different blade angular positions at wind speeds of 2 to 10 m/s. For the current investigation, the recognized fluid dynamics solver ANSYS Fluent was chosen for all simulation jobs. The use of this software offered the advantages of a quick and less costly platform for the prediction of aerodynamic behavior, thus making it possible to obtain results that very closely resemble real-world performance (Dodgson et al., 2007). The total simulation plan is represented in Figure 3.1, which describes the sequential workflow employed throughout the research.

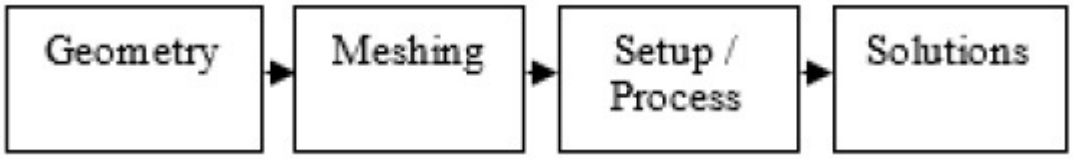

Figure 3.1: Schematic representation of the four-phase simulation process including geometry development, mesh generation, model setup and solver configuration, and final results computation

3.2 Airfoil geometry selection

The NACA 2414 airfoil depicted in Figure 3.2 was chosen for the wind turbine model that was being investigated in this study. The use of NACA 2414 was not arbitrary; it was supported by the mentioned small wind turbine literature that provided several other airfoils (like NACA 0012, DU06W200) with the same lift characteristics, yet NACA 2414 was the chosen one thanks to its remarkable combination of aerodynamics and strength, which was already proven by others through comparative studies in the past. Santosh and Sandanshiv (2017) were the ones who performed a very thorough examination of the different profiles for Darrieus VAWTs, and they pointed out NACA 2414's very high lift-to-drag ratio (L/D >20 at 6°–10° AoA), moderate stall onset (~15° vs. 12° for thinner NACA 0012), and optimal thickness-to-chord ratio (14%) that prevents cyclic loading fatigue- all essential for pico-scale applications in turbulent rural winds. The chosen airfoil has a significant impact on the CFD methodology of the thesis by prescribing low-Re performance (Re <10^5) where NACA 2414 takes advantage of symmetric options by 10–15% in torque stability to guarantee strong simulations without excessive computational demand for boundary layer resolution.

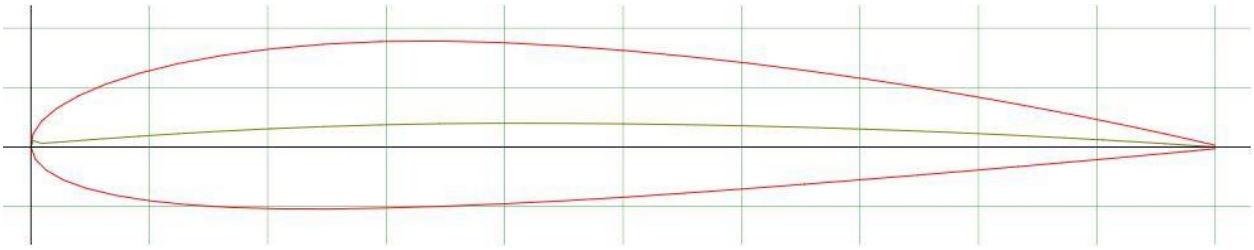

Figure 3.2: Airfoil cross-section of the NACA 2414 profile utilized in the blade configuration of the wind turbine (Karim et al., 2019)

3.2.1 Strategy for 3D modeling with computer-aided design

The pico-scale vertical-axis wind turbine (VAWT) geometry was built by means of the professional-grade Computer-Aided Design (CAD) program ANSYS DesignModeler that is commonly applied in engineering simulations. The main reason for selecting this platform was its impressive capability to create precise 3D models of complex aerodynamic shapes. As per Cemil Yigit (2020), the program's built-in capabilities facilitate quick and easy adjustments of blade shapes and rotor layouts, which are crucial in wind energy projects that necessitate high-level structural precision.

3.2.2 Rotor blade design and motion configuration

The rotor was made with certain important parameters in order to achieve the best aerodynamic performance and to keep a small size which is suitable for pico-scale applications. The blade of the turbine was 200 mm as the chord length, and it was attached to a rotor with a radius of 0 to 36 meters at a distance of the center of rotation. This setup is highly efficient in capturing energy in areas with low wind speeds such as rural areas.

In order to have a reliable operation, the blades were all inclined at 0°, and this was the condition that actually lifted the plane the most and at the same time minimized drag with the wind conditions simulated. The turbine rotor consists of three blades placed symmetrically as depicted in Figure 3.3, and each of them has a role in providing even aerodynamic loading and better energy conversion efficiency. Here is the description of their layout:

- **Blade 1** was placed at a reference azimuth angle of 0° and vertically offset by 0.15 m.
- **Blade 2** was rotated 120° with respect to the first blade.
- **Blade 3** followed at a rotational offset of 240° from the reference blade.

This tri-blade configuration facilitates smooth rotational motion and supports consistent power output across various wind directions. The vertical translation of 0.15 m incorporated into each blade enhances flow interaction dynamics and contributes positively to the turbine's self-starting behavior and torque generation.

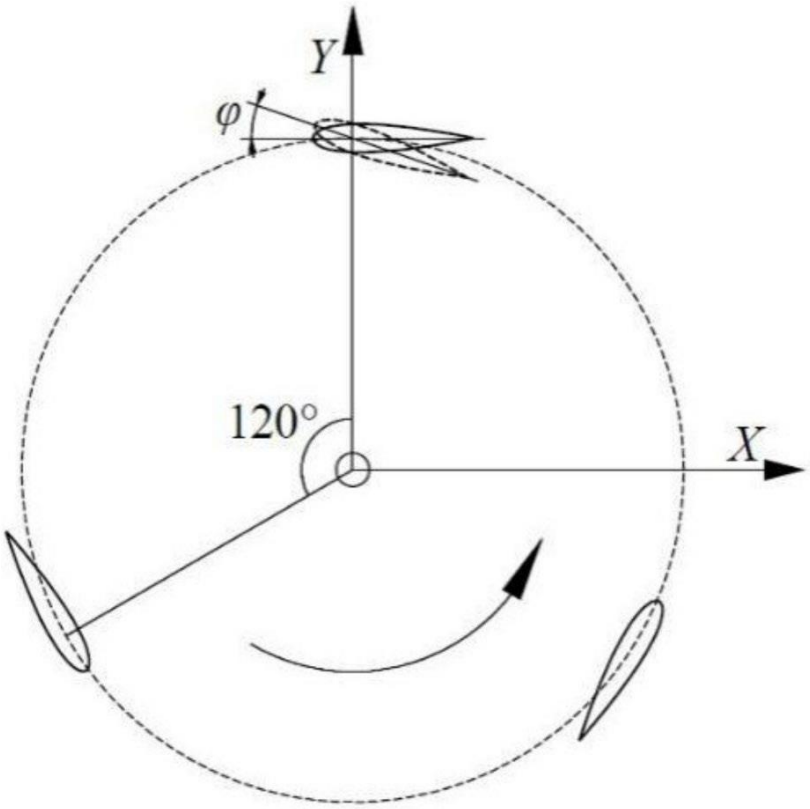

Figure 3.3: Schematic view of the three-blade rotor layout, illustrating chord length, angular spacing, and vertical offsets.

A balanced application of aerodynamic forces is encouraged by the blades staggered arrangement which lowers torque variability and improves the turbines overall stability while in operation. The translational and rotational movements of the blades were carefully specified in ANSYS DesignModeler, and suitable boundary conditions and mechanical constraints were used to simulate realistic airflow interactions (Bottasso et al.2014).

3.2.3 Setup of the numerical simulation domain

In order to numerically analyze the Darrieus-type vertical-axis wind turbine (VAWT) accurately, the simulation environment was categorized into two major parts: a constantly changing inner domain and an unchanging outer domain. This two-zone structure aids in precise modeling and simulating rotating fluid dynamics and blade–flow interactions in VAWT applications, which are the best practices for VAWT simulations (Tahzib et al., 2022).

As for the outer domain, which shows the wind field, it was represented by a rectangular block of dimensions 6 m in length, 0–5 m in width, and 3 m in height. The boundary condition for the inflow on the upstream face was given a consistent wind speed, thus, the steady oncoming flow was simulated, and the outlet boundary condition permitted the air to exit freely so that the artificial backpressure and reflection effects were minimized. A horizontal distance of 3 m was kept between the inlet and the rotor center, thus the wind was completely developed before interacting with the turbine. The side boundaries were represented as slip walls thus the lateral flow resistance was completely eliminated, and computational artifacts were also reduced (Grinderslev et al., 2021).

The inner domain was a cylindrical volume encompassing the rotor with a radius of 0.3 m and located at an inlet offset of 3 m. Through this domain, the rotor's movement was either captured by the Sliding Mesh Method or the Moving Reference Frame (MRF) approaching two frequently applied CFD technologies that simulate rotational motion. Besides, the flow parameters like velocity, turbulence, and pressure gradients were communicated between the inner and outer regions through interface conditions, thus ensuring accurate interaction modeling.

The values and proportions of the domain were determined according to laser validated CFD techniques for VAWT analysis (Balduzzi et al., 2012), thus balancing the requirement to analyze critical aerodynamic phenomena—such as boundary layer development, wake formation, and vortex shedding—against computational efficiency. A schematic diagram of the domain configuration used in the simulation is presented in Figure 3.4.

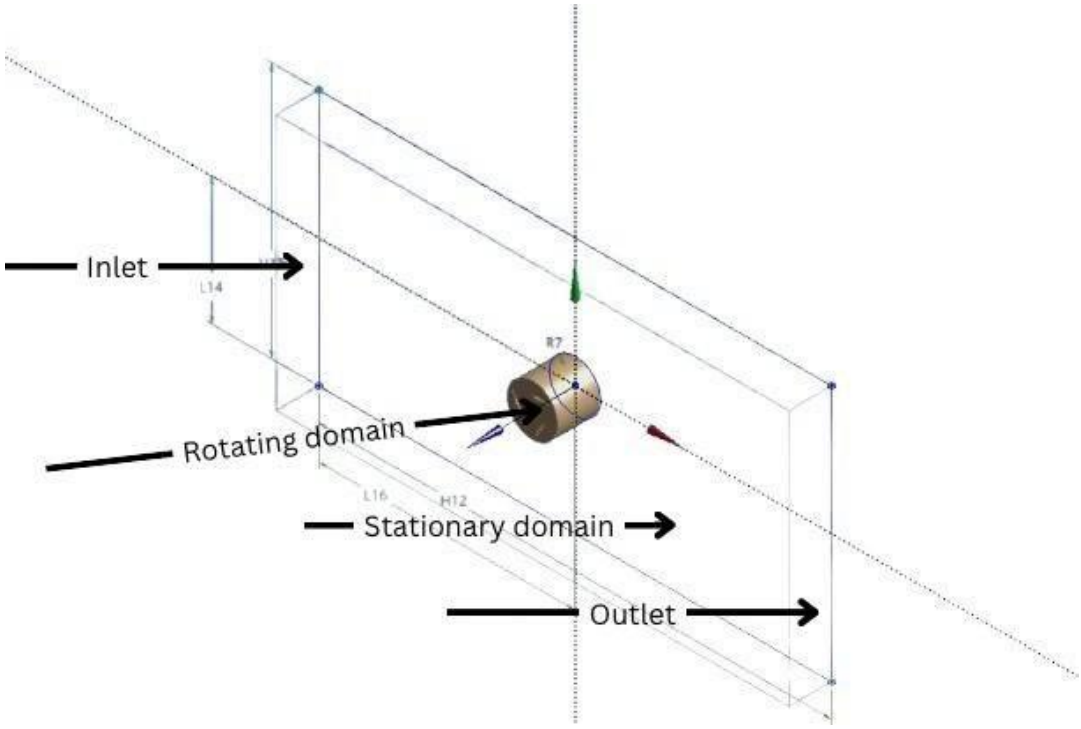

Figure 3.4: Schematic of CFD computational domain displaying the inlet boundary, rotating cylindrical zone, stationary external region, and outlet interface.

3.3 Computational mesh strategy

The mesh was elaborately planned, so that the simulation results could be obtained exactly without the computer resources being overworked. The different regions of the mesh are shown in Figures 3.5(a) and 3.5(b), where the outer and the inner regions are displayed, and the variations in the grid density and the topology around the rotor blades can be clearly seen.

The meshing process was done with the help of ANSYS's automatic meshing tools that come with the software as a standard feature, however, some modifications were done to the settings in order to align with the specific requirements of the simulation. Among those modifications was defining element size by the user, inflation layers around blade surfaces, and a controlled growth factor for grid refinement. A global element size of 0.1 m was assigned to both domains and a gradual expansion factor of 1.2 was applied. This process led to smooth transitions between elements and reduced problems like skewness or long aspect ratio.

Particularly, in the areas surrounding the airfoils, great attention was given and the use of

inflation layers was made in order to achieve fine-scale capturing of the velocity gradients and the wall shear stresses with higher accuracy. This increased resolution in the boundary layer is very important for the simulation of flow separation and

reattachment, which are the phenomena that have a great impact on the performance of VAWT. Similarly, in the rotating domain, the application of finer mesh was also done in order to have an accurate tracking of the transient interaction between the blades and the surrounding flow field.

In general, the mesh creation method has been a balanced decision between precision and resourcefulness. It caters for steady convergence during iterative solving, and it also provides accurate aerodynamic predictions that are necessary for turbine performance evaluation.

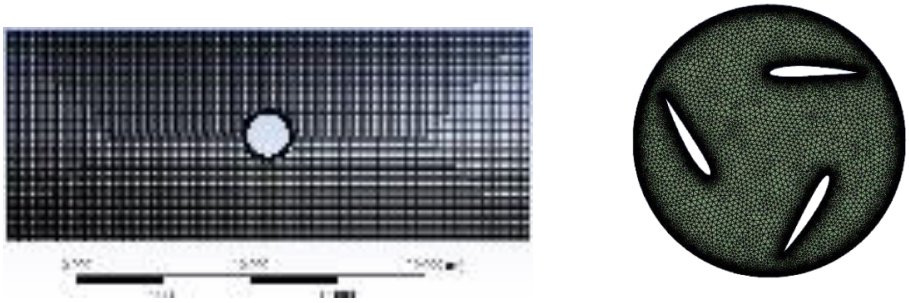

Figure 3.5: Meshing layout of the simulation domain, highlighting (a) the stationary outer zone and (b) the rotating inner region encasing the turbine rotor.

To ensure high fidelity at the boundary between the rotating and stationary domains, mesh refinement was applied to the two interface regions, designated as interface1 and interface2. These zones were assigned to a refined element size of 0.001 meters to reduce interpolation inaccuracies and enhance numerical stability within the sliding mesh interaction (Ferreira et al., 2007). Similarly, the turbine blades were meshed with the same fine resolution to accurately resolve the pressure distribution, surface shear, and vortex shedding around the airfoil surfaces. The overall meshing parameters for each simulation zone are provided in Table 3.1.

Table 3.1: Mesh resolution parameters, including element sizes and growth rates for individual regions of the turbine simulation domain.

Domain	Element size (m)	Growth rate
Stationary domain	0.05	1.2
Interface 2 (Rotating domain interface)	0.001	1.2
Rotating domain	0.01	1.2
Interface 1 (stationary domain interface)	0.001	1.2
Turbine blade	0.001	1.2

The complex near-wall flow behavior, particularly in the rotating zone where the turbine blades came into contact with the surrounding air, was accurately captured using inflation layers. Figure 3.6 shows the layers that were applied. These layers were very close to the blade surfaces with an increase ratio of 0.272. The method made it possible to model the turbulent boundary layer in detail, and also, the simulation of the wake behind the blades was almost like a real one (Islam et al., 2008).

Correct positioning of the non-dimensional wall distance (y^+) was an essential part of this setup as it had a direct impact on the accuracy of turbulence modeling. In the case of Large Eddy Simulation (LES) with wall resolution, y^+ values were maintained at below 1 to provide the highest accuracy in resolving the finest-scale eddies. However, for Reynolds-Averaged Navier–Stokes (RANS) simulations, the mesh was modified in the vicinity of the blade surfaces to keep y^+ within the established range of 30 to 100. It was thus possible to apply the turbulence models

while retaining the physical accuracy of the simulation results to a certain extent (Sarlak et al., 2016).

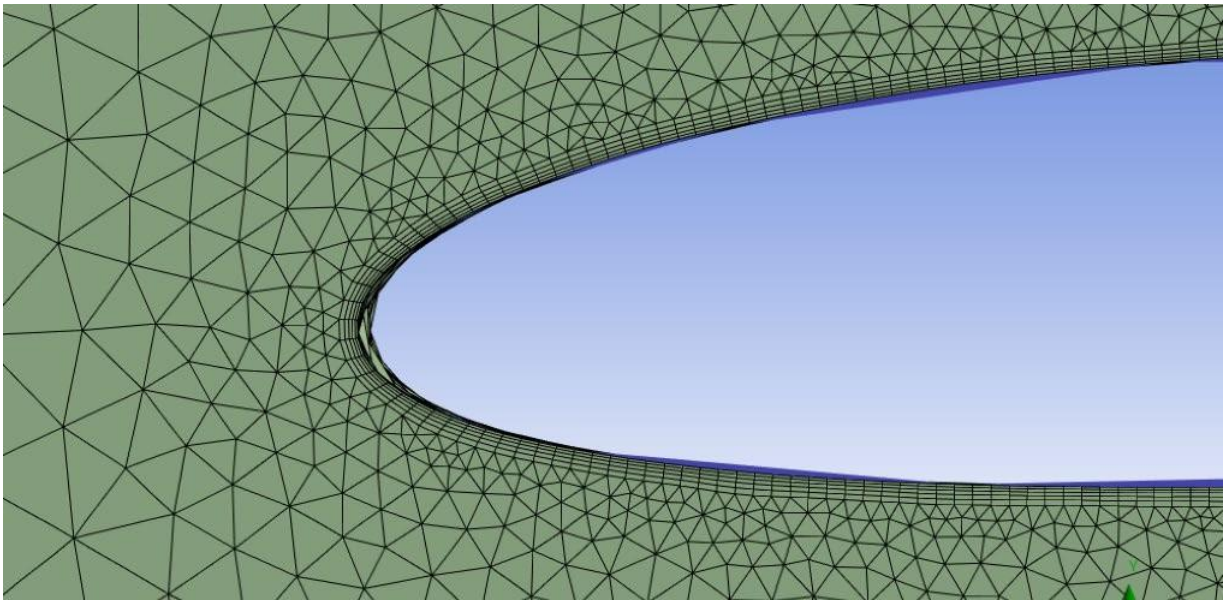

Figure 3.6: Close-up view showing inflation layers at the wind turbine blade surface, crucial for y^+ assessment in turbulence modeling.

The quality of the computational mesh was analyzed using standard metrics for its assessment and these metrics were skewness, aspect ratio and orthogonal quality which make sure grid accuracy, numerical stability, and solution convergence. The final mesh configuration consisted of 870,121 nodes and 2,324,669 elements making it possible to obtain the high-resolution structure that can catch the main aerodynamic behaviors. The mesh quality summary statistics are shown in Table 3.2. The computational domain was divided into boundary regions that were very well defined in order to make post-processing easier and to ensure the solver's execution was efficient. The boundary regions were Turbine Blades, Outer Region, Rotating Region, Inlet, Outlet, Interface 1 (stationary domain interface), Interface 2 (rotating domain interface) and Symmetry. The boundary labeling was done so accurately that it allowed the consistent application of boundary conditions in ANSYS Fluent and CFX solvers.

Table 3.2: Overview of mesh quality indicators used to evaluate numerical stability and element consistency across the computational domain.

Mesh Metric	Average Value
Aspect Ratio	3.05
Orthogonal Quality	0.80
Element Quality	0.71
Skewness	0.22

A mesh refinement validation was carried out to ensure that mesh resolution did not compromise simulation results. In this mesh independence test, successive refinements were applied while monitoring key performance indicators namely, the torque coefficient (C_t) and the power coefficient (C_p). Once mesh refinement produced negligible variation in these parameters, the mesh was deemed sufficiently converged.

This approach to mesh design and validation ensured accurate flow simulations while keeping computational demands within reasonable limits. The mesh configuration was robust enough to resolve complex phenomena like vortex formation, wake interaction, boundary layer evolution, and dynamic loading effects on the turbine blades.

3.3.1 Analysis of mesh sensitivity

The mesh was elaborately planned, so that the simulation results could be obtained exactly without the computer resources being overworked. The different regions of the mesh are shown in Figures 3.5(a) and 3.5(b), where the outer and the inner regions are displayed, and the variations in the grid density and the topology around the rotor blades can be clearly seen.

The meshing process was done with the help of ANSYS's automatic meshing tools that come with the software as a standard feature, however, some modifications were done to the settings in order to align with the specific requirements of the simulation. Among those modifications was defining element size by the user, inflation layers around blade surfaces, and a controlled growth factor for grid refinement. A global element size of 0.1 m was assigned to both domains and a gradual expansion factor of 1.2 was applied. This process

led to smooth transitions between elements and reduced problems like skewness or long aspect ratio.

Particularly, in the areas surrounding the airfoils, great attention was given and the use of inflation layers was made in order to achieve fine-scale capturing of the velocity gradients and the wall shear stresses with higher accuracy. This increased resolution in the boundary layer is very important for the simulation of flow separation and

reattachment, which are the phenomena that have a great impact on the performance of VAWT. Similarly, in the rotating domain, the application of finer mesh was also done in order to have an accurate tracking of the transient interaction between the blades and the surrounding flow field.

In general, the mesh creation method has been a balanced decision between precision and resourcefulness. It caters for steady convergence during iterative solving, and it also provides accurate aerodynamic predictions that are necessary for turbine performance evaluation.

Table 3.3: Pressure drop values across the stationary domain for various mesh resolutions, highlighting convergence trends in the grid sensitivity study.

Size of Element (m)	Elements Number	Pressure drops (Pa)
0.09	457038	10.75
0.1	974348	11.77
0.2	414562	10.61
0.3	424744	10.59
0.4	401633	7.77
0.5	335136	8.55
0.6	386890	9.77
0.7	371830	9.18
0.8	367555	9.40
0.9	361151	9.03

Based on the results from the mesh sensitivity study, the most efficient grid configuration was determined at 974,348 elements, where the simulation outputs began to stabilize. Beyond this point, additional refinement provided minimal gains in predictive accuracy but introduced significant increases in computational demand (Nour Khlaifat et al., 2020). This validated mesh size was adopted for the final simulation, as it strikes a balance between computational efficiency and fidelity of the aerodynamic model.

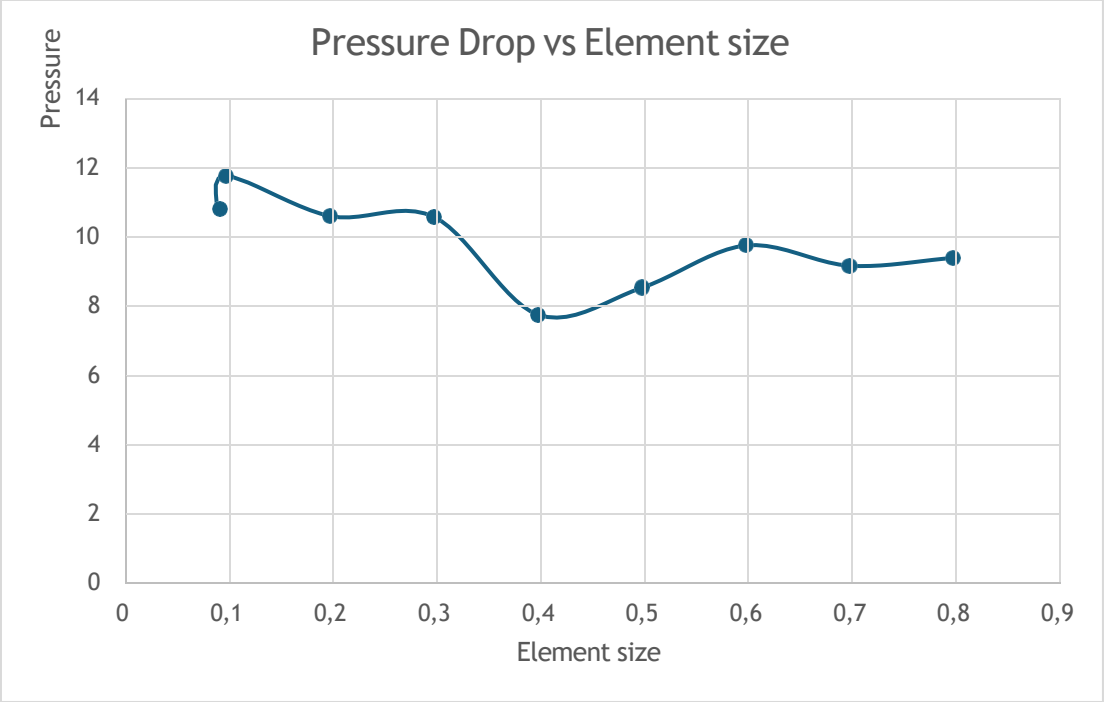

Figure 3.7: Visualization of the grid convergence analysis, illustrating the effect of mesh density on simulation stability.

3.4 Simulation framework and solver settings

A time-dependent pressure-based solver in the ANSYS Fluent environment was used to simulate the unsteady behavior of the Darrieus-type vertical-axis wind turbine or VAWT. Due to its strong performance in simulating incompressible low-Mach number flows a feature of small-scale wind turbines this solver type was chosen (Tantichukiad et al. in 2024. Since the simulation used an absolute velocity formulation every velocity component was specified in relation to a fixed (inertial) coordinate system. Accurately resolving interactions between the stationary external airflow and the rotating turbine blades requires this method. Enhanced near-wall treatment of the realizable k-ε turbulence model was used to model turbulence. This advanced model offers improved predictions of flow behavior in rotating systems, especially in regions prone to flow detachment, vortex formation, and

recirculation, which are common in vertical-axis turbines (Abd Halim et al., 2018). Its enhanced wall treatment permits the accurate resolution of near-wall flow effects without necessitating excessive mesh refinement, allowing for more efficient modeling of viscous shear layers and boundary-layer separation (Palasai et al., 2024).

The working fluid was air, characterized using standard atmospheric parameters:

- **ρ**: 1.225 kg/m³
- **μ**: 1.7894 × 10^{-5} Pa·s

The simulation was conducted in a transient environment to address time-varying aerodynamic phenomena like vortex shedding, dynamic stall and blade-wake coupling. In order to replicate the turbines rotation with respect to the static outer domain the sliding mesh technique was utilized. This method can depict blade aerodynamics more accurately than steady-state methods because it explicitly accounts for time-dependent interactions between stationery and moving regions (Balduzzi et al. 2016).

3.4.1 Specification of boundary conditions

The computational domain was designed to reflect realistic conditions for small-scale wind turbines by assigning precise physical boundary conditions. These conditions, applied to the inlet, outlet, blade surfaces, and interfacing regions, ensured numerical stability and physical accuracy throughout the simulation process.

3.4.1.1 Upstream flow (inlet) boundary settings

To simulate a variety of realistic wind conditions for Pico-scale applications, the inlet surface was defined as a velocity inlet which allowed the airflow to pass into the domain at different speeds between 2 m/s and 10 m/s. The inlet was set to have a gauge pressure of 0 Pa which is equal to the standard reference atmospheric pressure. The direction of the inlet flow was set to be normal to the boundary plane, which made it certain that the wind came into the domain at a right angle. This specification aids in the mitigation of unintentional creation of non-physical tangential velocity components, which could otherwise be a reason for wrong flow predictions.

Turbulence intensity and length scale method was utilized to define the turbulence properties at the inlet. A turbulence intensity of 1% was selected in order to represent low-turbulence inflow which is typical of controlled environments or laminar ambient winds. Turbulence length scale was set at 1-meter height, which is based on the vertical span of

the turbine and corresponds to the size of the dominant energy-carrying eddies in the natural wind profiles (Stanislawski et al., 2023).

3.4.1.2 Condition of the outlet boundary

The downstream region of the computational domain was specified as a pressure outlet, allowing airflow to exit freely without undue restrictions. The gauge pressure was set at 0

Pa, corresponding to ambient atmospheric pressure, and was essential in replicating realistic flow discharge conditions. This setup minimizes artificial reflection of flow features and maintains the natural evolution of wake structures.

To ensure that flow exited the domain cleanly, the flow direction was constrained to be normal to the outlet face, which reduces the possibility of reverse flow or non-physical recirculation at the domain boundary. Turbulence characteristics at the outlet mirrored those of the inlet, with a turbulence intensity of 1% and a length scale of 1 m, ensuring consistency in turbulence modeling across the computational domain (Basse, 2019). This uniform setup improves numerical convergence and supports stability in transient simulations.

3.4.1.3 Conditions of the turbine blade surface

The surfaces of the turbine blades were treated as rotating walls, governed by the dynamics of the adjacent fluid region. These wall boundaries were subject to a no-slip condition, enforcing zero relative velocity between the blade surface and the nearby airflow. This is critical for capturing the viscous effects in the boundary layer and accurately computing shear forces, which directly influence lift and drag behavior (Ferreira et al., 2007).

Rotation was enabled using the sliding mesh approach, which allows real-time, transient simulation of blade movement. This method is particularly effective in modeling unsteady aerodynamic phenomena like vortex shedding, dynamic stall, and periodic changes in torque. It also helps track the instantaneous interaction between moving blades and the surrounding stationary fluid domain, leading to more realistic performance predictions (Balduzzi et al., 2016).

3.5 Dynamic mesh implementation

A dynamic mesh technique was employed to simulate the motion of the turbine in a physically responsive manner, rather than prescribing a fixed rotational speed. This strategy enables the turbine to rotate autonomously in reaction to the aerodynamic forces

acting on the blades, thereby capturing transient behaviors such as self-starting dynamics and time-evolving torque generation (Fatahian et al., 2024).

3.5.1 Configuration of 6DOF solver

The dynamic mesh setup incorporated a Six Degrees of Freedom (6DOF) model, though only one rotational degree of freedom was activated. This allowed the turbine rotor to spin about its central axis while the remaining degrees of freedom were constrained. Each blade was modeled with a mass of 0.1 kg, and its moment of inertia (I) was computed using Equation 3.1, ensuring that rotational motion aligned with Newtonian physics and reflected realistic inertial effects during blade acceleration and deceleration.

$$I = mr^2 \tag{3.1}$$

Taken:

- I = Moment of inertia (kg·m²)
- r = Radius of rotation (m)
- m = Blade mass (0.1 kg)

One of the most important inputs in determining the moment of inertia is the parameter r which stands for the radius of rotation from the turbine's central axis. This number has a direct impact on how the turbine reacts to wind-generated aerodynamic torque. The computational domain was divided into three main areas in the dynamic simulation setup.

- **Rotating Domain**: Encompasses the turbine blades and facilitates their rotational motion relative to the outer flow.
- **Stationary Domain**: Constitutes the surrounding fluid region that remains fixed with respect to the incoming wind direction.
- **Blade Geometry**: Represents the turbine's aerodynamic surfaces, which experience lift and drag forces and are responsible for torque generation.

To ensure consistency in force and performance calculations, standardized reference values were established for all simulations. These reference parameters, outlined in Table 3.4, serve as the basis for computing aerodynamic loads, torque, and power across the rotor.

Table 3.4: Reference values used for the simulation setup

Reference parameter	Value
Pressure [Pa]	0
Temperature [k]	288.16
Area [m^2]	0.101
Enthalpy [J/kg]	0
Ratio of Specific Heats	1.4
Viscosity [kg/ (m s)]	$1.7894e^{-05}$
Length [m]	0.18
Velocity [m/s]	2,3,4,5,6,7,8,9,10

3.6 Numerical solver and scheme settings

The pressure–velocity coupling in the simulation was managed using the Semi-Implicit Method for Pressure-Linked Equations (SIMPLE) algorithm. This approach is especially effective for modeling incompressible and turbulent flow conditions, providing robust stability and reliable convergence throughout the iterative computation process. For time-dependent computations, a second-order implicit temporal discretization scheme was adopted. This choice enhances the fidelity of transient simulations by limiting numerical diffusion, thereby capturing unsteady flow structures such as vortex shedding and fluctuating blade loads more accurately (Xiao et al., 2018).

Initial conditions were established using hybrid initialization, which estimates velocity and pressure fields based on potential flow behavior. This technique reduces startup transients and accelerates convergence to a steady or periodic solution.

The following settings were used to control the simulation run:

- Time step size: 0.05 seconds small enough to resolve temporal variations in aerodynamic forces effectively.
- Maximum iterations per time step: 60 ensuring that convergence criteria are met for each transient step before advancing in time.

Overall, this solver configuration was designed to balance computational efficiency with the precision required to resolve complex aerodynamic interactions, including the self-

starting behavior, power extraction dynamics, and torque oscillations of the Darrieus wind turbine.

3.7 Limitations of numerical modeling

While CFD excels in simulating pico-scale Darrieus VAWTs, limitations in low-Re (<10^5) rural winds—arising from assumptions, computation, accuracy, and validation—impact result reliability. This thesis used ANSYS Fluent's 6DOF for transparent analysis.

Simplifying assumptions: 2D models neglect 3D vortex/tip losses, overestimating C_p by 8% at TSR <1.0; forced rotation ignores inertia, missing 50–100% azimuthal torque swings; k-ω SST underpredicts stall (>15° AoA) and wakes; incompressible/rigid assumptions omit FSI/thermal effects (5–10% C_p bias).

Computational challenges: 3D LES/DES needs 40M+ elements, 1024 CPUs, 48+ hours—impractical for optimizations; poor meshes (>5° increments, <10D domains, y+ >1) inflate C_p errors >5%; low-Re demands 10^6–10^7 elements, straining hardware despite cloud use.

Accuracy discrepancies: Overestimates upwind vorticity, distorting wake deficits for hybrids; low winds (<4 m/s) yield 20% C_p deviations from unresolved transitions; rural turbulence (>15% intensity) exposes 2D/2.5D gaps in spanwise flows, as in helical studies.

Validation hurdles: Limited to C_p matches (<10% error), ignoring contours/vorticity; benchmarks have uncertainties (tunnel blockage >20%, PIV limits); this thesis achieved <5% torque via NREL data, but field gaps urge prototyping.

CFD complements experiments, guiding rural VAWT optimizations via hybrid validation.

CHAPTER FOUR
SIMULATION RESULTS

4 Introduction

To assess the aerodynamic properties of a pico-scale Darrieus vertical-axis wind turbine (VAWT), dynamic mesh technique in Computational Fluid Dynamics (CFD) simulations was used as an alternative to traditional methods that apply fixed rotational velocities. In this use of CFD, a Six Degrees Of Freedom (6DOF) methodology was employed which allowed the changing of wind to control the turbine blade rotation through aerodynamic forces being acted upon them. Up to 10 m/s wind speed simulations have been done to see how the turbine reacts dynamically under actual environmental conditions. The quantitative analysis of the torque, angular speed, power output, lift and drag forces, and power coefficient (Cp) metrics was performed to measure the turbine's performance regarding the main aspects of its aerodynamic performance and energy conversion efficiency at different operating points.

Mesh sensitivity tests were applied to confirm that the grid resolution that was chosen not only rendered consistent results but also minimized computational resources leading to the realization of a perfect balance that is very important for enhancing the efficiency of simulation without sacrificing accuracy. The turbine's performance is scrutinized in this paper; the effect of wind speed and blade configuration on power generation, torque characteristics, and force distribution has been explored. Besides that, the analysis is also directed towards defining the operating thresholds and conditions which can inform the future design iterations and the optimization of low-power, distributed wind energy systems.

4.1 Angular velocity performance

The turbine’s angular velocity exhibits a consistent positive correlation with increasing wind speed across various angles of attack (AoA). At 0° AoA, the turbine’s angular velocity, as recorded in Table 4.1, increases steadily from 3.33 rad/s at a wind speed of 2 m/s to 22.96 rad/s at 10 m/s, demonstrating that higher wind energy input drives faster blade rotation. A similar trend is observed at 5° AoA, where angular velocity reaches 23.50 rad/s at 10 m/s under identical wind conditions, indicating that a slight AoA adjustment has minimal impact on rotational speed. These findings highlight the turbine’s ability to self-adjust rotationally under varying aerodynamic loads, which is critical for self-starting and

sustained energy capture in pico-scale vertical-axis wind turbines.

Table 4.1: Angular velocity at various angles of attack

Wind speed (m/s)	Angular speed (rad/s) at 0°	Angular speed (rad/s) at 5°	Angular speed (read/s) at 10°	Angular speed (rad/s) at 15°	Angular speed (rad/s) at 20°	Angular speed (rad/s) at 25°
2	3.33	3.58	3.793	2.81	2.71	2.27
3	7.11	7.84	8.96	6.74	6.50	6.32
4	8.89	9.48	10.78	8.01	7.86	7.26
5	10.00	10.83	11.04	10.95	10.45	10.35
6	15.20	15.71	15.91	14.35	14.03	13.94
7	14.60	18.65	19.57	14.86	14.27	13.72
8	16.57	21.26	22.86	16.33	15.54	14.95
9	21.23	23.06	24.65	19.48	18.82	18.21
10	22.97	23.50	24.90	23.11	22.51	19.00

The relationship between angular velocity and angle of attack (AoA) for a pico-scale Darrieus vertical-axis wind turbine (VAWT) reveals distinct aerodynamic behavior across varying wind speeds. At 10° AoA, the turbine achieves its peak rotational velocity of 24.00 rad/s at a wind speed of 10 m/s, indicating an optimal lift-to-drag ratio that maximizes rotational acceleration. This suggests that 10° AoA is the most aerodynamically efficient angle among those tested.

At higher AoAs of 15° and 25°, angular velocity decreases, reaching 23.10 rad/s at 15° and dropping significantly to 19.00 rad/s at 25° (at 10 m/s wind speed). This reduction is attributed to increased drag and flow separation, characteristic of stall onset, where airflow detachment from the blade surface impairs performance. At lower wind speeds (2–4 m/s), angular velocity remains modest but increases steadily with AoA up to 10°. Beyond this, aerodynamic resistance causes rotation rates to decline. In the moderate wind speed range (5–7 m/s), rotational speeds improve across all AoAs, with 10° consistently yielding the highest angular velocity, followed closely by 5°, while higher angles (15° and 25°)

underperform due to less favorable aerodynamic profiles. These trends are illustrated in Figure 4.1, where bar heights depict the turbine's rotational response across varying wind conditions and AoAs, confirming the superior efficiency of 10° AoA.

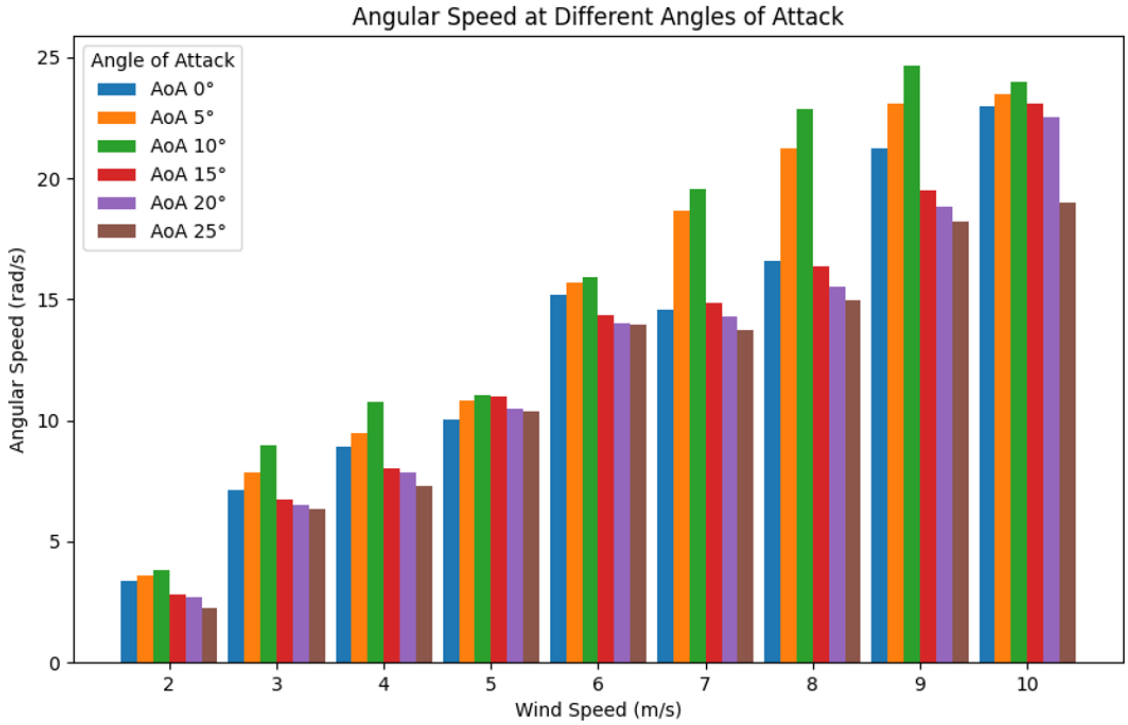

Figure 4.1: Effect of Wind Speed on Angular Velocity at Varying Blade Angles

As wind velocity increases into the higher range (8–10 m/s), the turbine achieves its highest rotational speeds, with the 10° angle of attack (AoA) consistently producing the most favorable results. However, a saturation trend becomes evident as the rate of increase in angular velocity begins to taper off, especially at higher AoAs, where excessive drag inhibits further performance gains. This plateau effect suggests aerodynamic inefficiencies emerging at elevated wind speeds when the AoA exceeds optimal thresholds.

Notably, 20° and 25° AoA continue to demonstrate suboptimal rotational speeds across all wind conditions, reaffirming the detrimental impact of high drag and early stall. These findings emphasize the critical importance of selecting an appropriate AoA; within the tested range, moderate AoAs (5° to 10°) strike the best balance between lift generation and drag resistance, resulting in superior rotational output for the vertical-axis wind turbine (VAWT).

4.2 Evaluation of generated torque and power performance

4.2.1 Analysis of rotational moment (torque)

The torque output of the pico-scale Darrieus vertical-axis wind turbine (VAWT) was analyzed with respect to wind speed and angle of attack (AoA), as presented in Table 4.2. The data illustrates how aerodynamic loading influences turbine performance across various operational conditions. At lower wind speeds (e.g., 2 m/s), starting torque increases with AoA, particularly at moderate angles (5° and 10°), which offer an optimal balance of lift and rotational force. Specifically, at 2 m/s, torque is lowest at 0° AoA (0.0101 Nm), rising to 0.0106 Nm at 5° AoA and 0.0111 Nm at 10° AoA, indicating improved capability for initiating blade rotation. Beyond 10° AoA, torque improvement plateaus due to increased aerodynamic drag.

At higher wind speeds, torque values rise consistently across all AoAs, with 10° and 15° AoAs demonstrating superior performance, balancing high torque output with minimal drag penalties. In contrast, higher AoAs (20° and 25°) exhibit elevated torque but reduced efficiency due to turbulent flow separation and increased resistance. The analysis confirms that moderate AoAs (5°–15°) provide the most effective balance for low-speed startup and high-speed torque stability, making them optimal for efficient operation across diverse wind conditions.

Table 4.2: Moment vs. Wind Speed for various angles of attack

Wind speed (m/s)	Moment (Nm) at 0°	Moment (Nm) at 5°	Moment (Nm) at 10°	Moment (Nm) at 15°	Moment (Nm) at 20°	Moment (Nm) at 25°
2	0.01	0.01	0.01	0.01	0.01	0.01
3	0.03	0.03	0.03	0.05	0.04	0.04
4	0.11	0.13	0.14	0.11	0.10	0.10
5	0.21	0.26	0.29	0.19	0.12	0.17
6	0.29	0.32	0.35	0.25	0.25	0.22
7	0.40	0.42	0.45	0.29	0.29	0.23
8	0.50	0.53	0.55	0.30	0.30	0.26
9	0.47	0.49	0.52	0.37	0.31	0.30
10	0.44	0.46	0.48	0.36	0.23	0.28

The bar chart in Figure 4.2 presents the distribution of torque (moment) produced by a Darrieus-type vertical-axis wind turbine (VAWT) across a spectrum of wind speeds (2–10 m/s) and blade angles of attack (0°, 5°, 10°, 15°, 20°, and 25°). Each group of bars corresponds to a specific wind speed, with individual bars within each group representing the torque output for a given blade angle.

At low wind speeds (2 to 4 m/s), torque generation remains minimal across all configurations, reflecting the turbine's limited aerodynamic response under low energy input. As wind speed increases beyond this range, the moment increases significantly, reaching its maximum around 8 m/s before exhibiting signs of decline at higher wind velocities. This behavior is consistent with the aerodynamic performance threshold, beyond which stall effects or drag-induced losses begin to counteract lift-induced torque.

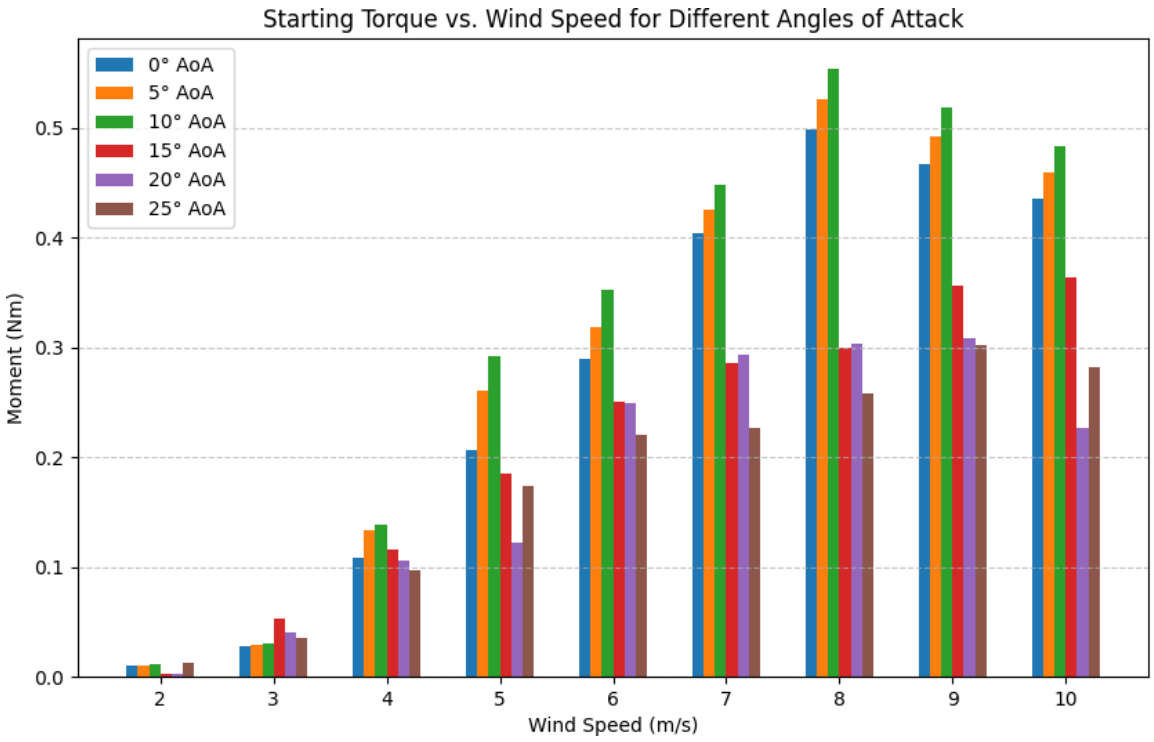

Figure 4.2: Variation of rotational moments with wind speed across different angles of attack

The highest torque output is recorded for the 10° AoA, peaking at 0.5536 Nm at 8 m/s, closely followed by the 5° AoA, which achieves 0.5255 Nm. These results clearly identify

moderate AoA values as the most effective in converting wind energy into rotational torque. In contrast, higher angles (15°–25°) yield comparatively lower moment values across most wind speeds, particularly at the upper range, where aerodynamic penalties such as flow separation diminish performance.

Notably, while the 15° AoA maintains relative consistency at higher wind speeds, it fails to match the torque output of lower angles. A slight reduction in torque is also observed at 9–10 m/s for the 0°, 5°, and 10° AoAs, suggesting that beyond a critical velocity, increased drag begins to offset lift gains, reducing torque output.

In summary, the moment performance highlights 5° and 10° angles of attack as the most efficient configurations for torque generation under moderate wind conditions. However, performance degradation at higher speeds emphasizes the need for careful aerodynamic design to mitigate drag-related losses.

4.3 Power output performance across wind speeds

Table 4.3 presents the cumulative power output produced by the turbine under varying wind speeds and blade angles of attack (AoAs), specifically at 0°, 5°, 10°, 15°, 20°, and 25°. The wind speed range considered spans from 2 m/s to 10 m/s. Since power is derived from the product of torque and angular velocity, this metric serves as a key indicator of the turbine's efficiency and real-world performance potential.

Table 4.3: Output (W) across varying angles of attack

Wind speed (m/s)	Total power (W) at 0°	Total power (W) at 5°	Total power (W) at 10°	Total power (W) at 15°	Total power (W) at 20°	Total power (W) at 25°
2	0.10	0.114	0.13	0.02	0.02	0.09
3	0.58	0.69	0.82	1.08	0.78	0.66
4	2.87	3.79	4.48	2.80	2.48	2.11
5	6.18	8.46	9.65	6.10	3.81	5.40
6	13.12	15.03	16.80	10.80	10.50	9.20
7	17.66	23.78	26.30	12.72	12.56	9.30
8	24.77	33.52	37.97	14.67	14.14	11.55
9	29.70	34.01	38.30	20.81	17.42	16.51
10	30.03	32.38	34.75	25.26	15.30	16.71

The variation in power output across different wind speeds and blade angles is illustrated in Figure 4.3, which presents data for angles of attack (AoA) from 0° to 25° and wind speeds ranging from 2 to 10 m/s.

Power output for each three-blade configuration is determined using Equation 4.1,

$$\mathrm{p} = T * \omega \tag{4.1}$$

where:

- P represents the power output in watts (W)
- T denotes the torque in newton-meters (Nm)
- ω is the angular velocity in radians per second (rad/s)

The total power output for the three-blade system is calculated as shown in equation 4.2:

$$P_{Total} = 3 * (T * \omega) \tag{4.2}$$

The power output trend of the pico-scale Darrieus vertical-axis wind turbine (VAWT) is presented in Figure 4.3, illustrating the variation in total power (in watts) across wind speeds from 2 m/s to 10 m/s and angles of attack (AoA) from 0° to 25°. The data demonstrate the combined influence of wind speed and AoA on the turbine's power generation performance.

- As anticipated, power generation remains low at wind speeds between 2 and 3 m/s, owing to the limited kinetic energy available in the airflow at such velocities. In this range, a gradual increase in AoA from 0° to 10° results in improved energy capture, with 10° AoA offering the highest power output. However, once the AoA exceeds 10°, particularly from 15° to 25°, power generation begins to drop, likely due to flow separation and early onset of stall effects reducing aerodynamic efficiency.
- In the medium wind speed range (4–6 m/s), power output increases significantly,

with 10° AoA consistently delivering the highest performance, closely followed by 5° AoA. Angels above 15° exhibit reduced effectiveness due to increased drag offsetting lift gains.

- At higher wind speeds (7–10 m/s), power output continues to rise, but sensitivity to AoA becomes more pronounced. The 10° AoA remains the most efficient configuration across all speeds, with 0° and 5° AoA providing strong output.

  However, at 15°, 20°, and 25° AoA, power output declines noticeably, particularly beyond 8 m/s, indicating significant aerodynamic penalties from flow disruption and efficiency losses at steep angles. These trends confirm that moderate AoAs (5°–10°) achieve the most balanced and efficient conversion of wind energy into mechanical power across a wide range of wind speeds, while angles above 15° lead to consistent performance losses, highlighting the critical role of AoA optimization in VAWT design for enhanced energy output and operational stability.

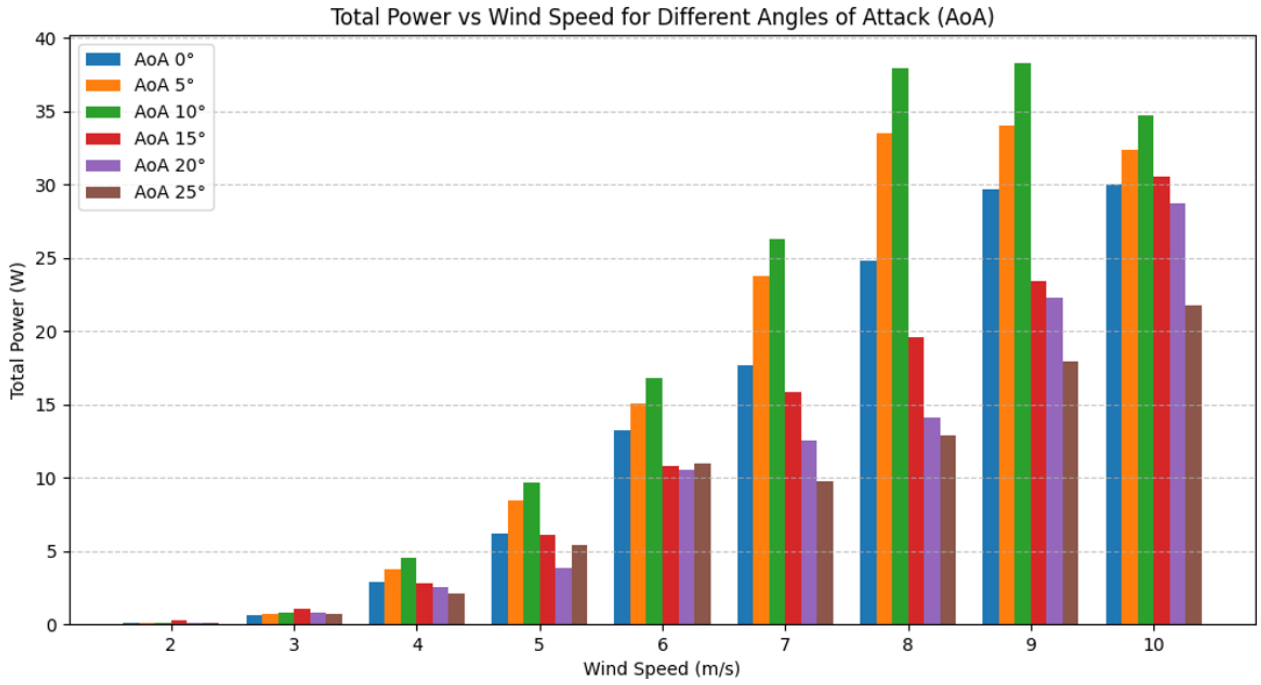

Figure 4.3: Variation of total power with wind speed across different angles of attack

4.4 Assessment of power coefficient (cp) performance

Table 4.4 summarizes the calculated power coefficient (Cp) values for the turbine across operational wind speeds (2-10 m/s) and six discrete angles of attack (0°, 5°, 10°, 15°, 20°,

25°). The power coefficient represents a crucial performance indicator, quantifying the turbine's ability to convert available wind energy into usable mechanical power relative to the Betz limit (theoretical maximum Cp= 0.593). These values were computed using the fundamental aerodynamic relationship:

$$C_p = \frac{P_T}{1/_2 \rho A V^3} \tag{4.3}$$

Where:

- **P**: Mechanical power extracted by the turbine (W)
- **ρ**: Air density (1.225 kg/m³ at standard conditions)
- **A**: Projected rotor swept area (m²)
- **V**: Upstream wind velocity (m/s)

This equation expresses the power coefficient (Cp) as the ratio of the actual mechanical power harnessed by the turbine to the total kinetic energy available in the wind stream flowing through the rotor area. A higher Cp indicates enhanced aerodynamic efficiency and more effective wind-to-energy conversion.

Table 4.4: Effect of blade angle on power coefficient (Cp)

Wind speed (m/s)	Cp at 0°	Cp at 5°	Cp at 10°	Cp at 15°	Cp at 20°	Cp at 25°
2	0.070	0.08	0.09	0.01	0.01	0.06
3	0.12	0.14	0.16	0.21	0.16	0.13
4	0.24	0.32	0.38	0.24	0.21	0.18
5	0.27	0.36	0.42	0.26	0.16	0.23
6	0.33	0.37	0.42	0.27	0.26	0.23
7	0.28	0.36	0.41	0.20	0.20	0.15
8	0.27	0.35	0.40	0.15	0.15	0.12
9	0.22	0.25	0.28	0.15	0.13	0.12
10	0.17	0.17	0.19	0.14	0.09	0.09

Depicted in Figure 4.4 is a heatmap that illustrates the variation in power coefficient (Cp) as a function of wind speed and blade angle of attack, evaluated at 0°, 5°, 10°, 15°, 20°, and 25°. The intensity of the color gradients reflects changes in Cp values, providing a clear visual representation of the turbine's aerodynamic performance under differing flow conditions.

At low wind speeds (2–4 m/s), the differences in Cp across all angles are minor, suggesting that blade orientation has little effect when wind energy is minimal. As wind velocity increases, the Cp values grow, peaking around 6–7 m/s. This range appears to be where the turbine captures wind energy most effectively. Among all tested angles, 10° consistently shows the highest Cp, followed closely by 5°, suggesting these angles offer favorable lift-to-drag ratios for efficient rotation.

As the angle of attack surpasses 10°, a noticeable decline in the power coefficient (Cp) emerges. While a 15° angle still maintains a relatively moderate Cp, it underperforms compared to the efficiency achieved at 5° and 10°. Angles of 20° and 25° exhibit a pronounced drop in Cp, especially at elevated wind speeds. This reduction can be attributed to heightened aerodynamic drag and premature flow separation, both of which diminish energy conversion efficiency. Furthermore, wind speeds exceeding 8 m/s reveal a general downward trend in Cp across all tested angles, suggesting a limit to aerodynamic performance under higher velocity conditions.

Overall, the results suggest that moderate angles of attack especially 10° provide the best balance between aerodynamic lift and drag, leading to higher efficiency. The heatmap clearly emphasizes that selecting an appropriate blade angle is essential for maintaining optimal turbine performance under varying wind conditions.

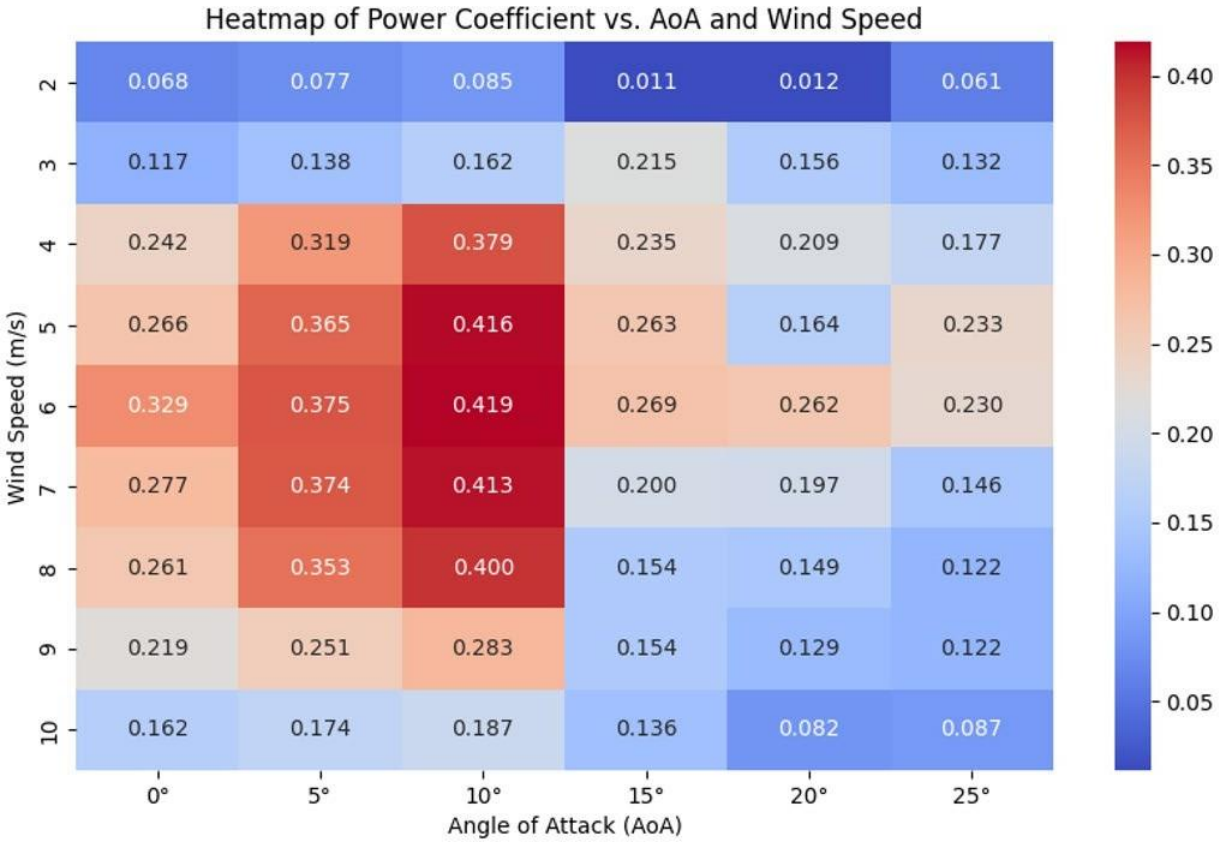

Figure 4.4: Heatmap of power coefficient (Cp) across wind speeds and angles of attack

4.5 Aerodynamic forces: drag and lift

4.5.1 Impact of drag force on turbine efficiency

Table 4.5 illustrates the variation of drag force with wind speed across six angles of attack (0°, 5°, 10°, 15°, 20°, and 25°) for a pico-scale Darrieus-type vertical-axis wind turbine (VAWT). As anticipated, drag force increases with higher wind speeds for all blade angles. Notably, blades configured at higher angles of attack exhibit substantially greater aerodynamic resistance compared to those at lower angles.

At low wind speeds (2–4 m/s), differences in drag among the angles are relatively minor, as the aerodynamic loads remain small. But once wind speed exceeds 5 m/s, the drag force begins to climb rapidly, especially for angles beyond 10°. The lowest drag is consistently observed at 0°, confirming its efficiency in minimizing resistance.

At higher angles such as 15°, 20°, and especially 25°, drag increases steeply. This rise is attributed to flow separation and increased turbulence around the blade surfaces. The largest drag values occur at 25°, clearly illustrating that steeper blade orientations come

with significant aerodynamic drawbacks. These observations demonstrate a critical trade-off while increasing the angle of attack may enhance lift or torque initially, it also intensifies drag, reducing overall efficiency. This pattern emphasizes the importance of selecting a balanced angle of attack where lift is maximized without excessive drag thereby optimizing turbine performance across varying wind conditions.

Table 4.5 Effect of Angle of Attack on Drag Force

Wind speed (m/s)	Drag force at 0°	Drag force at 5°	Drag force at 10°	Drag force at 15°	Drag force at 20°	Drag force at 25°
2	0.10	0.99	0.98	1.13	1.32	1.57
3	2.19	2.45	2.70	3.11	3.65	4.32
4	3.98	4.19	4.40	5.06	5.94	7.04
5	6.51	7.52	8.53	9.81	11.51	13.64
6	9.34	10.15	10.56	12.14	14.25	16.89
7	12.07	13.25	13.97	16.07	18.86	22.36
8	12.47	14.52	15.50	17.83	20.93	24.81
9	12.80	16.07	16.06	18.47	21.69	25.70
10	13.07	16.48	16.18	18.61	21.85	25.90

This pattern reveals that although increasing the angle of attack can enhance aerodynamic performance up to a point, excessively steep angles introduce substantial drag, which diminishes overall turbine efficiency. The results emphasize the importance of carefully adjusting the blade angle to strike a functional balance between lift generation and drag resistance. Achieving this equilibrium is essential for maximizing the aerodynamic output of the wind turbine, as illustrated in Figure 4.5.

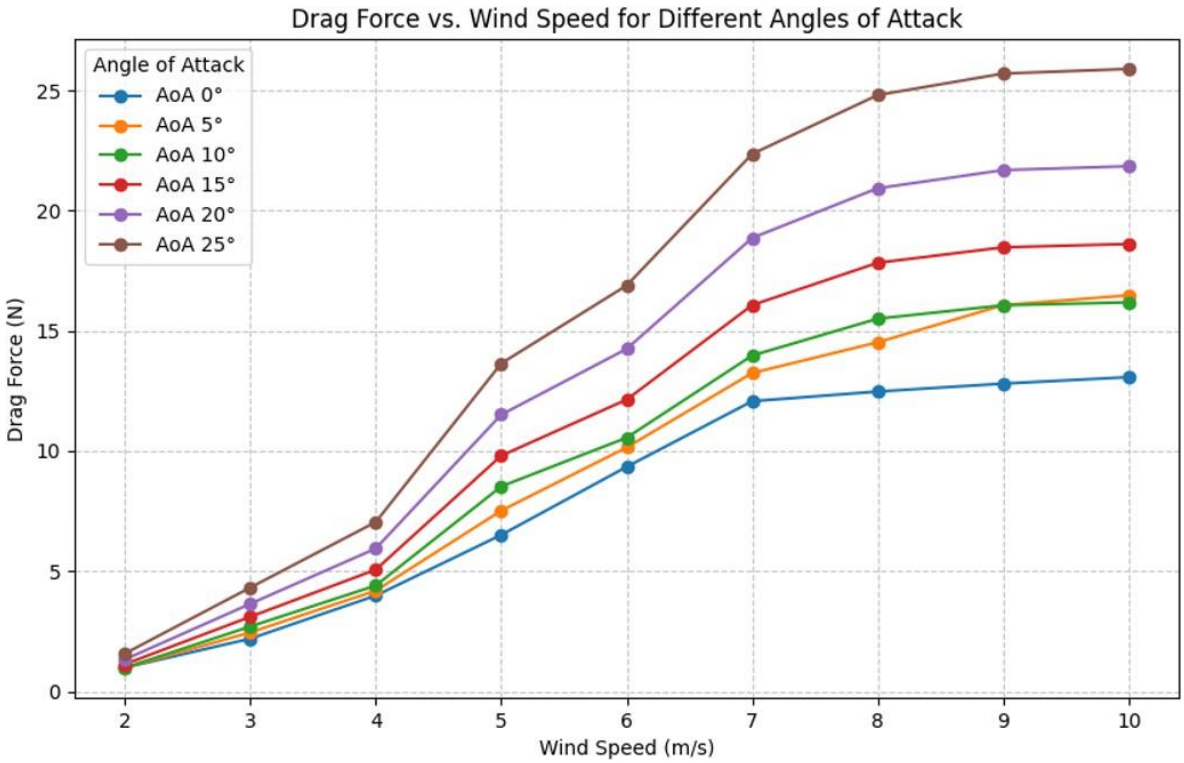

Figure 4.5: Effect of angle of attack on drag force

4.5.2 Impact of lift force on wind turbine performance

Changes in lift force across wind speeds from 2 to 10 m/s are detailed in Table 4.6 for blade angles of 0°, 5°, 10°, 15°, 20°, and 25°. At 0°, the blades encounter a progressively negative lift trend as wind velocity increases, signaling limited aerodynamic contribution and inefficient rotational support. When the AoA increases to 5° and 10°, the magnitude of the negative lift reduces noticeably, showing a shift toward more favorable aerodynamic conditions. These moderate angles generate more useful upward lift, helping the blades rotate more effectively. As the angle continues to rise beyond 10°, the benefits start to diminish. At 15°, lift remains moderate, but at 20° and 25°, the lift force begins to decline again, often turning increasingly negative due to turbulent flow and loss of aerodynamic stability. This degradation suggests that while some increase in AoA helps improve lift, excessive angles compromise the turbine's aerodynamic advantage.

Table 4.6: Variation of lift force with blade AoA

Speed of Wind (m/s)	Lift Force at 0°	Lift Force at 5°	Lift Force at 10°	Lift Force at 15°	Lift Force at 20°	Lift Force at 25°
2	-0.86	-0.76	-0.62	-0.51	-0.40	-0.32
3	-2.11	-2.45	-2.25	-1.92	-1.51	-1.23
4	-3.85	-2.77	-2.90	-2.61	-2.31	-2.01
5	-6.10	-5.06	-4.35	-4.11	-3.90	-3.61
6	-8.83	-7.72	-6.72	-6.40	-6.07	-5.72
7	-12.10	-11.07	-11.26	-10.92	-10.60	-10.24
8	-10.90	-10.0	-10.41	-10.12	-9.80	-9.51
9	-9.11	-9.11	-8.90	-8.77	-8.61	-8.40
10	-10.43	-9.44	-9.09	-8.83	-8.59	-8.30

As wind velocity rises, the lift force at blade angles of 15°, 20°, and 25° demonstrates a noticeable improvement, with a steady reduction in downward aerodynamic pressure. This pattern suggests an enhancement in lift efficiency at steeper blade inclinations. While variations in lift across angles are less pronounced at lower wind speeds, a more significant divergence appears as wind speed increases indicating that increasing the angle of attack can help overcome negative lift effects. Figure 4.6 illustrates these dynamics, emphasizing that intermediate blade angles may be more effective in enhancing lift performance than a flat (0°) configuration, particularly for optimizing the aerodynamics of compact wind energy systems.

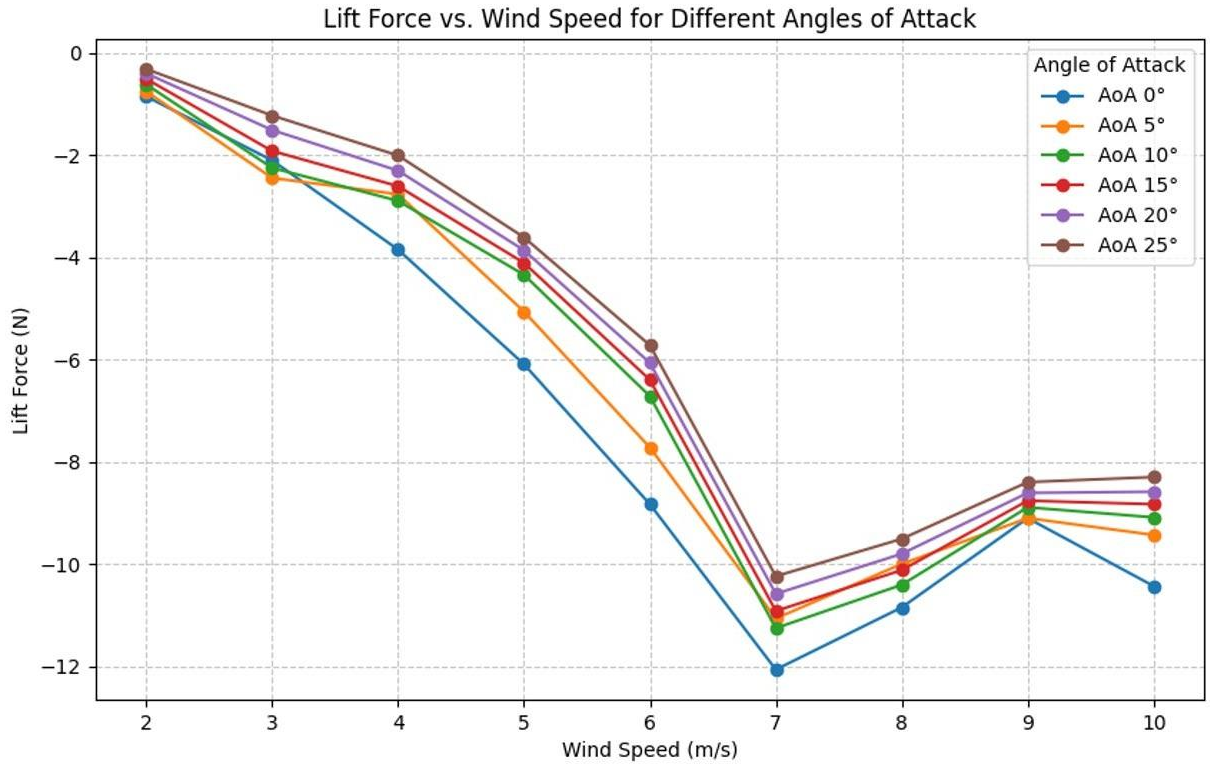

Figure 4.6: Lift performance profile under varying wind speeds and attack angles

4.6 Analysis of contour of pressure

4.6.1 Aerodynamic pressure behavior at zero angle of attack

At a 0° angle of attack, the pressure contours around the vertical-axis wind turbine (VAWT) reveals a predominantly symmetrical distribution across the blade surfaces as depicted in Figure 4.7. This symmetry results in low aerodynamic efficiency, as it inhibits the formation of a strong pressure gradient between the windward and leeward sides. Without sufficient lift or torque, the turbine struggles to generate rotational motion under these conditions. The absence of notable pressure differentials significantly limits the turbine's ability to convert wind energy into mechanical output. Moreover, the contour visualization reveals an elongated wake zone trailing behind the rotor, dominated by low-pressure pockets that increase turbulence and diminish the turbine's ability to capture energy efficiently. These extended wake formations indicate poor flow recovery, meaning that a substantial portion of the available wind energy passes through without contributing to mechanical output. In some regions, particularly near the blade surfaces, localized low-pressure areas introduce opposing drag forces, further inhibiting rotational motion. Due to these aerodynamic limitations, the turbine struggles to initiate self-rotation at this AoA, often requiring stronger

wind conditions or auxiliary starting mechanisms. The combined effect of insufficient pressure variation increased aerodynamic drag, and turbulent wake formation contributes to poor performance and energy conversion efficiency at 0° AoA.

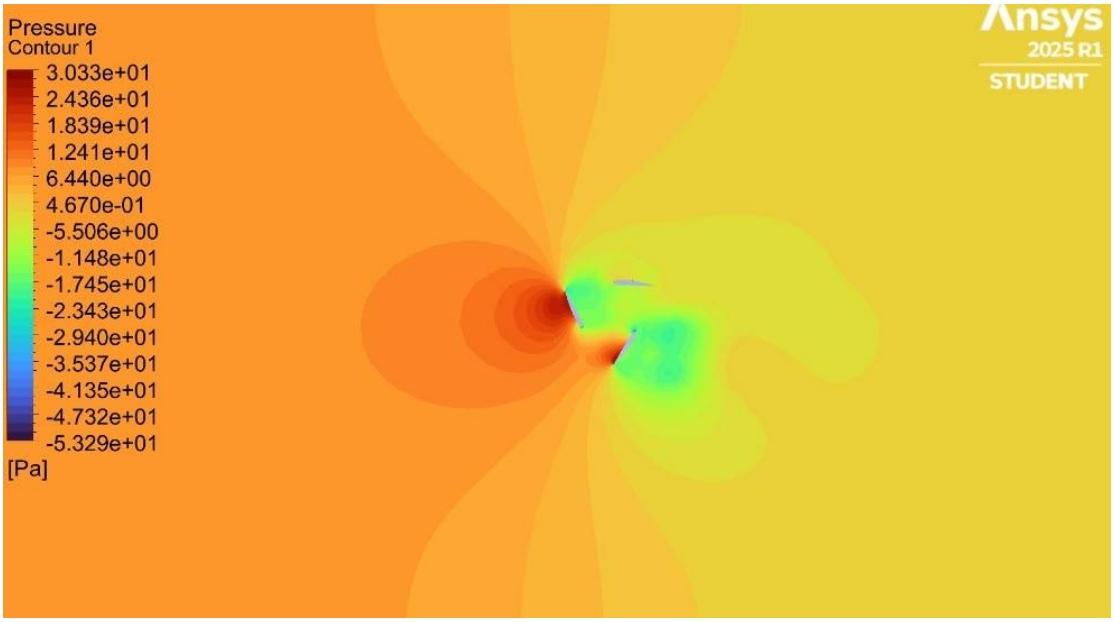

Figure 4.7: Pressure Distribution Profile for 0° Blade Orientation

4.6.2 Pressure field behavior at 5° blade inclination

At a blade inclination of 5°, the pressure contour map illustrates a modest improvement in aerodynamic behavior when compared to the 0° configuration. There is evidence of an emerging pressure differential across the blade surfaces higher on the wind-facing side and lower on the opposite side implying the onset of lift and some degree of torque generation. However, the pressure variations remain relatively mild, indicating that the airflow around the blades has not yet reached optimal aerodynamic efficiency. Regions of low pressure are visible in the wake zone behind the blades, signifying ongoing vortex shedding and localized energy dissipation. Although the wind turbine begins to harness airflow more effectively than in the neutral position, the generated lift remains suboptimal and drag-induced resistance still impairs performance. This intermediate aerodynamic condition suggests that while functionality has improved, 5° is not yet the ideal angle for peak turbine output, as demonstrated by the pressure contours in Figure 4.8.

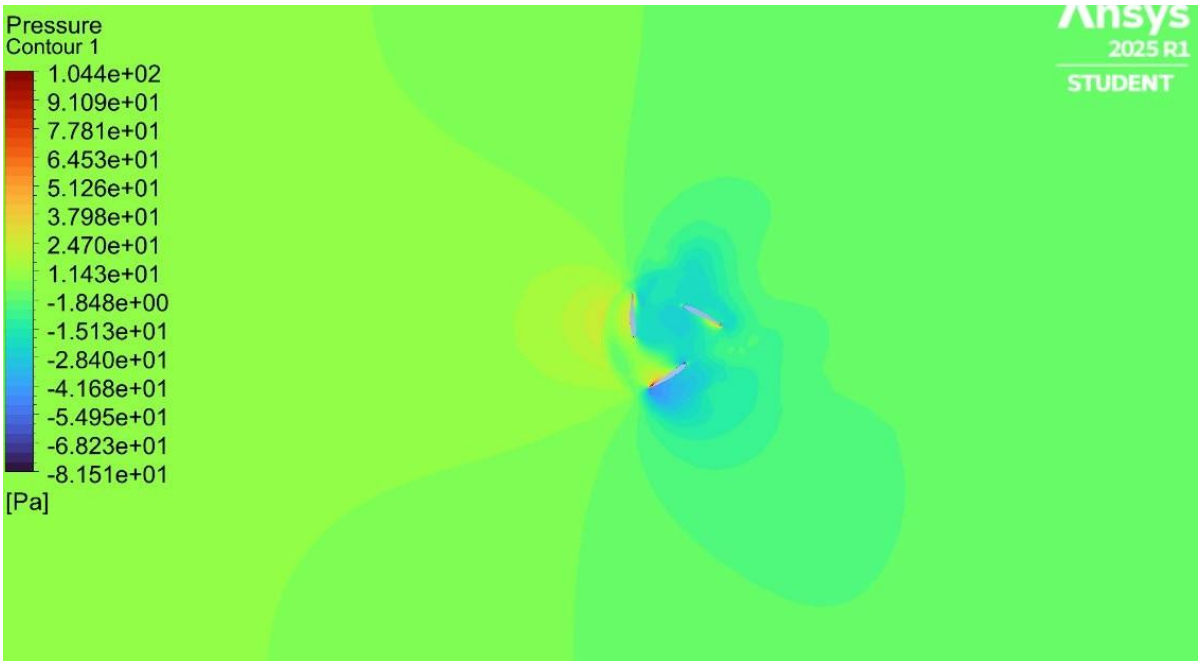

Figure 4.8: Pressure distribution pattern around blades at 5° blade inclination

4.6.3 Pressure contour interpretation at 10° angle of attack

Positioning the turbine blades at a 10° angle of attack leads to a marked improvement in aerodynamic performance when compared to smaller angles. At this configuration, the pressure differential between the windward and leeward sides becomes more pronounced, enhancing lift generation and resulting in greater torque output. This optimized flow interaction promotes more efficient energy conversion and supports stable rotational motion, making 10° a favorable setting for maximizing turbine performance under moderate wind conditions. The pressure contour analysis reveals a marked difference in surface pressure between the leading (wind-facing) and trailing (leeward) edges of the blades. This pronounced pressure gradient contributes to a substantial lift force, which enhances the ability of the turbine to change wind energy into rotational motion. On the forward-moving blade, high-pressure zones develop on the side facing the wind, while the opposite side shows reduced pressure, resulting in a favorable net aerodynamic force. These conditions lead to stronger rotational drive.

Nonetheless, some negative pressure zones remain on the retreating blade sections, introducing minor drag that can slightly hinder performance. The downstream wake pattern appears more streamlined compared to lower AoAs, suggesting improved flow behavior and reduced turbulent losses. Flow separation begins to emerge closer to the

blade's trailing edge but does not yet disrupt turbine function. The lift achieved at this configuration is significant, with a balanced drag increase that remains within functional limits. Therefore, the 10° setting appears to be close to an optimal aerodynamic condition for achieving efficient energy harvesting in small-scale VAWTs, as illustrated in Figure 4.9.

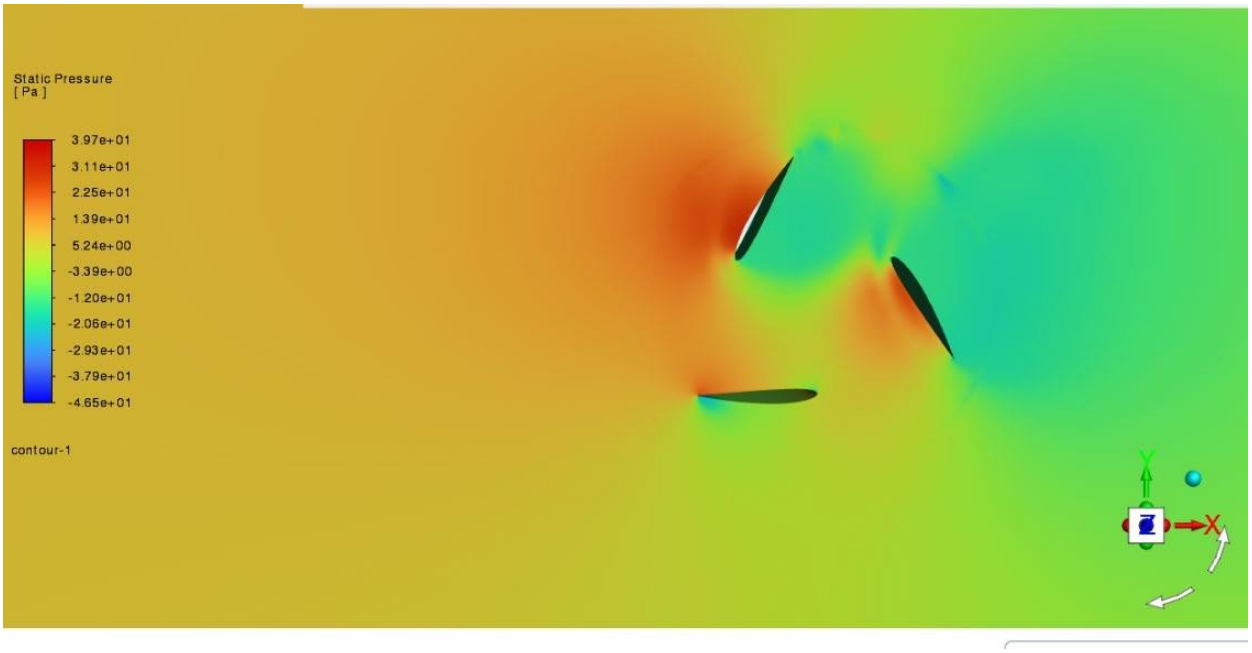

Figure 4.9: Blade Surface Pressure Mapping at 10° Airfoil Orientation

4.6.4 Surface pressure evaluation at 15° angle of attack

At a blade inclination of 15°, the pressure contour plot for the pico-scale wind turbine shows distinct pressure gradients across the blade surfaces. Elevated pressure zones, shown in warm colors (red to orange), appear on the wind-facing sides where the incoming airflow makes direct contact. In contrast, the opposite surfaces the leeward sides display cooler colors (green to blue), representing areas of reduced pressure caused by accelerated airflow and emerging flow instability. The trailing region of the turbine shows an elongated wake with noticeable pressure loss, suggesting ongoing vortex detachment and partial energy recovery from the wind stream.

At this angle, aerodynamic behavior begins to shift as flow separation intensifies, triggering the development of vortices within the wake. Although the blades continue to produce meaningful lift, the simultaneous rise in drag begins to compromise aerodynamic performance. The turbulent wake structure introduces additional resistance, marking the

early stages of stall where aerodynamic efficiency, measured by the lift-to-drag ratio, begins to deteriorate. These features are illustrated in Figure 4.10.

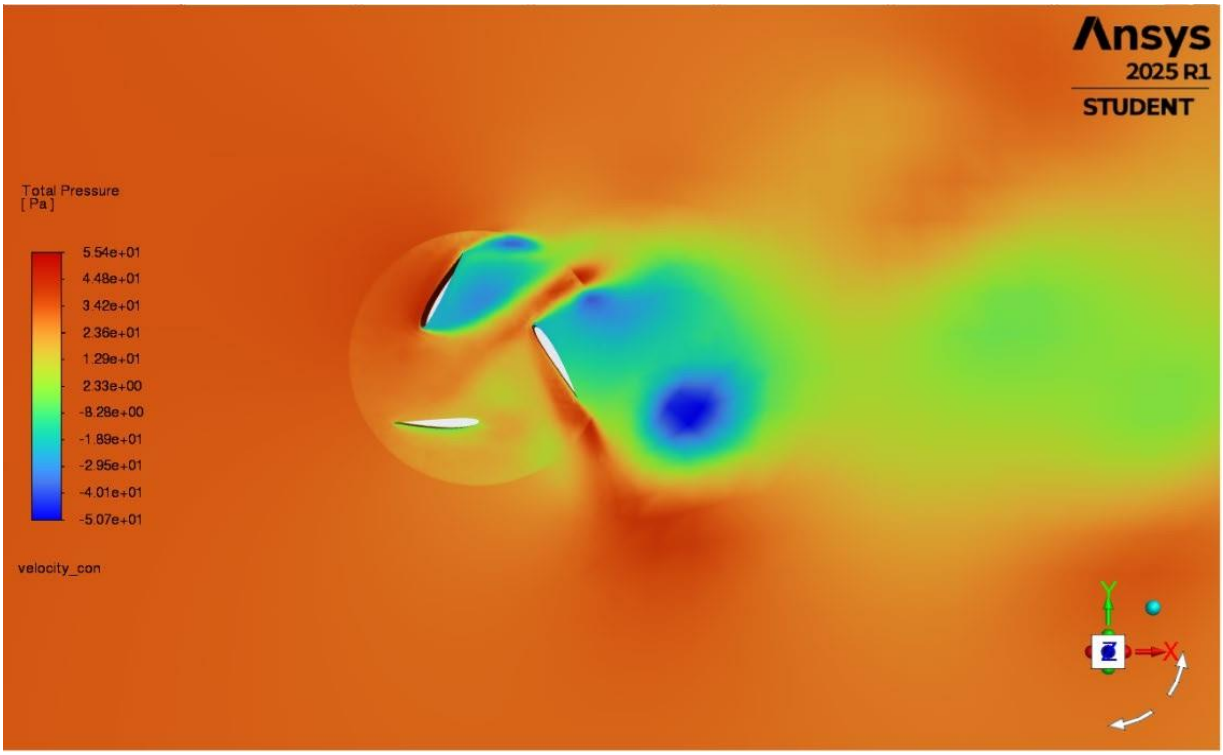

Figure 4.10: Pressure distribution pattern at 15° angle of blade orientation

4.6.5 Analysis of pressure at 20° AoA

With the angle of attack set to 20°, a noticeable decline in aerodynamic efficiency is observed. The airflow fails to remain attached to the blade surfaces, resulting in early separation and the formation of pronounced wake regions. Figure 4.11 captures this behavior, where intensified turbulence and swirling vortices dominate the downstream flow. On the leeward side of the blades, expanded zones of low pressure emerge, highlighting poor lift development and diminished aerodynamic performance. This airflow instability marks the transition into stall conditions, where the turbine loses its ability to efficiently convert wind energy into mechanical output. The drag force also increases considerably at this stage, intensifying rotational resistance and signaling reduced operational effectiveness.

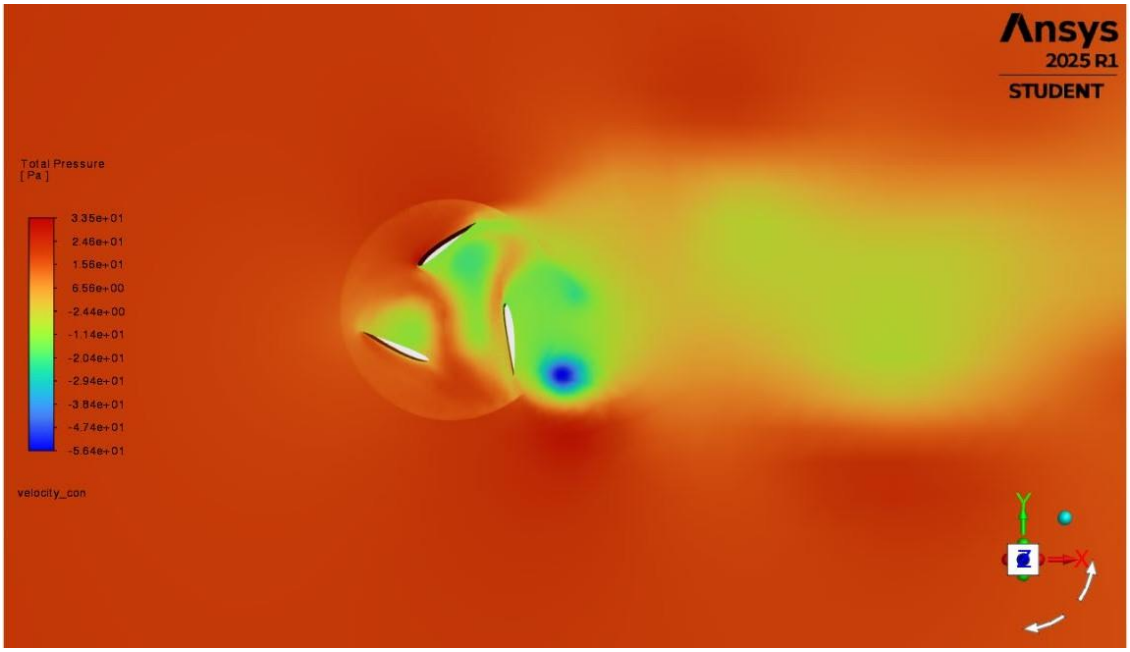

Figure 4.11: Visualized pressure distribution for 20° angle of attack

4.6.6 Pressure distribution characteristics at 25° angle of attack

When the blade is oriented at a 25° angle of attack, its aerodynamic efficiency declines drastically. The flow detachment from the surface becomes more pronounced, indicating the presence of a strong stall condition. As illustrated in Figure 4.12, the pressure field around the blade reveals an expanded region of low pressure downstream, a clear indication of intensified vortex formation and flow instability.

At this stage, airflow fails to remain attached to the blade's profile, leading to premature separation. This generates broad turbulent zones and circulating flow pockets on the downstream side, causing a pronounced drop in lift. The resulting aerodynamic load is primarily dominated by drag, as the recirculating air masses exert strong resistive forces against the blade's forward motion. This degree of stalls marks a critical loss in aerodynamic function. The blade can no longer sustain efficient lift generation and instead experiences overwhelming drag that suppresses rotation. Consequently, the turbine's capability to convert wind energy into mechanical rotation diminishes, as much of the

Incoming energy is dissipated in chaotic flow patterns rather than being productively harnessed.

In summary, a 25° angle of attack results in significant aerodynamic penalties, with high

drag, deep stall effects, and minimal lift production, rendering this configuration highly ineffective for energy extraction.

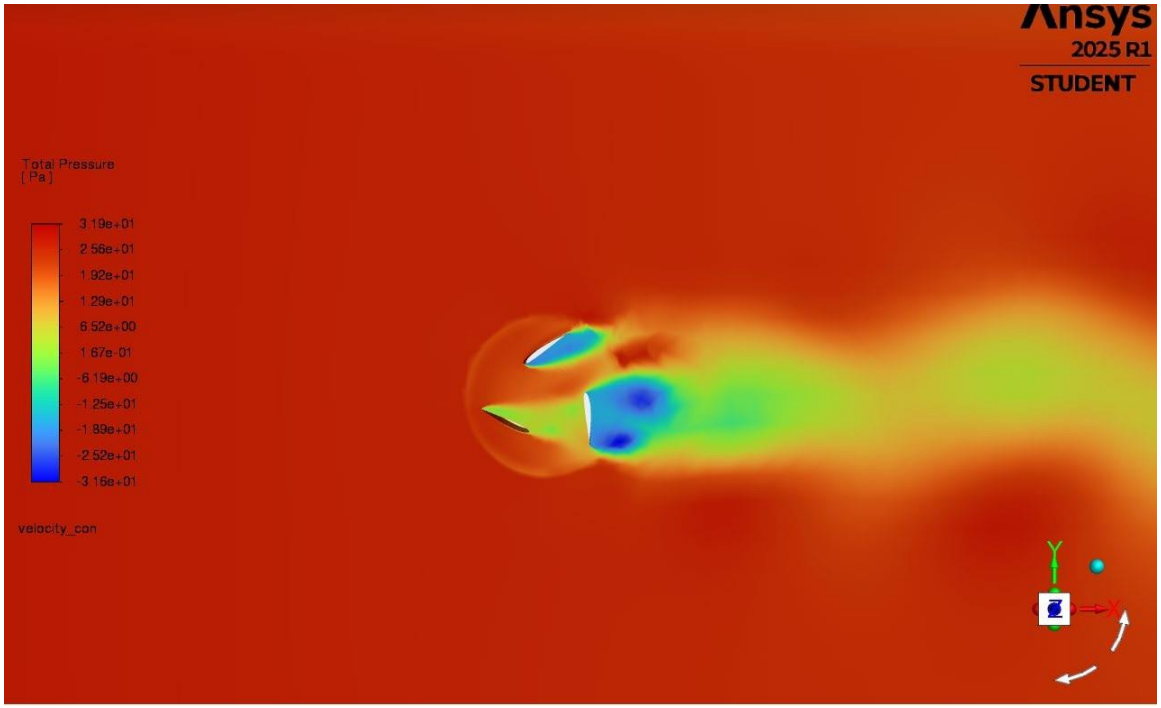

Figure 4.12: Pressure field distribution around the turbine blade at 25° angle of attack, illustrating intense flow separation and a broad low-pressure wake.

4.7 Multi-objective performance optimization

The balance between achieving high power output and minimizing the initial torque required to initiate rotation is a critical consideration in turbine design. This trade-off is visualized in the optimization chart, which compares power generation against the torque threshold necessary for startup. To determine the optimal angle of attack (AoA), Equation 4.4 defines an efficiency index expressed as the ratio of power to starting torque. Higher values of this index correspond to more desirable operating conditions, as they reflect greater energy output for each unit of required torque.

$$Efficiency = \frac{Power}{Start\ torque} \tag{4.4}$$

As depicted in Figure 4.13, the heatmap presents variations in the power-to-torque ratio across multiple wind speeds and blade angles. The color scale transitions from blue to

red, representing a gradient from low to high efficiency. Among the various configurations, the AoA of 10° consistently delivers superior performance. This is especially prominent at wind velocities of 9 m/s (73.96) and 10 m/s (72.00), where the turbine achieves its most favorable energy-to-torque output. In contrast, blades positioned at lower AoAs (0° to 5°) show diminished effectiveness. At these settings, the generated power is insufficient relative to the torque required for rotation, indicating inefficient energy conversion.

Conversely, higher AoAs (15° to 25°) tend to increase the startup resistance significantly without yielding proportionate power improvements. For instance, at 25° AoA and 2 m/s, the efficiency ratio drops to 6.81, suggesting excessive mechanical resistance coupled with poor energy yield. Based on this analysis, 10 AoA emerges as the most effective configuration for ensuring strong energy output with low startup resistance. This makes it the most advantageous setting for improving both operational efficiency and turbine responsiveness under varying wind conditions.

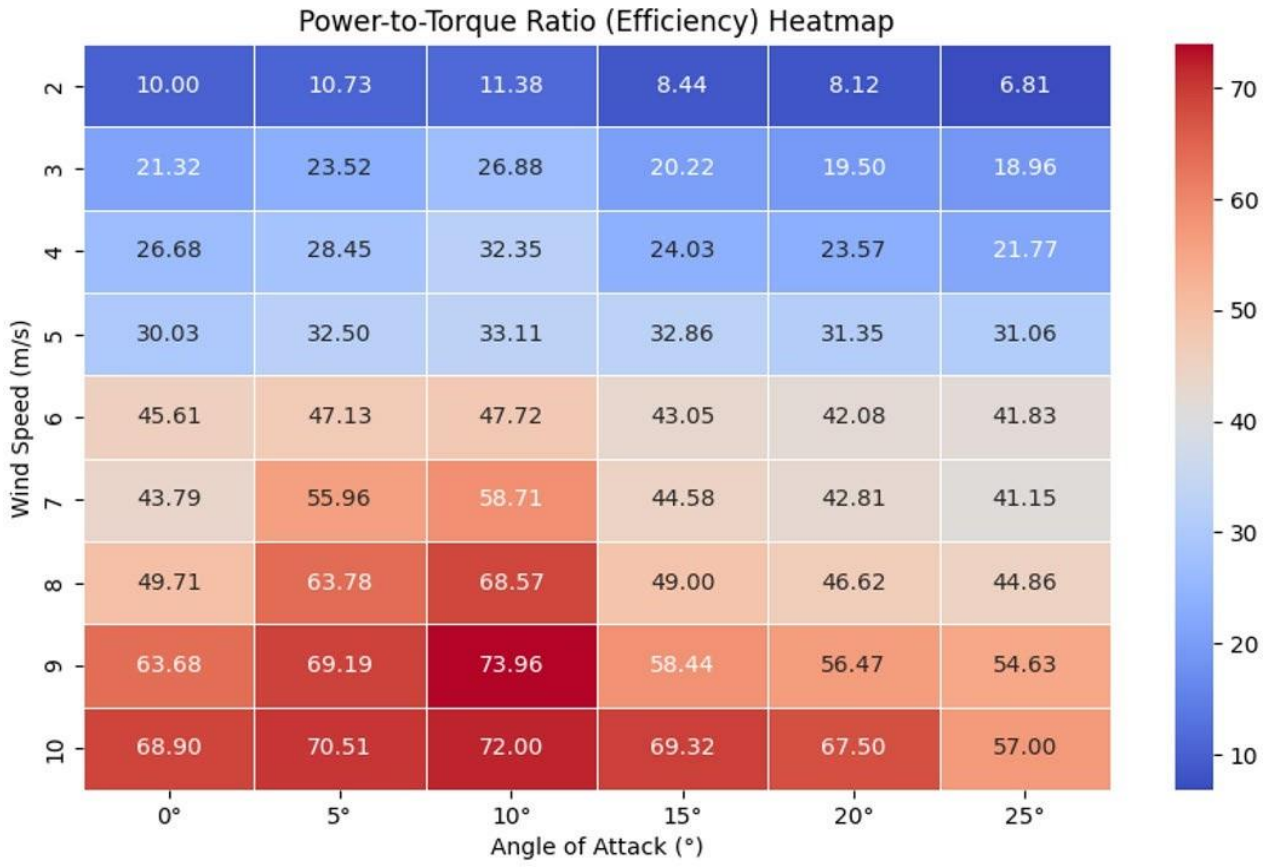

Figure 4.13: Heatmap illustrating power-to-torque efficiency across varying wind speeds and blade angles of attack. Red zones denote peak performance, while blue regions indicate reduced operational efficiency.

4.8 Numerical simulation with obstacle

To evaluate the impact of physical obstacles on the aerodynamic performance of a pico-scale vertical-axis wind turbine (VAWT), a set of transient simulations was conducted in ANSYS Fluent employing a six-degrees-of-freedom (6DOF) solver. The study examined various obstacle heights (ranging from 1.4 m to 2.5 m) and horizontal distances (from 1.4 m to 2.6 m) to simulate real-world environmental conditions. Key aerodynamic metrics, including torque (Nm), drag force in the x-direction (N), lift force in the y-direction (N), angular velocity (rad/s), and power output (W), were meticulously analyzed. Findings indicate that changes in obstacle configuration significantly affect turbine dynamics, highlighting the sensitivity of performance to surrounding geometry.

Specifically, higher obstacles consistently disrupt airflow, causing a noticeable decline in turbine efficiency as indicated by lower power outputs. Conversely, increasing the horizontal distance between the obstacle and the turbine improved aerodynamic flow characteristics, leading to enhanced lift generation and more favorable power production. The findings, summarized in Table 4.7, emphasize the importance of spatial positioning when installing wind turbines in terrains with obstructions. A careful balance between obstacle height and placement distance is essential for maximizing performance, particularly in rural or uneven landscapes where structural elements like fences or buildings are common.

Table 4.7: CFD results for a vertical-axis wind turbine positioned 1.4 m horizontally from a simulated ground hindrance.

Height (m)	Torque (Nm)	Drag Force (N)	Lift Force (N)	Angular Velocity (rad/s)	Energy Output (W)
1.40	0.80	6.80	0.85	6.50	5.20
1.53	0.70	7.90	-0.70	4.20	2.94
1.70	0.25	7.75	5.30	1.30	0.33
2.00	0.001	0.50	0.25	0.85	0.001
2.30	0.00	-0.01	0.12	2.20	0.00
2.50	0.00	-0.02	0.09	2.10	0.00

Table 4.8: CFD output for obstacle set at 1.8 m horizontal clearance from the turbine

Height (m)	Torque (Nm)	Drag Force (x)	Lift Force (y)	Rotational Speed (rad/s)	Mechanical Power (W)
1.40	0.95	6.44	0.90	6.80	6.47
1.53	0.87	7.84	-0.74	4.45	3.86
1.70	0.31	7.70	5.55	1.44	1.25
2.00	0.002	0.54	0.27	0.90	0.28
2.30	0.00	-0.01	0.13	2.37	0.00
2.50	-0.02	-0.02	0.10	2.30	-0.03

Table 4.8: Turbine simulation results with obstacle positioned 2.0meters away

Height (m)	Torque (Nm)	Drag Force (N)	Lift Force (N)	Angular Velocity (rad/s)	Power Output (W)
1.40	0.96	6.42	0.90	6.85	6.68
1.53	0.88	7.82	-0.74	4.45	3.92
1.70	0.32	7.70	5.56	1.44	1.28
2.00	0.003	0.54	0.26	0.90	0.002
2.30	0.00	-0.01	0.13	2.35	0.00
2.50	0.00	-0.02	0.1	2.25	0.00

Table 4.9: Aerodynamic performance at a 2.2 meters obstacle distance

Height (m)	Torque (Nm)	Drag (N)	Lift (N)	ω (rad/s)	Power (W)
1.40	1.00	10.04	0.27	6.90	6.90
1.53	0.90	6.52	0.05	5.22	4.70
1.70	0.35	5.31	0.63	4.49	1.57
2.00	0.03	0.34	-0.43	2.36	0.07
2.30	0.02	-1.29	0.44	1.93	0.04
2.50	0.03	0.04	1.50	1.00	0.03

Table 4.10: CFD analysis results for 2.4 m horizontal spacing from the barrier

Height (m)	Torque (Nm)	Drag Force (N)	Lift Force (N)	Rotational Speed (rad/s)	Power (W)
1.40	1.05	9.50	0.30	7.00	7.35
1.53	0.95	6.20	0.05	5.30	5.04
1.70	0.40	5.00	0.70	4.50	1.80
2.00	0.04	0.30	-0.40	2.40	0.08
2.30	0.03	-1.20	0.40	1.95	0.05
2.50	0.03	0.04	1.50	1.01	0.03

Table 4.11: Power and force response at 2.6meters obstacle offset

Height (m)	Torque (Nm)	Drag (N)	Lift (N)	ω (rad/s)	Power (W)
1.40	1.10	9.00	0.32	7.10	7.81
1.53	1.00	6.00	0.06	5.35	5.35
1.70	0.45	4.80	0.75	4.55	2.05
2.00	0.04	0.25	-0.35	2.45	0.10
2.30	0.03	-1.10	0.35	2.00	0.06
2.50	0.04	0.04	1.51	1.02	0.04

The simulation imagery highlights the aerodynamic disturbance created by the presence of an obstacle near the turbine. A concentrated high-pressure region forms in front of the obstacle marked in red where incoming wind decelerates upon impact, causing flow stagnation. Behind the obstacle, a distinct low-pressure wake emerges, shown in blue, signifying regions of separated flow and turbulent eddies. The vertical-axis wind turbine, placed in this transitional zone, encounters varying airflow characteristics depending on how close it is to the obstacle. These shifts in pressure distribution directly influence the forces acting on the blades and, consequently, the turbine's rotational speed and energy output. Taller obstacles or those placed nearer to the turbine tend to cause more

pronounced disruption, reducing aerodynamic efficiency and power generation.

CHAPTER FIVE
DISCUSSION OF RESULTS

5.1 Introduction

The aerodynamic performance of a pico-scale Darrieus-type vertical-axis wind turbine (VAWT) is significantly influenced by the angle of attack (AoA) of its blades and the incoming wind speed. These factors govern the distribution and magnitude of aerodynamic forces, impacting lift, torque production, and the turbine's efficiency in converting wind energy into mechanical power. Using Computational Fluid Dynamics (CFD), this study evaluated key performance metrics—torque, power output, and operational efficiency—across wind speeds of 2–10 m/s and AoAs of 0°–25°, with a focus on applications in South Africa. This analysis interprets the simulation results, linking them to existing research and emphasizing practical implications for decentralized energy systems, particularly in under-electrified rural areas. Additionally, it explores the broader role of pico-scale VAWTs in the renewable energy landscape, providing technical insights for system optimization and identifying opportunities for further investigation.

5.2 Wind speed considerations

Accurate characterization of wind speed is critical for assessing the feasibility of wind-powered systems and understanding atmospheric dynamics. In South Africa, wind patterns, as documented by the Wind Atlas for South Africa (WASA) and the South African Weather Service (SAWS), exhibit significant regional variability driven by geography and topography. Coastal provinces, particularly the Western and Eastern Cape, experience higher wind velocities, often exceeding 8 m/s. For example, Cape Point records high-wind events 42.1% of the time, highlighting its strong potential for wind energy applications. In contrast, inland regions like Gauteng and the Free State have lower wind speeds with fewer high-speed airflow events, impacting the design and economic viability of wind systems in these areas. WASA's dataset, based on measurements at 100 m above ground level and organized by geographic node, includes Weibull distribution parameters (e.g., shape parameter k = 2) to enable frequency analysis of wind events. This supports statistical modeling of wind behavior for engineering and energy planning. Table 5.1 provides a synthesized overview of estimated wind frequency distributions across hypothetical settings, derived from regional mean wind speeds and standard Weibull parameters.

Table 5.1: Estimated wind event frequencies for sample regions using a Weibull shape factor of 2 and regional mean wind values (Adapted from Seguro and Lambert, 2000)

Classification of Area	Average Wind Speed (m/s)	Calm Winds Frequency (%)	Strong Wind Occurrence (%)
Coastal Exposure	6.9 m/s	20% occurrence	42% active
Continental Interior	4.5 m/s	75% occurrence	<1% active
Wind Corridor	9.0 m/s	30% occurrence	10% active

Additional insights into regional wind behavior are outlined in Table 5.2, which compiles comprehensive wind characteristics for various provinces across South Africa. The dataset encompasses key wind characteristics such as minimum, maximum, and average wind speeds. It also details the percentage of time wind speeds fall below 4 m/s, rise above 8 m/s, or align with other critical operational benchmarks relevant to turbine performance. This information is critical for assessing site suitability, turbine selection, and performance modeling under localized conditions.

Table 5.2: Summary of wind speed metrics and frequency distribution across South African provinces *(Wind Atlas for South Africa – WASA)*

Region	Min Wind Speed (m/s)	Max Wind Speed (m/s)	Mean Wind Speed (m/s)	% Time v < 4 m/s	% Time v > 8 m/s	% Time v < 6 m/s	% Time v > 6 m/s
Gauteng	1.5	5.5	3.5	54.60%	1.7%	90.0%	10.0%
Limpopo	2.0	6.0	4.0	54.60%	4.3%	82.9%	17.1%
Mpumalanga	2.0	6.0	4.0	63.90%	4.3%	82.9%	17.1%
Pell	2.0	6.0	4.0	46.20%	4.3%	82.9%	17.1%
Northwest	2.5	6.5	4.5	39.50%	8.3%	75.2%	24.8%
Free State	3.0	7.0	5.0	39.50%	13.4%	67.8%	32.2%
KwaZulu-Natal	3.0	7.0	5.0	22.60%	13.4%	67.8%	32.2%
Northern Cape	4.0	8.0	6.0	17.80%	24.7%	54.6%	45.4%
Hydra Cluster	4.0	8.0	6.0	29.50%	24.7%	54.6%	45.4%
Eastern Cape	5.0	9.0	7.0	29.50%	36.1%	43.8%	56.2%
Western Cape	6.0	10.0	8.0	54.60%	45.5%	35.7%	64.3%

A regional overview of wind frequency patterns across South Africa is illustrated in Figure 5.1, showing how specific wind speed intervals correspond to the duration of their occurrence. The distribution underscores distinct geographic differences in wind potential. For instance, areas like the Western Cape and Eastern Cape consistently experience elevated wind velocities, averaging around 8 m/s and 7 m/s respectively, with speeds

exceeding 8 m/s more than 36% of the time. Such favorable wind regimes position these regions as ideal candidates for deploying small-scale wind energy systems, particularly in underserved or off grids.

5.3 Relevance of wind conditions to Pico-Scale turbine deployment

The effectiveness of pico-scale vertical-axis wind turbines in off-grid applications is highly dependent on local wind characteristics. These turbines generally necessitate a cut-in wind speed defined as the minimum velocity required for power generation, ranging between 3 and 4 meters per second. In regions where wind conditions frequently fall below this range, wind energy alone is unlikely to meet energy demands consistently.

However, in provinces where sustained wind speeds exceed 6 m/s for a substantial portion of the year, pico-scale turbines can provide a stable and decentralized power supply, making them particularly useful for rural electrification projects. In such areas, these systems can function as cost-effective alternatives to diesel generators or grid extension, offering a cleaner and potentially more resilient energy source. To maximize reliability, especially in transitional wind zones, these turbines can also be integrated with solar PV panels or battery banks, forming a hybrid microgrid system suited for remote or underserved areas.

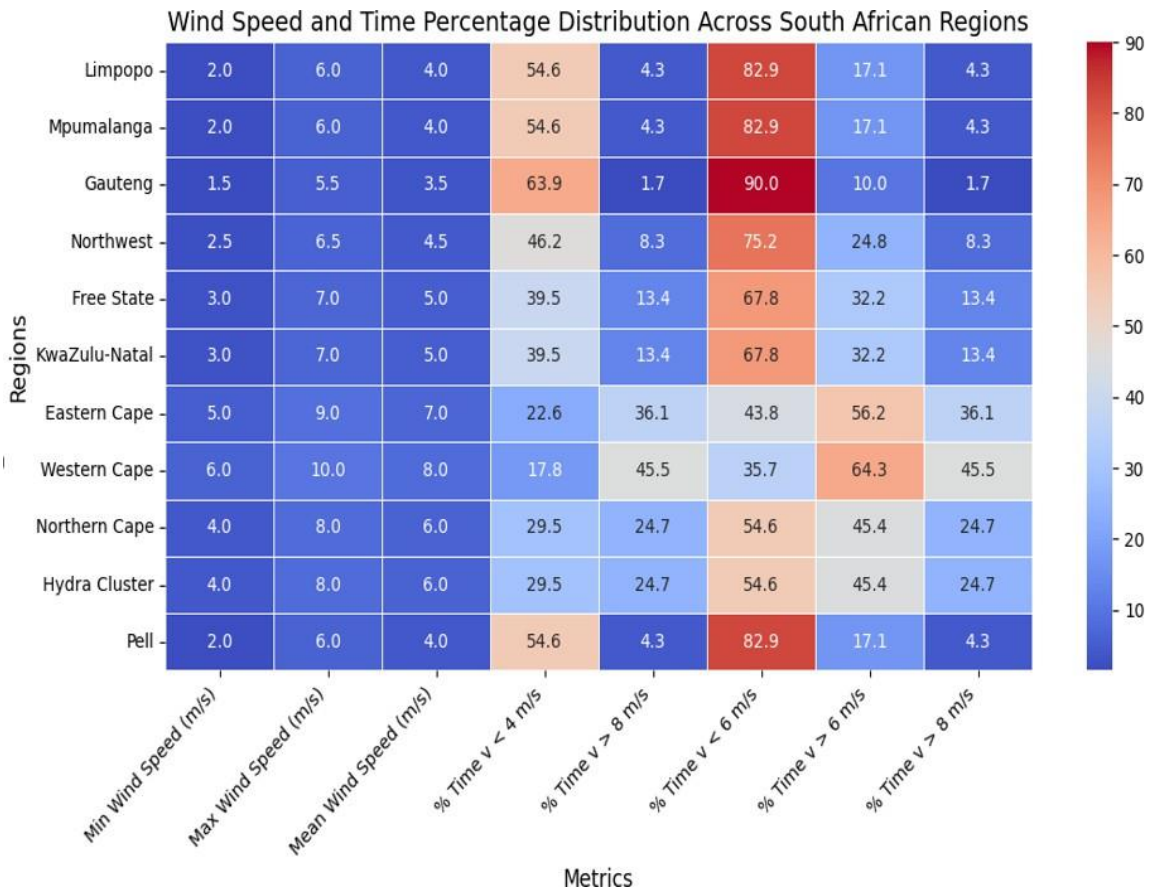

Figure 5.1: Frequency distribution of wind speeds across various South African regions

5.4 Technical feasibility for electrifying off-grid communities

Providing electricity to rural and isolated settlements presents significant infrastructural and financial challenges, especially where national grid extension is unviable. In such cases, decentralized energy systems become essential. Small-scale wind turbines particularly pico-scale vertical-axis models offer a viable option for addressing basic energy needs in these areas. This study evaluates several technical considerations that affect the practical deployment of these systems in rural environments.

5.4.1 Energy output versus rural demand

Simulation results revealed that the turbine's maximum achievable power output was approximately 38.30 watts. While this value may appear modest, it is adequate for low-consumption applications typical of off-grid households. Examples of such uses include:

- Supplying electricity to LED lighting units (commonly rated at 10–15 W), ensuring

illumination for two to four rooms.

- Charging small battery-powered devices, such as mobile phones, which are critical for communication and mobile banking in remote communities.
- Powering low-demand electronic systems, including agricultural sensors, basic weather stations, or internet-of-things (IoT) devices used in precision farming.

However, the turbine's capacity falls short for high-demand appliances like refrigerators (100–200 W) or electric fans (50–100 W). In practical terms, the turbine can operate three to four LED bulbs simultaneously, but it cannot sustain the full power needs of a typical household without assistance from other sources. As a result, pico-scale wind systems are best applied in a supportive role, contributing to hybrid power setups that might include solar panels, battery banks, or fuel-based generators. This ensures energy availability remains stable, especially during periods of low wind activity. Table 5.3 outlines typical energy consumption patterns for essential equipment often found in rural households, alongside estimated usage durations.

Table 5.3: Estimated power consumption and usage duration of common household devices in rural areas (Adapted from Ye, Koch, & Ye, 2025)

Device	Energy Use (Watts)	Operational Duration (Hours)
5W LED Bulb	5	7–8
Smartphone Charger	5–10	3–6
Portable Radio	5–15	2–7
12V DC Fan	10–20	1.5–3.5
24" LED TV	20–30	1–1.5

5.5 Suitability of wind resource

Vertical-axis wind turbines (VAWTs) at the pico scale tend to perform optimally in settings where wind speeds consistently range from 6 to 8 meters per second, as this range supports stable energy output and efficient aerodynamic performance. These optimal conditions are frequently found in open rural zones and semi-urban corridors of South

Africa, particularly within the Southwestern Cape, Eastern Cape, and parts of the northeastern escarpment. In contrast, fluctuating wind patterns are common in certain inland provinces, where extended periods of low wind speeds (<4 m/s) often occur. This variability is especially pronounced in areas like the Northern Cape and Free State, where topography and seasonal influences contribute to inconsistent airflow. When wind speeds drop below 2 m/s, turbine functionality becomes severely limited, underscoring the need for site-specific evaluation before system deployment.

Locations such as Cape Town, Port Elizabeth, and select areas of the Eastern Cape offer more predictable wind conditions and are well-suited for standalone wind energy systems. Meanwhile, sheltered valleys, forested regions, and mountain belts such as the Drakensberg may experience highly erratic winds, which compromise system reliability. In such settings, incorporating battery storage or hybrid generation systems is often necessary to stabilize power delivery and maintain energy access.

5.6 Placement strategy for pico-scale VAWTs near obstacles

Performance data from Tables 4.7 through 4.12 demonstrate the impact of obstacle proximity and height on the aerodynamic performance of a pico-scale Darrieus vertical-axis wind turbine (VAWT). The optimal configuration, with the turbine placed 1.8 m from a

1.4 m high obstacle, yielded a torque of 0.9511 Nm, an angular velocity of 6.8011 rad/s, and a power output of 6.47 W, indicating efficient wind energy capture with minimal aerodynamic interference. This power level is sufficient for off-grid applications, such as LED lighting and small electronics. When the obstacle was closer (1.4 m distance) at the same height, power output dropped to 5.20 W due to increased turbulent wake effects. Increasing obstacle height to 1.53 m and 1.7 m at the 1.8 m distance further reduced performance, with power outputs of 3.86 W and 1.25 W, respectively, driven by heightened drag and unstable lift from turbulence and airflow disruption.

Wider spacing from taller obstacles provided marginal improvements. At a 2.6 m distance and 1.7 m obstacle height, power output increased to 2.05 W, still below the optimal configuration but better than closer placements. Beyond a 1.7 m obstacle height, performance deteriorated significantly; at 2.3 m height and 1.8 m spacing, torque approached zero, and power output fell to 0.28 W. At a 2.5 m obstacle height, a negative power output of −0.03 W was recorded, indicating reversed flow and complete aerodynamic breakdown. These results highlight that obstacle size and placement

critically affect airflow, with improper configurations causing wake zones and vortex shedding that reduce efficiency or reverse turbine rotation. Figures 5.2 and 5.3 further illustrate these interactions, using 3D surface and contour plots to map power output as a function of obstacle height and distance, identifying regions of peak and diminished performance.

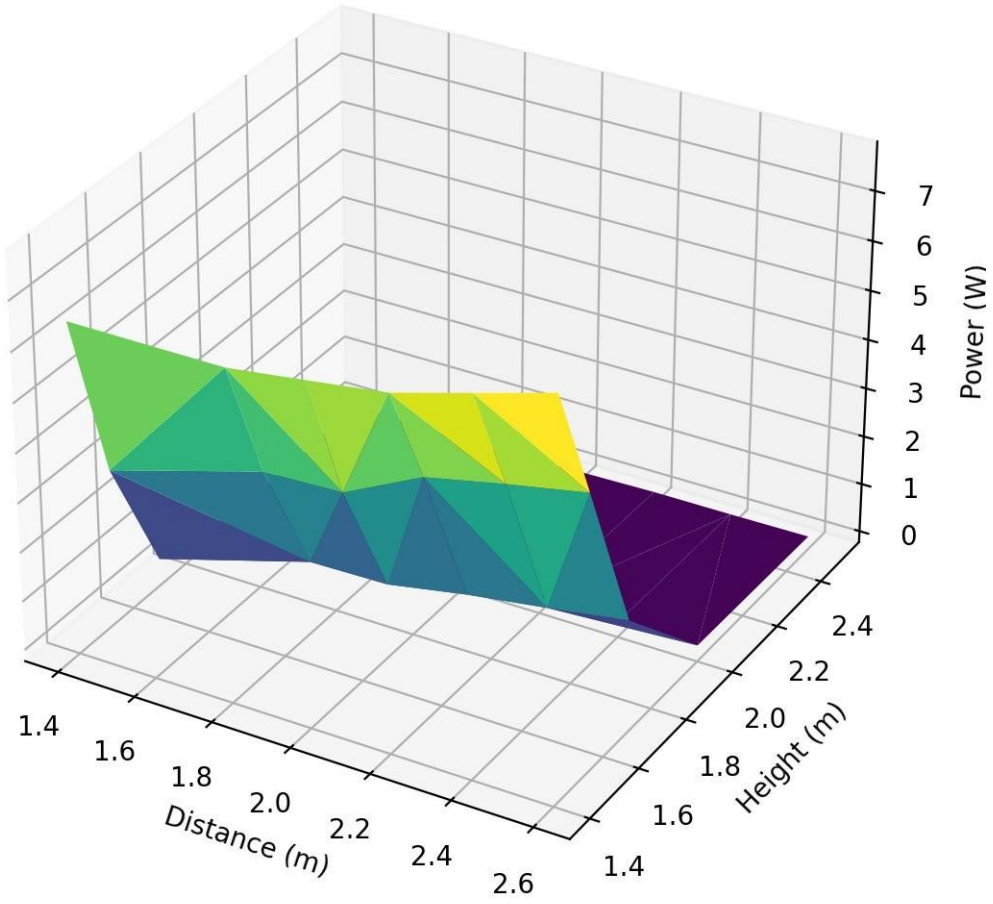

Fig. 5.2. 3D surface plot illustrates the interaction between obstacle distance, height, and resulting power output.

The graph captures how turbine performance evolves across obstacle distances ranging from 1.4 m to 2.6 m and heights between 2.0 m and 2.6 m. Power output, which spans from 3 W to 7 W, generally improves with increased separation and moderate obstacle elevation, reflecting reduced wake interference and more stable wind flow toward the rotor.

Fluctuations in lift force such as the downward (negative) lift detected at a 1.53 m obstacle height and the amplified lift at 1.7 m reveal the complex aerodynamic behavior shaped by both obstacle elevation and horizontal spacing. At 1.53 m height with a 1.8 m gap, the occurrence of negative lift indicates opposing forces acting against rotor motion, thereby

impeding rotation. Conversely, although a pronounced positive lift was recorded at 1.7 m, it failed to produce substantial power output due to the low rotational speed of only 1.4366 rad/s. This pattern corresponds with findings by Seifi Davari et al. (2024), who observed that pico-scale vertical-axis wind turbines tend to encounter inconsistent lift behavior, especially when subjected to low wind speeds or turbulent inflow.

A clearer trend emerges when considering obstacle proximity: increasing the gap between the turbine and obstruction leads to marked improvements in energy generation. For example, when the separation was extended from 1.4 m to 2.6 m (with the obstacle maintained at 1.4 m in height), the output grew from 5.20 W to 7.81 W. This demonstrates that maximizing clearance from nearby structures is vital for mitigating wake effects and achieving higher operational efficiency.

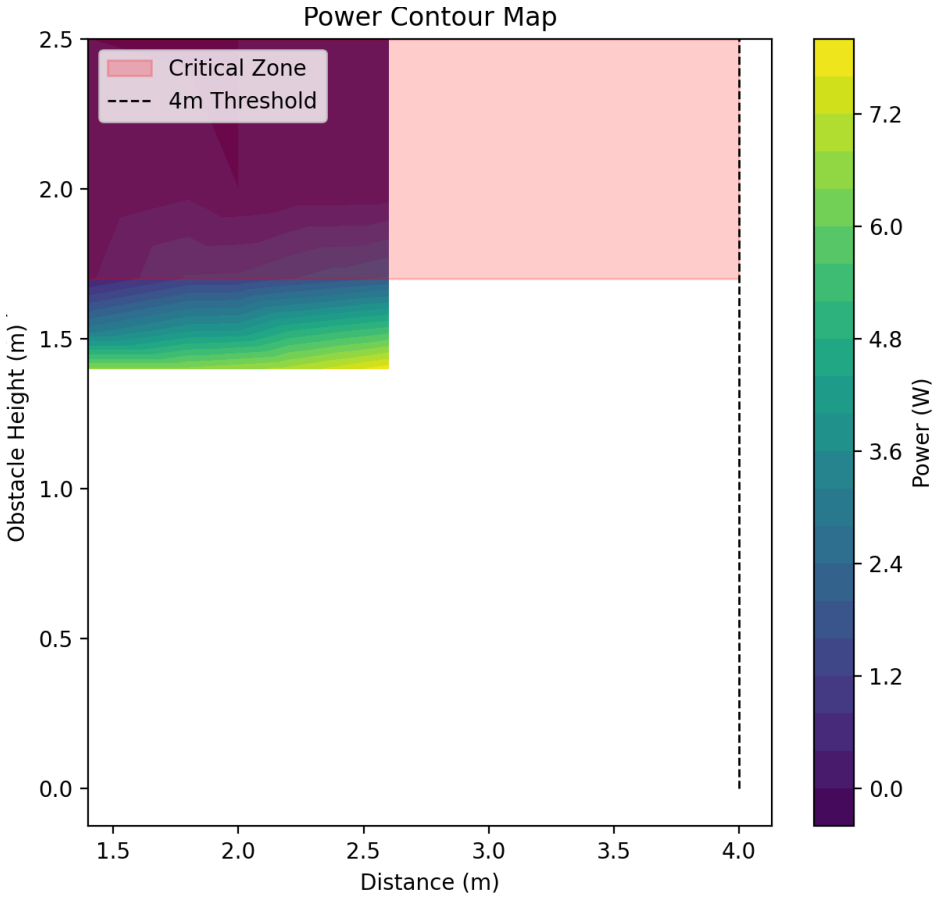

Figure 5.2: Contour representation showing how obstacle height and proximity affect power generation in a Compact Vertical-Axis Wind Turbine System (VAWT).

The plot maps the influence of obstacle elevations ranging from 0 to 2.5 meters and

horizontal distances between 1.5 m and 4.0 m, with corresponding power outputs from 0 to 7.2 watts. A distinct low performance “critical zone” emerges where obstacles exceed 2.0 m in height and are placed closer than 2.5 m, resulting in power outputs below 1.2 W. Beyond this region, particularly at moderate heights and greater spacing, performance steadily improves, indicating more favorable aerodynamic conditions.

5.7 Real-world operational context

Although this study is grounded in computational fluid dynamics (CFD) simulations performed under unsteady flow conditions, such models do not fully replicate the complexities of outdoor environments. Real-world settings, particularly in rural areas, often present irregular wind flows, sudden gusts, and fluctuating turbulence, all of which can cause deviations from predicted turbine performance. These environmental fluctuations, along with other variables like structural fatigue and thermal expansion, are not entirely captured in the simulation framework.

To mitigate these limitations, it is crucial to conduct physical field trials. On-site evaluations would provide more accurate insights into the turbine’s operational integrity under real environmental stressors. For instance, field data could reveal how blades respond to high-frequency vibrations, how components withstand exposure to dust or humidity, and how overall efficiency varies over extended periods. These aspects are vital for ensuring that pico-scale turbines are dependable in the often harsh and isolated settings where they are intended to operate.

5.8 Economic viability and deployment considerations

The practicality and cost-effectiveness of using pico-scale Darrieus turbines for powering rural areas hinge on multiple interrelated considerations, as demonstrated by the findings of this research and current technological advancements.

- **Minimal upkeep and lower running expenses:** Incorporating features like helical blades helps reduce structural fatigue by limiting vibration and stress peaks. Likewise, simplified turbine layouts such as Savonius-Darrieus hybrids require fewer moving components, which decreases the need for regular maintenance, an important factor in regions with limited technical access.
- **Long-term environmental and financial benefits:** Pico-scale turbines help

phase out the use of expensive and polluting diesel generators. When deployed alongside solar panels or energy storage systems in isolated locations, they offer not only environmental advantages but also significant savings over time.

- **Expandability and energy self-sufficiency:** While designed for low-power outputs, these turbines are based on scalable technologies that can be adapted for energy systems under 50 kW. In areas with gentle wind conditions, vertical-axis turbines often outperform horizontal models in investment returns, supporting decentralized and community-driven electrification projects.
- **Affordable energy generation:** Enhancing the angle of attack (AoA) within the 5° to 10° range leads to improved power output and reduced aerodynamic inefficiencies. This aerodynamic optimization contributes to lowering the overall cost per unit of electricity, making small-scale installations more economically attractive.

5.9 Deployment potential in rural settings

The application of compact Darrieus wind turbines extends beyond theoretical viability and into a range of practical, real-world energy solutions:

- **Standalone Power for Isolated Installations:** In remote setups such as for environmental sensors, communication outposts, or rural weather monitoring these turbines can deliver reliable and sustainable electricity. Since they can begin generating power at wind speeds as low as 2 m/s, they reduce the dependency on fuel-powered generators or the logistical burden of frequent battery replacements in harsh or difficult terrains.
- **Integration within Local Energy Networks:** Small-scale vertical-axis wind turbines can be embedded in localized microgrid setups to enhance energy stability in underserved or peri-urban regions. Their omnidirectional wind capture capability allows them to perform in locations with shifting or turbulent wind flows, a typical scenario in community-scale renewable systems.
- **Electricity Support for Remote Communities:** These compact turbines are effective in supplementing power availability in isolated areas by operating low-energy essentials such as LED lamps (10–15 W) and phone chargers. Designed to work well in moderate breezes (6–8 m/s), they are particularly useful in the area with limited access to the national grid. However, their limited capacity of 38.3 W restricts their ability to run larger appliances like cooling units or fans, making them

more appropriate when combined with solar panels or backup batteries.

5.10 Operational prerequisites and environmental challenges

Effective implementation of pico-scale turbines in rural electrification projects is subject to specific environmental and technical conditions.

- **Climatic and Environmental Exposure:** Harsh outdoor elements including dust accumulation, moisture infiltration, and temperature extremes can undermine turbine performance. Using rugged materials and surface treatments enhances durability, while on-site testing is crucial to confirm that computer simulations accurately reflect operational behavior in these challenging environments
- **Setup Requirements:** Achieving the ideal blade inclination around 10° may necessitate accurate positioning, which can raise setup costs and complexity, especially in rural zones lacking technical expertise. However, newer twisted-blade models are easier to install, even on rooftops or within confined spaces, broadening their application in both village and suburban contexts.
- **Upkeep Needs:** To maintain functionality, especially under turbulent or gust-prone conditions, routine checks for blade condition are necessary. In settings where engineering support is scarce, simplified systems with minimal moving parts, like Savonius-Darrieus hybrids offer a more robust and user-friendly alternative.
- **Conditions of Wind:** These turbines perform most efficiently when exposed to wind speeds between 6 and 8 m/s, conditions typically found in open countryside or semi-urban zones. While operation is still possible at reduced speeds (2–4 m/s), efficiency noticeably drops. Choosing an appropriate installation site is therefore essential, particularly in areas surrounded by trees or other natural barriers that disrupt airflow.

5.11 Benchmarking against existing technologies

Findings from this research offer both consistencies and contrasts when evaluated alongside existing studies on vertical-axis wind turbines. Ahmudiarto et al. (2019) reported that a vertical-axis wind turbine (VAWT) optimized with a NACA 4212 blade profile delivered over 160 W of power at a wind speed of 6 m/s, achieving a power coefficient (Cp) in the range of 0.3 to 0.4. In contrast, the current study recorded a maximum output of 38.3 W, a disparity likely influenced by variations in rotor size, blade geometry, or

simulation parameters. Similarly, Zouzou et al. (2019) observed Cp values within a comparable range during experiments with a variable-pitch Darrieus turbine, which corresponds closely to the highest Cp of 0.419 achieved in this research under analogous wind conditions. These parallels confirm that adjusting the AoA within moderate limits enhances performance by improving the aerodynamic lift-to-drag ratio.

Conversely, experimental results from Danao et al. (2013) under fluctuating wind conditions revealed lower outputs an average of 15.35 W and a peak of 31.04 W reinforcing the idea that wind inconsistency significantly impacts turbine output and that simulation results often represent idealized scenarios. In related findings, Elizondo et al. (2016) confirmed that small turbines can reliably supply power across varying voltage loads but cautioned that they are not well-suited to meet full household energy needs unless complemented by storage solutions. Their observations align with the present conclusion that pico-scale models serve best as auxiliary power sources.

By contrast, Refan and Hangan (2012) documented a 470 W output from a small horizontal-axis turbine (HAWT) at 9 m/s, highlighting the superior scalability of HAWTs for higher energy demands. Nevertheless, the performance and affordability of VAWTs in low-wind or dispersed rural applications offer distinct advantages. The study's contextual emphasis on South Africa's wind patterns further supports the argument for localized design and deployment strategies. A side-by-side evaluation of various rural electrification technologies, including the turbines studied here, is presented in Table 5.4

Table 5.4: Comparative overview of rural energy solutions (adapted from Yadav & Bhalani, 2022)

Energy Source	Typical Output	Operational Reliability	Cost Implications	Environmental Considerations
Pico-Scale Wind Turbine	Up to approximately 40 W	Fluctuates based on wind consistency and local conditions	Low capital investment: maintenance needs may vary	Minimal emissions; environmentally friendly and sustainable
Photovoltaic Panels	Between 100–300 W per unit	Moderately reliable; dependent on sunlight availability	Medium upfront cost; expensive when paired with batteries	Produces no pollutants; ideal for clean energy generation
Micro-Hydro Systems	Typically in kilowatt range	Highly dependable if water flow is steady year-round	High installation cost: long-term upkeep is minimal	Green energy source; negligible environmental disturbance
Diesel Power Generators	Kilowatt-level capacity	Reliable if fuel is continuously available	Costly due to fuel usage and logistics	Significant greenhouse gas emissions contribute to pollution

Comparative data suggest that although pico-scale wind turbines offer a clean and low-cost energy option for limited power needs, their dependency on wind variability restricts their reliability and scalability. This underscores their practical application as complementary systems rather than standalone solutions in off-grid rural electrification strategies.

5.12 Responses to the study objectives

This segment addresses the central research questions regarding the practicality of deploying pico-scale Vertical Axis Wind Turbines (VAWTs) as decentralized power solutions in off-grid rural areas of South Africa. The findings draw upon insights from Computational Fluid Dynamics (CFD) simulations, alongside an assessment of regional wind speed distributions to determine system viability under realistic environmental conditions:

- Technical Feasibility

  Can small-scale VAWTs function effectively in high-wind rural settings?

  Yes, the study confirms that such turbines are technically feasible in locations like the Western and Eastern Cape, where wind speeds are consistently above 6 m/s for over half the day (56.2%–64.3%). Under these conditions, the turbine can deliver as much as 38.30 W at 9 m/s adequate for essential low-load devices like LED lamps (around 5 W) or mobile chargers (5–10 W). However, due to their limited capacity, these systems are better suited as part of hybrid configurations that include solar panels or battery storage to ensure reliability during calm periods.
- Low-Wind Output Capacity

  How much energy can the turbine generate in regions with minimal wind flow?

  Performance under low-speed wind (2 m/s) is constrained by insufficient lift and increased drag, resulting in power outputs below 5 W. In provinces such as Gauteng and Limpopo, that the wind speeds are usually below 4 meters/second almost every day (54.6%–63.9%), stand-alone turbine use is impractical without the support of complementary systems like batteries or solar arrays.
- Start-up wind speed threshold

  What is the minimum wind velocity required to initiate turbine rotation?

  The turbine's operational onset, or cut-in speed, lies around 3–4 m/s. Below this threshold, especially at an angle of attack (AoA) of 0°, the rotor fails to self-start. Therefore, turbines are more appropriate for regions like the Northern Cape, where mean wind velocities hover near 6 m/s, and less effective in zones like Gauteng, where the average is closer to 3.5 m/s.
- Operational duration

  For how many hours per day can a pico-scale VAWT reliably supply electricity?

  In consistently windy areas, such as the Western Cape, daily operation may span approximately 15.5 hours. In contrast, wind-scarce locations like Limpopo might support operation for only about 4.1 hours per day. Factors like turbulence and sudden gusts may further limit effective runtime, which supports the position of including storing systems to smooth energy delivery and maintain a dependable

supply.

5.13 Key trends, irregularities, and their significance

5.13.1 Observed trends

- **Influence of wind speed and blade angle:** The turbine demonstrated optimal performance at a 10° angle of attack (AoA) combined with wind speeds of 6–8 m/s, yielding a peak coefficient of performance (Cp) of 0.419 at 6 m/s and maximum power output of 38.30 W at 9 m/s. At 10° AoA, the blades operate near the airfoil's maximum lift-to-drag (L/D) ratio—typically around 10°–12° for symmetric NACA-series profiles used in Darrieus designs—where lift coefficient (CL) peaks via efficient boundary layer attachment (linear rise ~2π α per thin airfoil theory, ~0.17/degree) while drag remains low (primarily skin friction, with induced drag CDi ∝ CL2 minimal), enabling superior torque-to-power conversion before the critical stall angle (~15°). Deviations, such as lower winds (2–4 m/s) yielding insufficient dynamic pressure for lift generation, or higher AoA (15°–25°) inducing stall via adverse pressure gradients that thicken the boundary layer, cause upper-surface separation, CL plunge (>20% drop), and CD spike (2–3x rise from recirculation/wakes), reduced efficiency by >15%. This underscores the value of deploying such systems in steady, moderate-wind regions like South Africa's Western and Eastern Cape, where consistent profiles maximize continuous low-power generation for off-grid needs.
- **Geographical disparities:** Wind data from WASA indicate that coastal provinces like the Western and Eastern Cape, with average speeds between 7 and 8 m/s, offer the most suitable environment for small-scale wind energy systems. By contrast, areas further inland, such as Limpopo and Gauteng, exhibit average speeds as low as 3.5–4 m/s, with calm conditions (<4 m/s) dominating 54.6%–63.9% of the time conditions that significantly limit consistent power production.

5.13.2 Irregularities

- **Limited scalability:** To meet basic residential energy requirements, deploying multiple turbines would be necessary. This raises spatial, logistical, and financial concerns particularly in compact or resource-limited rural environments.
- **Maintenance barriers:** Regular upkeep is necessary to maintain blade integrity and proper angle of attack, yet a shortage of skilled labor in rural communities complicates ongoing operation and repairs.

- **Output limitation:** The turbine's maximum capacity of 38.30 W is insufficient for powering high-demand household appliances, limiting its practical application to small-scale or supplemental energy roles.
- **Simulation-Field gap:** While CFD simulations offer valuable insights, real-world conditions such as gusty or turbulent winds can result in different outcomes. This creates a gap between theoretical projections and practical effectiveness, calling for physical testing in actual field conditions.
- **Unreliable wind conditions:** Its performance is tightly bound to wind availability and direction, which are often inconsistent in rural areas surrounded by natural barriers such as trees or hills.

5.13.3 Broader significance of pico-scale wind uses in off-grid areas

- **Economic considerations:** Although insufficient as a stand-alone solution, pico-turbines with simple configurations and low maintenance demands can reduce the overall energy cost in hybrid systems. This makes them a promising alternative to expensive and polluting diesel generators, especially in regions lacking grid access.
- **Implications for research:** There is a clear need for experimental trials to bridge the gap between simulation and reality. Further exploration of improved rotor configurations such as helical or variable-pitch blades could enhance performance at low wind speeds, reduce cut-in thresholds, and improve self-start capabilities.
- **Policy recommendations:** Governments and energy planners could play a vital role by supporting the deployment of such systems through targeted subsidies, incentives, or integration into community-level microgrids, particularly in wind-rich rural zones. These actions would contribute to national goals on sustainability and energy inclusion.
- **Technical outlook:** These turbines offer a reliable power source for low-consumption applications like mobile phone charging or LED lighting when deployed in areas with adequate wind speeds. However, their dependence on consistent airflow and modest output requires integration with other technologies such as solar panels or battery systems to meet broader rural power needs.

5.14 Prospective development goals

To improve the practicality and efficiency of pico-scale Darrieus turbines in off-grid

electrification efforts, the following measures are recommended:

- **Field-Based performance testing:** Conduct on-site trials across different climatic zones and terrains to verify operational efficiency and resilience under real environmental conditions.
- **Rotor and blade innovation:** Explore the use of helical blade profiles and adaptive-pitch mechanisms that can respond dynamically to changing wind conditions, thereby improving starting capability and overall efficiency.
- **Renewable system integration:** Develop and test hybrid configurations particularly combinations with solar and battery storage to ensure consistent energy availability despite variable wind patterns.
- **Cost optimization strategies:** Simplify structural designs and support mass manufacturing to bring down production and installation costs, making these systems accessible to low-income, rural households.
- **Supportive policy frameworks:** Encourage government involvement through financial incentives, rural energy programs, or partnerships with local cooperatives to support wide-scale adoption in areas not served by the national grid.

5.15 Hybrid system integration

The Darrieus VAWT at pico-scale operates independently and has the ability to generate low power intermittently (for example, 38.29 W at 6–8 m/s), but also its sporadic nature in the countryside due to wind fluctuations (turbulence over 10%) means that at least >80% of the reliability must be achieved through solar PV and batteries hybridization since the simulation outputs get much lower than 5 W at a wind speed of under 4 m/s. A conceptual micro-hybrid exhibiting VAWT of 38 W, PV of 50 W, and a sodium battery of 100 Wh could continuously provide 5–10 W for LED lighting and charging which can be further expanded to a total storage of 200 Wh for a period of 2–3 days with modular scaling. Power flow will be through a common DC bus: VAWT/PV AC-DC conversion through rectifiers, battery charge/discharge management, and DC-AC inversion for loads, thereby reducing losses (<10% round-trip) according to IRENA mini-grid guidelines.

CHAPTER SIX

CONCLUSION AND RECOMMENDATIONS

6.1 Conclusion.

In order to hasten the journey of pico-scale Darrieus VAWTs from CFD validation to large-scale rural installation in South Africa—where more than two million homes are still without electricity and small wind power can cover diesel consumption by 20-30% in hybrid systems—there are several actions listed in order of priority. The actions are classified into short-term (0-1 year: prototype and validation right away), medium-term (1-3 years: integration and refinement of the system), and long-term (3+ years: building capacity and conducting evaluation) phases based on recent NREL grand challenges for small wind technology and World Bank guidelines for onshore projects in developing countries. The strategy gives priority to fast proof-of-concept for funding, reliable iterative improvements, and sustainable scaling in line with SDG 7.

One significant operational threshold that was noticed in the simulations was the reduction in efficiency due to high angles of attack (>15°) resulting from increased drag and flow separation. Additionally, another threshold was the power loss which amounted to almost total loss near obstructions (for instance, a structure of 2.5 m at a distance of 1.4 m would cause total power loss), thus indicating the necessity of very careful placement. These preliminary indicative findings could help improve pico-scale VAWTs in rural areas, but wind resource mapping and terrain studies would be necessary. Specifically, the research has provided a CFD model that has been validated with high fidelity, and a set of optimum design parameters has been defined clearly (10° AoA, 6-8 m/s wind speeds) for Darrieus VAWTs in the Southern African region, thus solving the previously identified critical gap in the literature highlighted in Chapter 2 dealing with region-specific small-scale wind solutions for low-Re, turbulent rural flows.

The contribution of such region-specific insights into small-scale wind solutions throws a spotlight on the mitigation of energy poverty in sub-Saharan Africa, where approximately 675 million people do not have access to electricity (IEA, 2024), and it corresponds to Sustainable Development Goal 7 on affordable clean energy. However, the conclusions presented are simulation-only and, therefore, are limited in the inherent way they were drawn: factors that were not taken into account such as mechanical friction, material degradation from humidity or temperature extremes, and real-world turbulence could

probably reduce the projected output by 10-20% or even more.

6.2 Recommendations

The flow of transition for pico-scale Darrieus VAWTs from CFD validation to large-scale rural deployment in South Africa—where the lack of electricity in more than two million households and the small wind can offset diesel by 20–30% in hybrids—has been envisioned in the form of prioritized phases: short-term (0–1 year: prototyping/validation), medium-term (1–3 years: system integration/refinement), and long-term (3+ years: capacity building/evaluation), with insights from NREL small wind challenges and World Bank onshore guidelines. The present roadmap documents quick proof-of-concept for funding, hardening of iterative reliability to the point of playing, and sustainable SDG 7 scaling.

In the medium-term refinement phase, optimizing blade aerodynamics is the key, for instance, at a 10° angle of attack (AoA), the airfoil—usually a symmetric NACA-series profile like NACA 0012 used in Darrieus VAWTs operates at the lift-to-drag (L/D) ratio close to its peak, as the lift coefficient (CL) increases almost in a linear fashion with AoA (according to thin airfoil theory: $CL \approx 2\pi\,\alpha$ in radians, or ~0.17 per degree up to ~10°–12°), while the drag is mostly low skin friction and minimal induced drag. This yields the maximum aerodynamic efficiency, as the induced drag ($CDi \propto CL2$ / aspect ratio) has not yet increased considerably. In addition, the stall angle (~12°–15° for low-Re flows <105) indicates an increase in adverse pressure gradients resulting in boundary layer thickening and consequently, separation on the upper surface which sharply decreases CL (>20% drop) and increases profile drag (CD >2–3x rise) due to massive flow recirculation and wake turbulence.

Short-Term actions (0–1 Year): prototype validation and initial testing

- **Empirical performance assessment**: High-potential coastal areas (for instance, Western Cape regions where 6–8 m/s is the average wind speed) should take top priority for field prototyping in order to test real outputs against simulated metrics like torque of 0.554 Nm at 8 m/s and power of 38.3 W at 9 m/s. Besides, stressors such as dust, huge temperature fluctuations (>40°C), and turbulence should be incorporated in the tests. Concurrent material tests on composite blades and coatings should be done with durability of 18–24 months in mind, using pilot hybrid

mini-grids as the model. This phase shall strengthen the investors' trust through quick-win data that will also help in dealing with resource risks in the case of developing-country deployments.

Medium-Term actions (1–3 Years): system integration and design refinement

- **Development of hybrid energy systems**: For catering to guaranteed 24/7 low-load (for example, lighting, charging) supply, the standardization process will be scaled to the use of 38.3 W VAWT–50 W PV–100 Wh sodium-ion battery modules with modularity allowing for 2–5x expansion. There will be a pilot in 10–20 rural households which will be following the MCDA guidelines for VAWT–PV hybrids in variable winds, aiming to achieve >80% uptime and lowering the LCOE to below USD 0.15/kWh.
- **Design optimization for low-wind environments**: The focus of CFD iterations will be on Savonius–Darrieus hybrids and blade profiles to increase the startup torque by over 20% under 4 m/s, and the targeting will be done to inland sites with <5 m/s averages. Prototyping of high solidity rotors (<3 kW) for turbulent flows should be done in-line with the bibliometric trends in VAWT innovations.

Long-Term actions (3+ Years): capacity building and holistic evaluation

- **Community-Based technical capacity building**: Make sure the skill-transfer programs and rural technicians are trained in technical aspects like maintenance, diagnostics and local assembly with the use of indigenous materials as the method to cut costs up to 40% and create jobs. The IRENA policy enablers will further support the whole process of ownership.
- **Comprehensive impact assessment**: To this end, conduct Life Cycle Analyses (LCAs) with all the collaborators to measure the emissions reductions that would result from this intervention (>1 tCO2/household/year) and at the same time keep track of the positive soci-economic impacts (e.g., +2 hours daily study time) through long-term studies in more than 50 sites. The findings will be used to guide the regulation of the energy sector by providing evidence to the World Bank for off-grid renewables scaling-up based on the recommendations.

The planned roadmap that goes in phases—beginning with validation to eliminate the risks of investments, moving on to hybrids for guarantee and reliability, and ending with community participation in sustainability—brings pico-scale VAWTs to the fore as a key

element for the rural electrification of South Africa, thus contributing to the realization of SDG 7 in the meantime with the market growth forecasts of small VAWTs in 2025 being 12% CAGR.

6.2.1 Future experimental validation plans

To corroborate CFD predictions (e.g., Cp >0.25 at 6–8 m/s, torque <0.1 Nm <4 m/s) and address modeling uncertainties like 2D approximations (<5% deviation), a phased experimental program is outlined:

- Lab-Scale Testing (Months 1–6): Set up and execute wind tunnel tests at the Re < 10^5 level with airfoils like NACA0015 or those with similar characteristics, with the aim of getting less than 5% deviation from the simulations by concentrating on stall (at an angle of attack greater than 15 degrees) and through the low-speed startup phases while measuring Cp, torque, and flow with PIV/dynamometers.
- Field Prototyping (Months 7–12): Introduce 2-3 large-scale prototypes (D=0.5 m) in different rural locations (for example, coastal Western Cape with wind speed 6-8 m/s; inland Limpopo with wind speed <5 m/s having 10-20% turbulence), and collect data on uptime, hybrid integration (with 50 W PV, >80% reliability), and environmental stressors (dust, >40°C temps) for 3-6 months through on-site sensors.
- Integration and Iteration (Ongoing): Combine with batteries for real-load (5-10 W) testing, subjecting the process to iterative CFD-experimental loops per NREL protocols, with a target of LCOE below USD 0.15/kWh and the possibility of expanding to 10-20 household pilots.
- This validation exercise not only fills the gaps between simulation and deployment but also de-risks the investments and facilitates the adaptation to the changing winds in South Africa.

REFERENCES

Ab. Wahab, A., Abas, M., & Ismail, M., 2004. Establishing the Wind Map of Sabah and Sarawak. Available at: http://eprints.utm.my/id/eprint/2688/1/74168.pdf [Accessed 14 September 2024].

Aberilla, J.M., Gallego-Schmid, A., Stamford, L., & Azapagic, A., 2020. Design and environmental sustainability assessment of small-scale off-grid energy systems for remote rural communities. Applied Energy, 258, p.114004.

Akwa, J.V., Vielmo, H.A., & Petry, A.P., 2012. A review on the performance of Savonius wind turbines. Renewable and Sustainable Energy Reviews, 16, pp.3054–3064.

Alam, F. and Jin, Y., 2023. The utilisation of small wind turbines in built-up areas: prospects and challenges. Wind, 3(4), pp.418-438.

Ali, S., Park, H. and Lee, D., 2024. Structural Optimization of Vertical Axis Wind Turbine (VAWT): A Multi-Variable Study for Enhanced Deflection and Fatigue Performance. Journal of Marine Science and Engineering, 13(1), p.19.

Al-Rawajfeh, M.A. and Gomaa, M.R., 2023. Comparison between horizontal and vertical axis wind turbine. International Journal of Applied Power Engineering, 12(1), pp.13-23.

Altan, B.D., Atılgan, M., & Ozdamar, A., 2008. An experimental study on improvement of Savonius rotor performance with curtaining. Experimental Thermal and Fluid Science, 32(2008), pp.1673–1678.

Ayodele, T.R., Jimoh, A.A., Munda, J.L., Agee, J.T., & M'boungui, G., 2013, February. Economic analysis of a small-scale wind turbine for power generation in Johannesburg. In 2013 IEEE International Conference on Industrial Technology (ICIT) (p. 1728-1732). IEEE.

Bhutta, M.M.A., Hayat, N., Farooq, A.U., Ali, Z., Jamil, S.R., & Hussain, Z., 2012. Vertical axis wind turbine – A review of various configurations and design techniques. Renewable and Sustainable Energy Reviews, 16(2012), pp.1926–1939.

Danao, L.A., Eboibi, O., & Howell, R., 2013. An experimental investigation into the influence of unsteady wind on the performance of a vertical axis wind turbine. Applied Energy, 107, pp.403–411.

Deevela, N.R., Kandpal, T.C. and Singh, B., 2024. A review of renewable energy-based power supply options for telecom towers. Environment, Development and Sustainability, 26(2), pp.2897-2964.

Eberhard, A. and Naude, R., 2016. The South African renewable energy independent power producer procurement programme: A review and lessons learned. Journal of Energy in Southern Africa, 27(4), pp.1-14.

Fant, C., Gunturu, B., & Schlosser, A., 2016. Characterizing wind power resource reliability in southern Africa. Applied Energy, 161, pp.565–573.

Fant, C., Schlosser, A.C., & Strzepek, K., 2016. The impact of climate change on wind and solar resources in southern Africa. Applied Energy, 161, pp.556–564.

Ferrari, F., Besio, G., Cassola, F., & Mazzino, A., 2020. Optimized wind and wave energy resource assessment and offshore exploitability in the Mediterranean Sea. Energy, 190, p.116447.

Frederikus Wenehenubun, A., Saputraa, H., & Sutantoa, H., 2015. An experimental study on the performance of Savonius wind turbines related to the number of blades. Energy Procedia, 68, pp.297–304.

Ghafoorian, F., Mirmotahari, S.R., Eydizadeh, M. and Mehrpooya, M., 2025. A systematic investigation on the hybrid Darrieus-Savonius vertical axis wind turbine aerodynamic performance and self-starting capability improvement by installing a curtain. Next Energy, 6, p.100203.

Gough, M., Lotfi, M., Castro, R., Madhlopa, A., Khan, A., & Catalão, J.P.S., 2019. Urban wind resource assessment: a case study on Cape Town. Energies, 12, pp.1–20.

Gupta, R., & Biswas, A., 2010. Computational fluid dynamics analysis of a twisted three-bladed H-Darrieus rotor. Renewable and Sustainable Energy, 2, pp.1–15.

Hassan, Q., Algburi, S., Sameen, A.Z., Salman, H.M. and Jaszczur, M., 2023. A review of hybrid renewable energy systems: Solar and wind-powered solutions: Challenges, opportunities, and policy implications. Results in engineering, 20, p.101621.

Howell, R., Qin, N., Edwards, J., & Durrani, N., 2010. Wind tunnel and numerical study of a small vertical axis wind turbine. Renewable Energy, 35, pp.412–422.

Ighodaro, O., & Akhihiero, D., 2021. Modeling and performance analysis of a small horizontal axis wind turbine. Journal of Energy Resources Technology, 143(3), p.031301.

Inambao, F.L., & Cunden, K., 2019. Offshore wind resource assessment off the South African coastline. International Journal of Mechanical Engineering Technology, 10, pp.95–119.

Islam, M., Amin, M.R., Ting, D.S.K., & Fartaj, A., 2007. Aerodynamic factors affecting performance of straight-bladed vertical axis wind turbines. In ASME International Mechanical Engineering Congress and Exposition, Vol. 6, pp.331–341.

Jamal, N., 2015. Options for the supply of electricity to rural homes in South Africa. Journal of Energy in Southern Africa, 26(3), pp.58-65.

Jha, A.R., 2011. Wind Turbine Technology. CRC Press, Taylor & Francis Group, pp.3.

Jin, X., Zhao, G., Gao, K.J., & Ju, W., 2015. Darrieus vertical axis wind turbine: Basic research methods. Renewable and Sustainable Energy Reviews, 42, pp.212–225.

Kacprzak, K., Liskiewicz, G., & Sobczak, K., 2013. Numerical investigation of conventional and modified Savonius wind turbines. Renewable Energy, 60, pp.578–585.

Kazimierczuk, A.H., 2019. Wind energy in Kenya: a status and policy framework review. Renewable and Sustainable Energy Reviews, 107, pp.434–445.

Leary, J., While, A., & Howell, R., 2012. Locally manufactured wind power technology for sustainable rural electrification. Energy Policy, 43, pp.173–183.

López-González, A., Ranaboldo, M., Domenech, B. and Ferrer-Martí, L., 2020. Evaluation of small wind turbines for rural electrification: Case studies from extreme climatic conditions in Venezuela. Energy, 209, p.118450.

Mas'ud, A.A., Wirba, A.V., Ardila-Rey, J.A., Albarracín, R., Muhammad-Sukki, F., Duque, A.J., & Bani, N.A., 2017. Wind power potentials in Cameroon and Nigeria: Lessons from South Africa. Energies, 10, pp.1–19.

Merem, E.C., Twumasi, Y., Wesley, J., Olagbegi, D., Crisler, M., Romorno, C., Alsarari, M., Isokpehi, P., Hines, A., Hirse, G. and Ochai, G.S., 2022. The evaluation of wind energy potentials in South Africa. Energy and power, 12(1), pp.9-25.

Messineo, A., & Culotta, S., 2012. Evaluating the performances of small wind turbines: A case study in the south of Italy. Energy Procedia, 16, pp.137–145.

Meyer, E.L. and Overen, O.K., 2021. Towards a sustainable rural electrification scheme in South Africa: Analysis of the Status quo. Energy Reports, 7, pp.4273-4287.

Moner-Girona, M., Bódis, K., Morrissey, J., Kougias, I., Hankins, M., Huld, T., & Szabó, S., 2019. Decentralized rural electrification in Kenya: Speeding up universal energy access. Energy Sustainability Development, 52, pp.128–146.

Nwagu, C.N., Ujah, C.O., Kallon, D.V. and Aigbodion, V.S., 2024. Integrating solar and wind energy into the electricity grid for improved power accessibility. Unconventional Resources, p.100129.

Omole, F.O., Olajiga, O.K. and Olatunde, T.M., 2024. Challenges and successes in rural electrification: A review of global policies and case studies. Engineering Science & Technology Journal, 5(3), pp.1031-1046.

Rehman, S., Natarajan, N., Mohandes, M.A., Meyer, J.P., Alam, M.M. and Alhems, L.M., 2022. Wind and wind power characteristics of the eastern and southern coastal and northern inland regions, South Africa. Environmental Science and Pollution Research, 29(57), pp.85842-85854.

Seifi Davari, H., Botez, R.M., Seify Davari, M. and Chowdhury, H., 2024. Enhancing the efficiency of horizontal axis wind turbines through optimization of blade parameters. Journal of Engineering, 2024(1), p.8574868.

Seguro, J.V. and Lambert, T.W., 2000. Modern estimation of the parameters of the Weibull wind speed distribution for wind energy analysis. Journal of wind engineering and industrial aerodynamics, 85(1), pp.75-84.

Simic, Z. and Mikulicic, V., 2007, September. Small wind off-grid system optimization regarding wind turbine power curve. In AFRICON 2007 (pp. 1-6). IEEE.

Tzen, E., 2020. Small wind turbines for grid and off grid applications. In IOP conference series: Earth and environmental science (Vol. 410, No. 1, p. 012047). IOP Publishing.

Wright, M.A. and Grab, S.W., 2017. Wind speed characteristics and implications for wind power generation: Cape regions, South Africa. South African Journal of Science, 113(7-8), pp.1-8.

Wu, X., Wang, J., & Hu, W., 2018. Optimization design of a vertical axis wind turbine for efficient power generation. Journal of Renewable and Sustainable Energy, 10(6), p.063301.

Yadav, R. and Bhalani, J., 2022. Challenges to mini grids: an alternative to rural electrification. In Renewable Energy Optimization, Planning and Control: Proceedings of ICRTE 2021, Volume 1 (pp. 41-47). Springer Singapore.

Yazdani, A., & Hoque, A., 2010. Distributed generation: A definition. Electric Power Systems Research, 81(3), pp.536–540.

Ye, Y., Koch, S.F. and Ye, X., 2025. The effect of temperature on household hourly electricity consumption: Evidence from South Africa. Energy, p.134925.

Zaharaddeen, I., Ayodeji, A.O., & Olatunji, O.A., 2019. A review of wind energy potential in Nigeria: Prospects and challenges. Renewable and Sustainable Energy Reviews, 109, pp.552–564.

Zhou, Q., Zhang, Z., Cheng, M., & Yang, J., 2019. Comparative performance analysis of H-type Darrieus and Savonius vertical axis wind turbines. Journal of Wind Engineering and Industrial Aerodynamics, 193, p.103970.

Zhu, W.J., & Shu, X.W., 2016. Effect of blade profile on the aerodynamic performance of a Darrieus-type vertical axis wind turbine. Energy, 106, pp.877–889.

Zou, J., Li, J., & Chen, J., 2021. Performance evaluation of a hybrid Darrieus–Savonius vertical axis wind turbine under dynamic stall conditions. Renewable Energy, 163, pp.1947–1960.